TURUN
YLIOPISTO
UNIVERSITY
OF TURKU

PHOTOLUMINESCENCE QUENCHERS IN DRUG DISCOVERY

Emmiliisa Vuorinen

TURUN YLIOPISTON JULKAISUJA – ANNALES UNIVERSITATIS TURKUENSIS
SARJA – SER. AI OSA – TOM. 659 | ASTRONOMICA – CHEMICA – PHYSICA – MATHEMATICA | TURKU 2021

TURUN
YLIOPISTO
UNIVERSITY
OF TURKU

PHOTOLUMINESCENCE QUENCHERS IN DRUG DISCOVERY

Emmiliisa Vuorinen

TURUN YLIOPISTON JULKAISUJA – ANNALES UNIVERSITATIS TURKUENSIS
SARJA – SER. AI OSA – TOM. 659 | ASTRONOMICA – CHEMICA – PHYSICA – MATHEMATICA | TURKU 2021

University of Turku

Faculty of Science
Department of Chemistry
Detection Technology
Drug Research Doctoral programme

Supervised by

Docent Harri Härmä, Ph.D.
Department of Chemistry
University of Turku
Turku, Finland

Kari Kopra, Ph.D.
Department of Chemistry
University of Turku
Turku, Finland

Reviewed by

Professor, Nico Hildebrandt
University of Rouen Normandie,
Laboratoire COBRA
Normandy, France

Andrew Stephen, Ph.D.
NCI-Frederick
Leidos Biomedical Research, Inc.
Frederick, Maryland, USA

Opponent

Assistant professor, Bogdan Iulius Florea
Leiden University
Leiden Institute of Chemistry
Leiden, Netherlands

ISBN 978-951-29-8706-1 (PRINT)
ISBN 978-951-29-8707-8 (PDF)
ISSN 0082-7002 (Print)
ISSN 2343-3175 (Online)
Painosalama, Turku, Finland 2021

The road goes ever on

Over rock and under tree,
By caves where never sun has shone,
By streams that never find the sea;
Over snow by winter sown,
And through the merry flowers of June,
Over grass and over stone,
And under mountains in the moon.

Roads go ever ever on
Under cloud and under star,
Yet feet that wandering have gone
Turn at last to home afar.
Eyes that fire and sword have seen
And horror in the halls of stone
Look at last on meadows green
And trees and hills they long have known.

The Road goes ever on and on
Out from the door where it began.
Now far ahead the Road has gone,
Let others follow it who can!
Let them a journey new begin,
But I at last with weary feet
Will turn towards the lighted inn,
My evening-rest and sleep to meet.

–J.R.R. Tolkien

UNIVERSITY OF TURKU
Faculty of Science
Department of Chemistry
Emmiliisa Vuorinen: Photoluminescence quenchers in drug discovery
Doctoral Dissertation, 134 pp.
Drug Research Doctoral Programme
November 2021

ABSTRACT

During the drug discovery process molecular libraries containing millions of molecules are screened to find a single potential drug with the highest potency and efficacy over unwanted side-effects. The whole drug development process usually takes more than a decade and requires billions of euros. Thus, new methods with improved cost and time effectiveness are vital for both improving primary screening of molecular libraries and verifying the results obtained via secondary screens.

Drug discovery often utilizes methods based on photoluminescence, the emission of light from a luminophore molecule excited by photon absorption, e.g. fluorescence. The methods monitor changes in photoluminescence that are initiated by an event in the assay e.g. interaction of protein and ligand. In some methods, the detectability of the change can be enhanced by decreasing the luminescence of non-interacting luminophores by quenching. Some luminophores are quenched by water but others require dedicated quencher molecules e.g. the acceptor molecules quenching donor luminophores in Förster resonance energy transfer (FRET).

In the work presented in this thesis, the addition of a soluble quencher was utilized for developing two photoluminescence-based assays suitable for drug discovery for studying protein-ligand interactions (PLI), protein-protein interactions (PPI), and protease activity. The first method developed, QTR-FRET, utilizes soluble quencher to decrease the emission of non-interacting donor luminophore thus preventing it from interfering in the monitored acceptor channel. QTR-FRET improves conventional TR-FRET by permitting the investigation of low affinity PLI interactions requiring high donor luminophore concentrations and by enabling multiplexing via monitoring PLI and subsequent PPI. The second method, the Protein-Probe, was developed to measure the emission of external luminescence probe during its interaction with a target protein. The emission of non-interacting probe is reduced by soluble quencher. The Protein-Probe is suitable for monitoring the PLIs via their effect on the thermal stability of protein and the protease activity via the digested protein substrate. The Protein-Probe has 50-fold improved sensitivity compared to conventional methods.

KEYWORDS: Drug discovery, Method, Photoluminescence, Quenching, FRET

TURUN YLIOPISTO
Matemaattis-luonnontieteellinen tiedekunta
Kemian laitos
EMMILIISA VUORINEN: Loistevalon sammuttajat lääkekehityksessä
Väitöskirja, 134 s.
Lääkekehityksen tohtoriohjelma
Marraskuu 2021

TIIVISTELMÄ

Varhaisen lääkekehityksen aikana miljoonia molekyylejä sisältävistä molekyylikirjastoista seulotaan lääkemolekyyli, joka vaikuttaa sairauteen mahdollisimman tehokkaasti välttäen haitallisia sivuvaikutuksia. Yleensä lääkekehitysprosessi kestää yli vuosikymmenen ja kuluttaa miljardeja euroja. Tämän vuoksi uusia aika- ja kustannustehokkaita menetelmiä tarvitaan parantamaan ensisijaista seulontaa sekä varmistamaan niiden tulokset toissijaisella seulonnalla.

Varhaisessa lääkekehityksessä hyödynnetään usein menetelmiä, jotka perustuvat fotoluminesenssiin, eli valon tuotantoon luminofori molekyylistä, joka on virittynyt fotonin imeytymisen vuoksi, kuten fluoresenssiin. Menetelmät tarkkailevat luminesenssiin vaihtelua, minkä saa aikaan tapahtuma määrityksessä kuten proteiinin ja ligandin vuorovaikutus. Joissain menetelmissä tapahtuman havaitsemista voidaan tehostaa sammuttamalla sitoutumattomien luminoforien luminesenssia. Jotkut luminoforit voidaan sammuttaa vedellä, mutta toiset vaativat erillisen molekyylin kuten Förster resonanssi energiasiirron (FRET) luovuttaja luminoforeja sammuttavat vastaanottaja molekyylit.

Tässä väitöskirjassa liukoisen sammuttajan lisäystä käytettiin kehittämään kaksi lääkekehitykseen soveltuvaa fotoluminesenssimenetelmää, jotka tarkkailevat proteiini-ligandi (PLV), proteiini-proteiini vuorovaikutuksia sekä proteaasien aktiivisuutta. Ensimmäiseksi kehitetyssä QTR-FRET menetelmässä sammuttajaa käytetään vähentämään sitoutumattomien luovuttaja-luminoforien valon tuotantoa, jolloin niiden aiheuttama häiriö vastaanottajamolekyylin luminesenssia mitattaessa vähenee. QTR-FRET mahdollistaa korkeaa luovuttajapitoisuutta tarvitsevien matalan affiniteetin PLV:en sekä kahden linkittyneen vuorovaikutuksen tarkkailun yhteisestä kaivosta. Toinen kehitetty menetelmä, Protein-Probe, mittaa erillisen koettimen luminesenssia sen sitoutuessa proteiiniin. Sitoutumattoman koettimen luminesenssi himmentyy liukoisen sammuttajan vaikutuksesta. Protein-Probella voi tarkkailla PLV:ia proteiinien lämpöpysyvyyden välityksellä, sekä proteaasien aktiivisuutta niiden hajottamien substraattiproteiinien kautta. Protein-Probe menetelmän herkkyys on 50-kertainen verrattuna vastaaviin menetelmiin.

AVAINSANAT: Lääkekehitys, Menetelmä, Fotoluminesenssi, Sammutus, FRET

Table of Contents

Abbreviations

ADMET	Absorption or administration, distribution, metabolism, excretion, and toxicological properties
AZA	Acetazolamide
CA	Carbonic anhydrase
CTA	Clinical trial application
DARPin	Designed ankyrin repeat proteins
DEL	DNA-encoded libraries
DMTA	design-make-test-analyze
DNA	Deoxyribonucleic acid
DSF	Differential scanning fluorometry
EC_{50}	Half-maximal effective concentration
EDTA	Ethylenediaminetetraacetic acid
Eu^{3+}	Europium (III) ion
FDA	Food and drug administration
FRET	Förster resonance energy transfer
GDP	Guanosine diphosphate
GFP	green fluorescent protein
GLP	Good laboratory practice
GPCR	G protein-coupled receptor
GTP	Guanosine triphosphate
HSA	Human serum albumin
HAT	Histone acetyltransferase
HIDC	1,1,3,3,3′,3′-hexamethylindodicarbocyanine iodide
HOMO	highest occupied molecular orbital
HTRF	Homogeneous Time Resolved Fluorescence
HTS	High throughput screening
HSPG	Heparan sulfate proteoglycan
ISO	International Organization of Standardization
ITC	Isothiocyanate conjugation
IC_{50}	Half maximal binding affinity
LANCE	Lanthanide Chelate Excite

LUMO	lowest unoccupied molecular orbital
NAD(H)	Nicotinamide adenine dinucleotide
NAD(P)H	Nicotinamide adenine dinucleotide phosphate
MDH	Malate dehydrogenase
MG	Malachite green
PET	Photoinduced electron transfer
PLI	Protein-ligand interaction
PPI	Protein-protein interaction
PTM	Post-translational modification
PTX	Pertussis toxin
Qdot	Quantum dot
QRET	Quenched resonance energy transfer
QTR-FRET	Quencher modulated time-resolved Förster resonance energy transfer
RAF-RBD	The Ras binding domain of the c-Raf kinase protein
RO5	Lipinski Rule of Five
Tb^{3+}	Terbium (III) ion
T_m	denaturation temperature
TR	Time-resolved
TR-FRET	Time-resolved Förster resonance energy transfer
TRL	Time-resolved luminescence
TSA	Thermal shift assay
SA	Streptavidin
SAR	Structure-activity relationship
S/B	Signal-to-background
SOS	Son of sevenless
S_0	Ground state
S_2	Excited singlet state
T_1	Triplet state
β2AR	β2-adrenoreceptor
1,8-ANS	8-Anilinonaphthalene-1-sulfonic acid
2,6-TNS	2-(4-toluidino)-6-naphthalenesulfonic acid

List of Original Publications

This dissertation is based on the following original publications, which are referred to in the text by their Roman numerals:

I Markku Syrjänpää, Emmiliisa Vuorinen, Sakari Kulmala, Qi Wang, Harri Härmä, Kari Kopra. QTR-FRET: Efficient background reduction technology in time-resolved förster resonance energy transfer assays. *Analytica Chimica Acta*, 2019; 1092: 93–101.

II Kari Kopra, Emmiliisa Vuorinen, Maria Abreu-Blanco, Qi Wang, Ville Eskonen, William Gillette, Arto T. Pulliainen, Matthew Holderfield, Harri Härmä. Homogeneous Dual-Parametric-Coupled Assay for Simultaneous Nucleotide Exchange and KRAS/RAF-RBD Interaction Monitoring. *Analytical Chemistry*, 2020; 92: 4971–4979.

III Emmiliisa Vuorinen, Salla Valtonen, Ville Eskonen, Taru Kariniemi, Jelena Jakovleva, Kari Kopra, Harri Härmä. Sensitive Label-Free Thermal Stability Assay for Protein Denaturation and Protein–Ligand Interaction Studies. *Analytical Chemistry*, 2020; 92: 3512–3516.

IV Emmiliisa Vuorinen, Salla Valtonen, Nazia Hassan, Randa Mahran, Huda Habib, Morteza Malakoutikhah, Kari Kopra, Harri Härmä. Protease Substrate-Independent Universal Assay for Monitoring Digestion of Native Unmodified Proteins. *International Journal of Molecular Sciences*, 2021; 22: 6362

1 Introduction

The process of drug discovery and development takes 10 to 15 years, costs billions of euros, and necessitates multidisciplinary efforts.[1–3] In the early phases of drug discovery, molecular libraries spanning millions of molecules are screened with primary assays for hit compounds directed against the target biomolecule involved in the disease.[4–6] The initial hit compounds are confirmed with secondary assays, and their number expanded during the hit-to-lead process, which aims to enhance their selectivity and potency towards the target biomolecule.[7,8] The hit-to-lead process results in lead compounds that are further optimized to improve their absorption and efficacy before preclinical investigation and guarantee their safety for clinical trials in humans.[9,10] If the clinical trials result in a candidate drug with satisfactory efficacy against the target disease without endangering the health of the patient, the drug development process has been successful.[11–13]

The clinical trials are the most expensive part of the drug development process. Thus, high quality drug discovery screening and validation is needed to avoid later phase *dead-ends* by avoiding drug candidates with too low efficiency towards the disease or significant health concerns. The initial drug discovery screening for hit compounds employs high-throughput screening (HTS) with primary screening methods.[14] In the hit-to-lead stage, a variety of secondary screening methods aim to verify the results obtained previously. Both *in vivo* and *in vitro* assays are used for lead optimization. For preclinical testing, an increasingly human-like environment, i.e. from cell culture to mice models, is used.[9,10] Since the process of drug discovery requires wide range of different methods, e.g. for screening verification and safety evaluation, new and improved methods are always of interest. Ideally the assays should be sensitive, robust, and simple for automation purposes. The selection of the assay often comes down to the balance between reliability and cost- and time-effectiveness.[15] Assays can be divided into heterogenous assays which utilize separation of unbound reporter or analyte and homogenous which require no separation steps. Although heterogeneous assays provide higher sensitivity and robustness, homogenous assays are often used. Homogenous assays based on photoluminescence are increasingly popular nowadays.

Photoluminescence is a type of luminescence that releases the excess energy obtained through photon absorption by the emission of light. The photon absorption excites an electron in the luminescent molecule to a higher energy state. Depending on the relaxation pathway of the excited electron, different types of photoluminescence, such as fluorescence, are emitted. The relaxation pathway also affects the wavelength of the emission and the emission lifetime.[16–18] Some luminescent molecules like phosphors and lanthanide chelates have significantly longer lifetimes than typical fluorochromes. In time-resolved (TR) measurement, this property is used to minimize short-lived background signals from the instrument and environment.[17,19–21] Most photoluminescence methods focus on monitoring the changes in luminescence emission associated with alterations in the assay system such as interactions of proteins or changes in their structure. The luminescence emission is often produced by luminescent labels conjugated to studied proteins or external luminescent probes such as fluorescent dyes interacting with different biomolecules. The intensity of the emission can be decreased by quenching in either a dynamic or static quenching format. Dynamic quenching is based on molecular collision, e.g. energy or electron transfer between the luminophore donor and quencher acceptor. During static quenching, the luminophore and quencher form a complex, which releases the absorbed excess energy in non-radiative forms, such as heat and molecular vibrations. These two quenching formats are not mutually exclusive, and in some cases, it is difficult to determine which format is employed.[17,22,23]

A wide range of assay methods are based on photoluminescence quenching. The well-known FRET method, is based on dynamic quenching and the energy transfer between the donor and acceptor labels. FRET assays are often performed with luminescence labels with long-lived emission that enable time-resolved FRET measurements.[17,24–26] FRET assays, such as LANCE and HTRF, are especially useful for investigating protein interactions with other proteins or small molecular ligands, and some methods enable membrane protein studies featuring living cells, such as Tag-lite and QRET.[27–30] One approach is based on the dynamic quenching properties of water on common fluorescent dyes. In this case, the fluorescence is only emitted when the dye is not in close contact with water but bound to biomolecules such as proteins or lipid membranes. This binding can be affected by structural changes in the biomolecule, like protein denaturation, leading to measurable changes in the fluorescence emission. Differential scanning fluorometry (DSF) is one such method and is often employed for studying the thermal stability and aggregation of proteins.[31–34]

The work presented in this thesis was focused on developing two new methods for drug discovery purposes, in particular for secondary screening with potential use for primary screening. The methods were homogenous microtiter plate assays based

on photoluminescence quenching and designed for protein interaction and digestion studies. In publication **I**, quencher mediated time-resolved FRET (QTR-FRET) provided an improvement on conventional TR-FRET for studying protein-ligand interactions (PLI) by decreasing the donor emission interference in the acceptor channel with a soluble quencher. The quencher addition increased the signal to background ratio (S/B ratio) and enabled the investigation of low affinity interactions requiring high donor concentrations. Publication **II** proved the capability of QTR-FRET for single well PLI and protein-protein interaction (PPI) monitoring with two model assays. In publication **III,** a new Protein-Probe method was developed for investigating the thermal profiles of target proteins and ligand binding to the target. The Protein-Probe method is based on an external luminescent probe binding to a range of proteins, particularly in their denatured form and affected by the soluble quencher in the assay solution. In publication **IV,** the Protein-Probe was utilized for the evaluation of protease digestion activity with several unmodified substrate proteins.

2 Literature Review

In this review of literature, methods based on FRET and photoluminescence quenching via water are considered in the context of the drug discovery process. First, the drug development process and the importance of assay development are introduced. Then the principles of photoluminescence and quenching are presented. Finally, methods based on dynamic quenching effects of water and FRET, akin to those developed during my thesis, are described. The main focus of this review is on the versatility of photoluminescence quenching for assay development in the interest of drug discovery.

2.1 The Drug development process

The development process for a single new drug takes on average of 10 to 15 years and can cost over billions of euros.[1–3] It has evolved to a highly controlled process in order to regulate the unnecessary and life threatening side-effects of drugs like thalidomide causing embryopathy and diethylstilbestrol, causing cancers, birth defects and developmental abnormalities.[35,36] Regulated development ensures the safety and efficiency of novel drugs in a cost effective way by relying on streamlined assays and methods during all its phases (**Figure 1**). This chapter focuses on the phases of drug discovery and especially early drug discovery. The early drug discovery of classic small molecular ligand is described as an example.

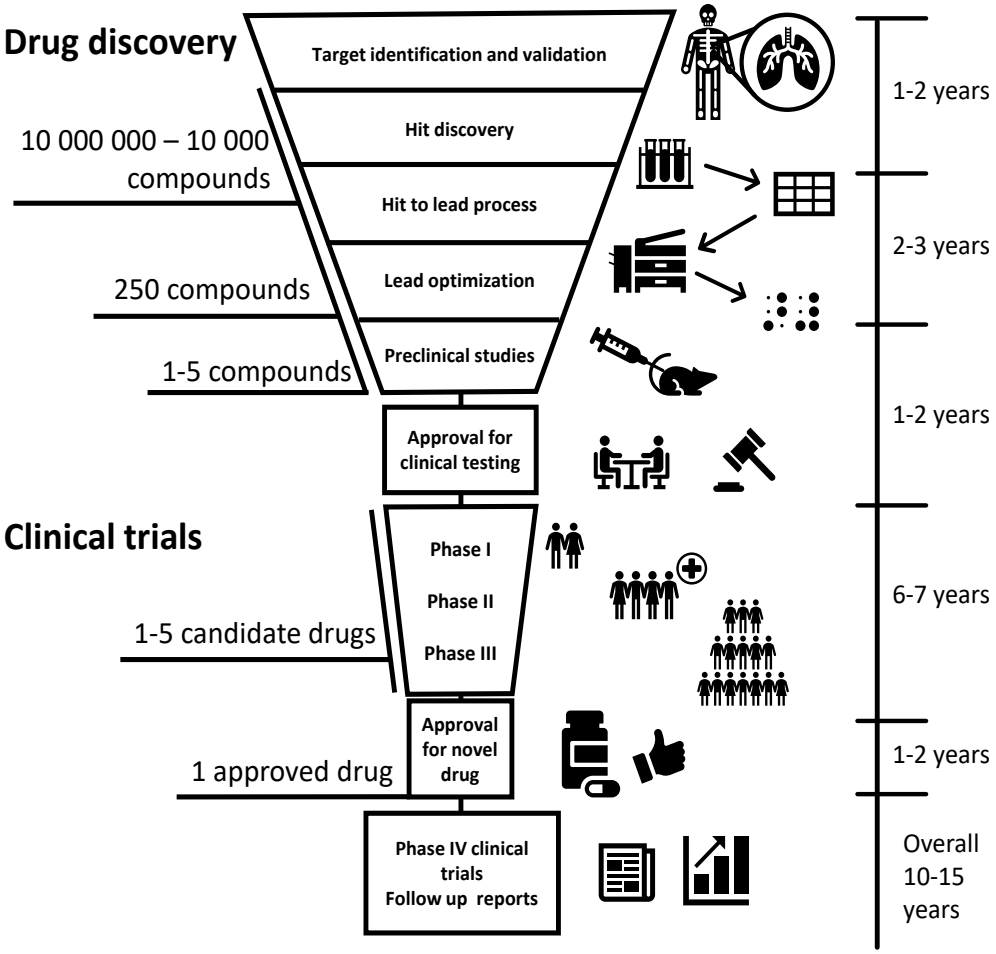

Figure 1. A Drug development process investigates millions of molecules to produce an as effective and safe drug as possible. The process is divided into drug discovery and clinical trials and can take up to 15 years and cost billions of euros. The drug discovery begins with target identification and validation, which determine the target for the drug compound based on its involvement with the disease. The selected target is then assayed in primary screening with molecular libraries to discover hit compounds that interact and affect the target in a desired manner. These hit compounds are then further developed during the hit-to-lead process to improve their potency and selectivity towards the target and produce lead molecules. The leads are then optimized for pre-clinical trials where only approximately 200 compounds remain. Pre-clinical studies select up to five candidate drugs for clinical trial approval application and subsequent clinical trials. The clinical trials focus on proper usage and risk/benefit ratio of the drug. Clinical trials are separated into 4 phases with an increasing number of voluntary participants. The first three phases are conducted before applying for market approval for novel drug and if granted the safety and efficiency of the marketed drug is monitored in the final phase IV.

2.1.1 Target identification & validation, and molecular libraries

Drug development starts from an unmet clinical need for an improved drug with reduced side-effects, or need for a novel drug for a disease without appropriate medicine.[37] To begin with, the drug discovery process requires knowledge of the disease and its underlying cause. This is the focus of target identification, which utilizes pre-existing knowledge gathered on gene and protein identification, along with the importance of the target for metabolism and signaling.[38] This biological target is often a gene or a protein, such as a receptor, enzyme or ion channel, involved in the disease. The chosen target must be druggable, ergo its binding with a potential drug must affect its function in a health beneficial way, without significantly interfering with other important metabolic pathways.[39]

In traditional small molecule drug development, the target validation research establishes the involvement of the target in the disease and the binding site for the potential drug molecules. The biological activity and importance of the target are investigated and the effects of potential modulation for toxicity and disease efficacy are assessed. Extensive target validation helps to avoid project termination in the later drug development phases due to undruggability or inefficiency of the target. Rapid target validation and invalidation are enabled by genetic methods, computer modeling, biochemical and cellular assays.[40] The most optimal target is highly selective, suitable for both biochemical and cellular assays, and has existing biological markers for evaluating the modulation responses accurately and reproducibly.[41,42] The chosen target determines which molecular libraries contain ligands suitable for screening.[3,40,43–45]

Molecular libraries contain an array of compounds with recorded information on their properties, such as structure, purity, quantity, and physiochemical characteristics. Depending on their application, these libraries can be categorized into diversity oriented libraries and focused libraries. Diversity oriented libraries contain a wider array of molecules with distinct structures and properties for screening a board range of biological activities.[46] Focused libraries function in either a target-focused or ligand-focused manner, and consist of a set of structurally similar compounds designed for a specific purpose, e.g. inhibition of specific enzyme. Focused libraries can contain approved drug molecules with known safety profiles or compounds with known toxicity profiles.[5]

Molecular libraries operate on the basis a chemical space, i.e. the area covered by all possible molecules under established principles and conditions, where a potential ligand for the target can be found. The chemical space containing all possible drug molecules is vast and only fraction of it is covered by molecular libraries.[47,48] To increase the coverage, traditional small molecule libraries can be generated from a range of different sources, e.g. by exploring natural compounds, *in*

silico methods, structure or fragment-based approach, hybrid molecule design, and repurposing drugs.[3,4,49] Traditionally, many drugs have originated from nature and multiple molecular libraries are still collected from or based on natural compounds.[50] Living organisms have been modified to produce new compounds, such as antibiotics, which are released by mold or fungi to battle against bacteria.[51,52] Another approach for producing novel molecules for libraries is based on mimicking the structure of a natural ligand or substrate of the target. *In silico* methods aid this process through computational analysis and artificial intelligence.[53–57] In the fragment based approach, small molecular fragments with low affinity towards the target are combined to produce molecules with increased affinity.[58,59] Novel compounds can be produced with the hybrid technique by conjugating molecular fragment or multiple molecules.[60,61] Existing and approved drug molecules have also been collected for drug repurposing libraries. This approach minimizes failures caused by toxicity since the molecule has already passed toxicity evaluation.[62–64]

In traditional small molecule libraries, the drug-likeness of compounds play an important role in improving the likelihood of the compound passing absorption, distribution, metabolism, excretion, and toxicity (ADMET) testing in later stages of drug discovery. The drug-likeness of compounds can be evaluated with sets of chemical parameters, such as Lipinski Rule of Five (RO5). RO5 states that for the compound to be orally active drug in humans it must contain no more than five hydrogen bond donors and ten hydrogen bond acceptors. Additionally the compounds must be highly lipophilic with octanol-water partition coefficient (log P) below 5 and the molecular mass of the compound cannot exceed 500 daltons. These rules are not absolute and many exceptions exist, e.g. antibiotics and vitamins, but RO5 nevertheless functions as a starting point.[65–67]

The number of novel compounds in traditional small-molecule libraries has been greatly increased by the development of combinatory libraries such as DNA-encoded libraries (DEL).[5,6,68] Combinatorial libraries enable storage of the whole library in one mixture for production of millions of compounds in a single synthesis process.[5] DEL achieves this by attaching an identifiable strand of DNA to each ligand compound, splitting the sample, and modifying the ligand and DNA-strand before pooling the samples once again. The process can be repeated multiple times for an increasing number of unique compounds in the library. When the DEL library is screened, target bound ligand-DNA is separated from unbound ligand-DNA compounds and identified by decoding the DNA strand by e.g. Sanger sequencing or mass spectroscopy. In addition to combinatory libraries, custom libraries based on an initial screen with virtual libraries have become a viable option.[69]

2.1.2 Hit compound discovery

Hit compound discovery focuses on finding potential drug molecules and novel molecular structures based on their interactions with the target and effect on its modulation. An optimal hit compound leads to a desired effect on the target for diminishing the disease function and progression while having a minimal impact on normal biological functions. Hit discovery utilizes screening of molecular libraries to identify the hit compounds. As the libraries can span millions of molecules, high throughput screening (HTS) is utilized to accelerate the process and reduce overall costs. HTS operates by a combination of robotics,[70] computing,[71] liquid handling machinery[72] and highly sensitive readers, enabling the screening of a minimum of 10 000 samples per day.[73] Rapid HTS, also called ultra HTS, is capable of screening 100 000 samples in day.[74,75] The HTS format is mostly restricted to a microtiter plate format, with 384 or more wells per plate.[76]

In simple terms, HTS operates through an automated system that combines the reagents from stock plates into a test plate to perform the screening assay and observe the reaction with an automated detection device. From the results, the most interesting compounds, i.e. the initial hits, are selected based on their interaction with the target or effect in the assay. The initial hits are then rescreened under different conditions in multiple assays to ensure their effect on the target.[3,14] The assays utilized in hit discovery vary from whole organism *in vivo* assays to biochemical and cell based *in vitro* assays (**Figure 2**).[77] Although *in vivo* assays can provide highly accurate models of human morphology and physiology, they are rarely applied due to their relative complexity. However, zebrafish based methods have increased in popularity.[78] *In vitro* cellular assays and high content screening provide an opportunity to study the pharmacological activity of hit compounds and their influence on cell growth and proliferation. The effects of hit compounds on transcription and translation of proteins along with complex signaling pathways can be studied. Cellular assays mostly utilize a monolayer of viable cells in the assay test plate and screen the molecular libraries against multiple targets.[77,79–81] The biochemical assays, which are mainly used in classic small molecule drug design, focus on the interactions of screened ligands with purified target proteins or the effect of screened inhibitors on enzyme functions. These assays are popular due to their simplicity and often function in a competitive format in which the known ligand is displaced by the screened hit compound. The enzymatic assays often measure the activity of the enzyme in a non-competitive assay format. The monitoring of biochemical assays is mostly conducted optically via absorbance and luminescence, such as fuorescence.[77,82,83]

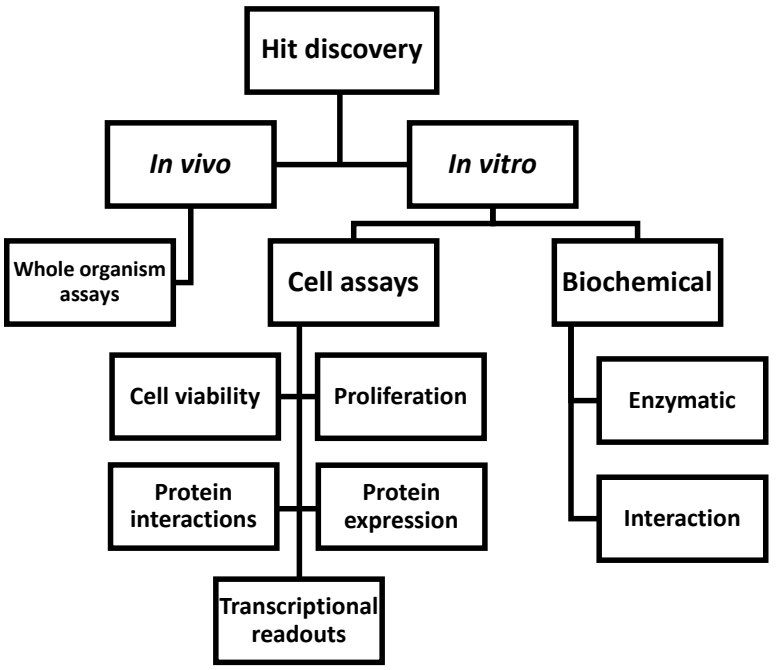

Figure 2. Assay types used in hit discovery. *In vivo* assays provide accurate models for human morphology but are less popular compared to simpler *in vitro* cellular and biochemical assays. Cell based *in vitro* assays focus not only on the effects of the screened compounds on the target biomolecule but also the whole metabolism and signaling of the cell. Biochemical assays are more focused and investigate specific interactions of target and screened ligands and the effects of ligands on enzymatic targets.

HTS continues to develop as robotics, computational power and assay methods advance aiming to reduce the costs and time consumption of screening millions of molecules.[3,14] Although the aim of HTS is to achieve low cost assays, e.g. ~0.1 dollar/assay, with increasing library sizes and multiple HTS rounds this may amount to millions. These costs highlights the importance of not only molecular library selection and focused library utilization but also the significance of cost effective assays for reduced hit discovery expenses. Thus developing new assays is of high interest for drug discovery.

For an assay to be suitable for drug discovery, it must be extremely reliable and robust with Z' factor (**Equation 1**) values over 0.5 and a coefficient of variation (%CV) (**Equation 2**) of under 10 %. Both Z' factor and %CV equations utilize standard deviations (σ) and mean values (μ) to evaluate the assay. Ideal assay also has a signal-to-background (S/B) ratio (**Equation 3**) of over 3 but, if the results have low variety values below 3 are acceptable. The assays must also be robust and allow slight changes to improve performance or convenience. For example, since most molecules in the libraries are stored in DMSO, the assay components must tolerate

at least 10 % DMSO.[15,76] In addition, for ease of automation, the assay must operate with as low a number of steps and reagents as possible. Thus, label-free and homogenous methods are most optimal, albeit they have lower sensitivity compared to heterogeneous assays with a labelled target.[84] Low sensitivity increases material consumption, costs, and can lead to other difficulties, such as solubility problems and spontaneous protein aggregation in biochemical assays relying on purified target proteins. Many biochemical assays are often designed for only a single target in some specific instance, which lowers their versatility.[3,14,85]

$$Z'factor = 1 - \frac{(3\sigma_{positive} + 3\sigma_{negative})}{|\mu_{positive} - \mu_{negative}|} \quad (1)$$

$$\%CV = \frac{\sigma}{\mu} \times 100\ \% \quad (2)$$

$$S/B\ ratio = \frac{\mu_{max}}{\mu_{min}} \quad (3)$$

2.1.3 Hit-to-lead, lead optimization and pre-clinical studies

The hit-to-lead process aims to produce optimal lead molecules by hit confirmation and expansion, which improve the potency and selectivity of the hit towards the target. The acquired lead compounds are optimized for improved efficiency and absorption, and preclinical investigation is performed to finalize safety for clinical trials.

During the first stage of hit-to-lead, hit confirmation, the hit compounds are retested to confirm their activity with the target and to establish an initial ranking based on their efficiency. The efficiency is determined by generating dose response curves and verifying the half maximal binding affinity (IC_{50}) and half maximal effective concentration (EC_{50}). Hit compounds presenting false positives, assay interference, aggregation, or other problems, such as intellectual property issues and toxicity, are excluded. Hit confirmation initially relies on the same primary assays as hit discovery, generating dose response curves and retesting hits to ensure that errors leading to false positives during hit identification are eliminated. Remaining false positives are cleared by biochemical or cell-based counter-assays, which do not contain the target molecule, and orthogonal secondary screening assays, which provide distinct output from the primary assay in different assay conditions. The cell based assays also investigate the cytotoxicity of hit compounds either alongside or after these assays. Finally the false positives are eliminated by differing secondary assay formats e.g. by cell based secondary assays if primary assay was biochemical.[4,7] The subsequent hit expansion step is used to screen analogues to determine structure-activity relationships (SAR) and find those with the highest selectivity and affinity towards the target and with lowest toxicity. Hit expansion

follows a design-make-test-analyze (DMTA) cycle, starting with hypothesis generation based on 3D models, existing SAR and ADMET data on similar compounds, and patents.[86,87] The designed hit analogues can be synthesized, or chemically modified from hit compounds to create derivatives or chosen from a library. The assays utilized during test phase mimic those in hit validation and the analysis creates new design hypothesis for another cycle. Careful analysis of unsuitable molecules can result in improvements in the next cycle.[3,4,8]

Lead optimization converts lead compounds to suitable candidates for pre-clinical evaluation. It focuses on solving ADMET deficiencies to ensure that the potential drug is absorbed and properly distributed to the site of action in body before effectively metabolized and excreted without toxic metabolites. During lead optimization the large-scale manufacturing issues, such as additional preservatives and other inactive ingredients, are also considered.[3,10] The optimization follows a DMTA cycle and begins with modification of the molecular structure of the lead compound based on desired properties.[86–88] The modifications are mostly carried out by organic synthesis or biotechnological methods, aided by *in silico* modeling, if the structure of lead and target are known. The modifications are studied initially with *in vitro* methods before performing *in vivo* tests, which especially target toxicology investigation. Orthogonal methods based on cells and animal models are used to mimic physiological conditions. Lead optimization results in hundreds of compounds for pre-clinical testing and provides an estimation of their priority.[9,89]

The main aim of preclinical testing is to ensure the safety of candidate drugs for clinical trials. The testing evaluates the pharmacokinetics and pharmacodynamics of candidate drugs and establishes safe doses for clinical trials. Pharmacodynamics focus on investigating the effect of the drug on the biological environment depending on the concentration, whereas pharmacokinetics observe how the drug is distributed and eliminated during metabolism. The pre-clinical tests are determined depending on the intended use of the candidate drug. For a typical drug, the tests include cell viability, proliferation, angiogenesis and apoptosis assays, along with *in vitro* permeability, toxicity and transporter testing and animal model studies.[90] Preclinical testing follows good laboratory practices (GLP), which define the minimum requirements for research including study conduct, equipment, protocols, reports and quality assurance.[91,92] Other regulatory aspects such as in International Organization of Standardization (ISO) quality management standards, animal ethic requirements and 3 R principle of reducing waste, reusing and recycling may apply as well. Adherence to these regulations is required for attaining approval for clinical trials, e.g. in the USA from the Food and Drug Administration (FDA). A complete clinical trial application (CTA) includes results and analysis of all pre-clinical studies and detailed plan on the clinical trial. Approval of CTA can take up to two years and FDA may request further investigation when necessary.

2.1.4 Clinical studies

Clinical studies investigate the efficiency and safety of the drug on human participants. The clinical trial is divided into four parts and adheres to the principles of ADMET. In the initial Phase I trials the safety of the drug is studied on under hundred healthy volunteers. In Phase II the efficiency of the drug on the targeted disease or condition is investigated with thousand patients suffering from the said disease condition. This phase focuses on the short-term effects of the drug on the patient's condition and if drug shows promise, preparations for the large-scale Phase III trial are initiated. In Phase III the proper dosage, administration and labeling instructions of the drug are determined. Possible interactions with other medication are also investigated and the overall benefit/risk ratio is determined. Other studies are also conducted, such as planning of full-scale production and testing required for drug approval application. In USA, this New Drug Application can run 100 000 pages, and more information may be requested before approval or rejection during two years.[93,94]

After approval and drug marketing, the Phase IV studies begin to investigate the long-term effect and efficiency of the drug. Since the drug is distributed to a large population of patients, the opportunities to study its effects increase. These studies often focus on complications, such as side effects and drug interactions, as well as investigations on the drug effects on specific subgroups of patients, such as patients suffering from other existing conditions such as diabetes. Organizations responsible for approving the drug also require updates and periodic reports about the process of the studies.[11–13]

2.2 Principles of quenching in photoluminescence

Luminescence is the emission of light in the ultraviolet, visible, or infrared region of the electromagnetic spectrum. The source of the released excess energy determines the luminescence type, which are described as photo-, cathodo-, chemi-, electro-, mechano-, radio- and thermoluminescence.[17] The focus of this thesis is photoluminescence, which refers to energy release due to photon absorption. The photo-, chemi- and mechanoluminescence also include subtypes. For photoluminescence these are fluorescence and phosphorescence, and their mechanisms will be further discussed in this chapter.[95–97]

Quenching of photoluminescence refers to decreasing the intensity of emitted photoluminescence. Quenching is categorized into dynamic and static quenching, and occurs mainly by the following mechanisms: intersystem crossing, Förster resonance energy transfer (FRET), Dexter interactions or electron exchange, and photoinduced electron transfer. Two examples of dynamic quenching, the quenching of fluorescent dyes by water and FRET, are examined in more detail during this chapter, as they are significant for the assays developed during this thesis.

2.2.1 Photoluminescence

Photoluminescence is a form of luminescence caused by electromagnetic radiation and photon absorption.[16,17] The electromagnetic radiation leads to photon excitation of electrons to higher energy level. These electrons return to the non-excited state through a relaxation processes and release part of the absorbed energy as photoluminescence emission. Photoluminescence can be described by the parameters of intensity, quantum yield and lifetime. The intensity of luminescence refers to the number of photons emitted, typically per second. This can vary significantly between various substances. Quantum yield (ϕ) compares the number of photons emitted to the number of photons absorbed (**Equation 4**). This observation provides an indication of the proportion of the energy lost in a non-emitting form and the efficiency of the luminescence. The quantum yield can be defined by the decay of the excited state, where k_f is the rate constant for spontaneous emission of radiation and $\sum_i k_i$ is the sum of all rates of excited state decay. The-$\sum_i k_i$ term includes the decays not related to emission, such as dynamic quenching and non-radiative relaxation.[17,18] The fluorescence lifetime refers to the time the exited electron spends in the higher energy level before emission (**Equation 5**). This often follows first-order kinetics, where $[S_1]$ refers to the concentration of exited molecules at the timepoint t and $[S_1]_0$ to the concentration at ground state. Γ refers to the decay rate which is the combination of non-radiative Γ_{nrad} and radiative Γ_{rad} decay rates (**Equation 6**).[17,98]

$$\Phi = \frac{k_f}{\sum_i k_i} = \frac{Photons\ emitted\ (count)}{Photons\ absorbed\ (counts)} \quad (4)$$

$$[S_1] = [S_1]_0 e^{-\Gamma t} \quad (5)$$

$$\Gamma_{tot} = \Gamma_{nrad} + \Gamma_{rad} \quad (6)$$

Multiple forms of photoluminescence exist and to describe and distinguish them the Jablonski diagram is often employed (**Figure 3**). Jablonski diagram visualizes the electronic states of the photoluminescent molecule.[17,98,99] The photoluminescence is initiated when a luminescent molecule absorbs electromagnetic radiation. This absorption of energy excites an electron of the molecule from the ground state (S_0) to an excited singlet state, such as S_1 or S_2 (**Figure 3**). In the case of fluorescence, the electron relaxes back to the S_0 through electron relaxation, which generally has a lifetime of around 10 ns. Compared to fluorescence, phosphorescence has a much longer lifetime, typically on the millisecond scale. This is the result of the intersystem crossing of the electron from the S_1 state to the excited triplet state T_1 (**Figure 3**). During this intersystem crossing, the spin of the exited electron reverses leading to the excited electron at T_1 having a spin of the same direction with the electron at ground

state S_0. The transition from T_1 to S_0 is forbidden due to the spin symmetry of the electrons. Thus the spin must reverse before the excited electron can relax to S_0 and emit phosphorescence. For this reason, the T_1 is sometimes called the forbidden state. In specific cases, when the spin of the exited electron at T_1 reverses, it returns to S_1 before relaxing to S_0 resulting in delayed fluorescence (**Figure 3**).[17,100]

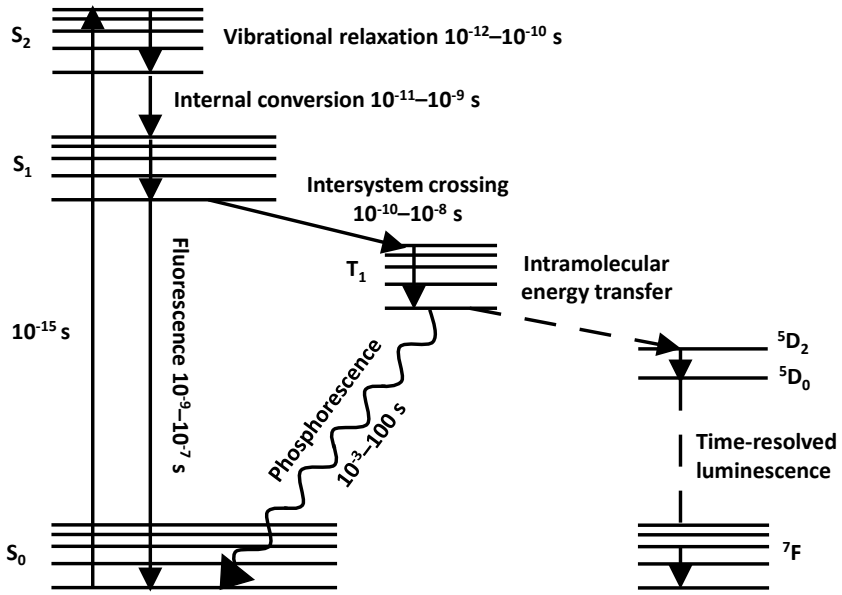

Figure 3. This Jablonski diagram describes three types of photoluminescence processes; fluorescence, phosphorescence and time-resolved luminescence (TRL). For these types, the process of initial excitation is identical; photon absorption excites an electron from ground state to the excited singlet state S_2 and it relaxed to S_1 through vibrational relaxation and internal crossover. In the case of fluorescence, the electron relaxes from S_1 to S_0 and emits the released energy with a general lifetime of 10 ns. For phosphorescence and TRL, the electron shifts from S_1 to the triplet state T_1 by intersystem crossing. Relaxation from T_1 to S_0 results in phosphorescence emission, which has an average lifetime between 1 and 10 ms. For TRL, an intramolecular energy transfer occurs from the excited organic chelate to the emitting lanthanide ion, resulting in the relaxation of chelate and excitation of a lanthanide ion electron to ^5D. TRL is emitted when the excited electron relaxes to ^7F and has a lifetime of between 1 and 0.1 ms.

Photoluminescence measurements can be classified as steady-state and time-resolved measurements. The more commonly used steady-state measurements are performed with continuous exposure to light and recording of the emission. Steady-state measurements are most suitable for fluorescence due to its nanosecond timescale. Time-resolved measurements record the decay of the photoluminescence after excitation by a brief pulse of light. Time-resolved measurements provide more information than steady-state measurements, which only present an average of the time-resolved decay. Time-resolved measurements can distinguish two fluorophores with similar spectral

information on the basis of their decay times, and monitor the luminescence of the target fluorophore after background autofluorescence has ceased. The latter type of "time-domain measurements" do not technically monitor decay time. Instead, a steady-state intensity measurement of time-resolved luminescence (TRL) is performed after the excitation pulse (**Figure 4**). In most cases the intensity is measured after an initial delay of hundreds of microseconds, during which the background luminescence decays, and as a several hundred microseconds long measurement window. This cycle of excitation, delay and monitoring is performed multiple times to observe an average value of the intensity during the measurement window. TRL monitoring uses mostly lanthanides such as terbium (Tb^{3+}) and europium (Eu^{3+}) exited through organic chelate, since the lanthanides have weak absorption properties. The energy absorption of the organic chelate excites an electron from S_0 to T_1 before the energy is transferred to the lanthanide through intramolecular transfer. The lanthanides emit by forbidden transitions involving 4f orbitals from ^7F to ^5D (**Figure 3**). This leads to the aforementioned low absorption properties and long lifetime of the lanthanide chelate TRL emission.[17,19–21]

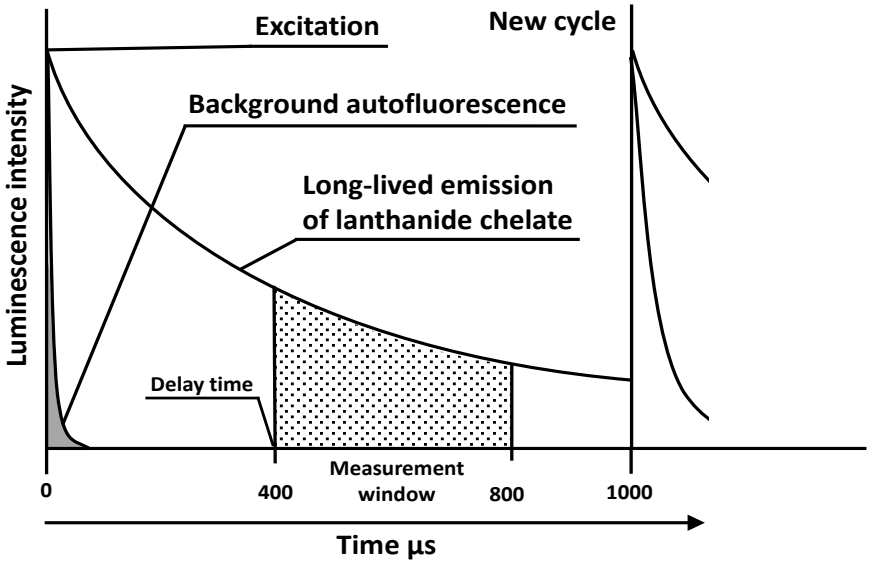

Figure 4. The timescale of TRL monitoring. During TRL monitoring the short-lived background signal, consisting mainly of environment emission of the assay plate and assay components, decays faster than the long-lived emission of lanthanide chelates. This property enables the monitoring of TRL after several hundred µs when the since decayed background emission will not interfere in the measurement window. This will enhance observed S/B ratio and improve the reliability and sensitivity of the method.

During the photoluminescence process, some of the absorbed energy is released as measurable radiative emission. The remaining energy is released in non-radiative forms, mainly through internal conversions as well as vibrational and rotational

relaxation.[17,98,101] During internal conversion, the electron rapidly relaxes from a higher to lower electronic state, such as from S_2 to S_1 or from S_3 to S_1, in a picosecond timescale (**Figure 3**). In addition to these non-radiative energy release processes, solvent relaxation, energy transfer, and rotational relaxation can decrease the energy released. The non-radiative energy loss between excitation and emission is visible in the spectrum of the molecule as Stokes shift (**Figure 5**). Stokes shift refers to the fact that the peak of the excitation spectrum is monitored at lower wavelength compared to the peak of the emission spectrum due to the energy loss between excitation and emission. The emission occurs at a higher wavelength since the energy levels decrease as the wavelength increases.[17,102] Depending on the non-radiative energy loss, the luminescent molecules have different levels of Stokes shift, e.g. fluorescein and Cy5 have Stokes shifts of 24 nm and 19 nm, respectively.[103,104] Lanthanide chelates also have large differences between their excitation and emission wavelengths, e.g. 350 nm with Eu^{3+}-chelates.[105] Stokes shifts are affected by environmental conditions, such as solvent polarity, which may lead to an increased Stokes shift. A larger difference between excitation and emission peaks is a useful phenomenon for sensitive fluorescence detection, as emission wavelength can be readily separated from excitation, preventing interferences and improving multiplexing possibilities.[106,107]

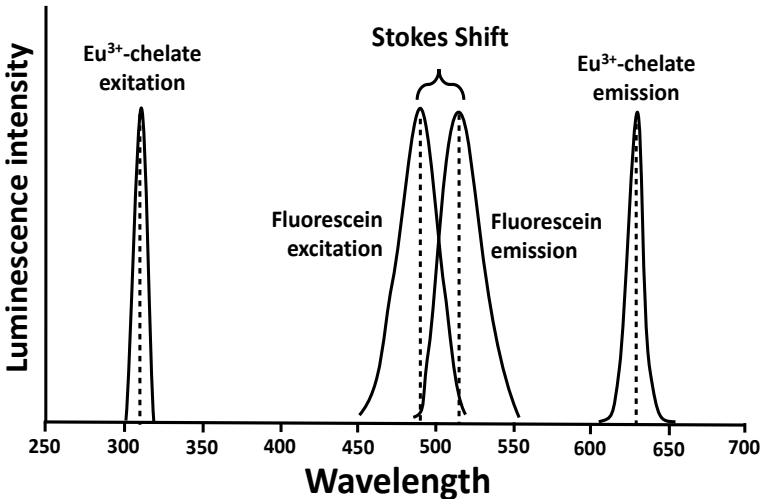

Figure 5. The difference between excitation and emission wavelengths of luminophores are distinct for individual molecules. The emission wavelength of luminophore is higher compared to the excitation wavelengths since excitation requires more energy than what is released during emission. The energy loss is due to non-radiative forms of energy release, such as internal conversion and vibrational relaxation, occurring prior to emission. The difference between the excitation and emission wavelengths of molecule is called Stokes shift. For example, fluorescein has an average Stokes shift of 25 nm, whereas the difference between excitation and emission of Eu^{3+}-chelate is approximately 350 nm. Stokes shift can be affected by the polarity of the surrounding environment, as more polar environments lead to increased Stokes shift.

2.2.2 Quenching of photoluminescence

Quenching of photoluminescence refers to a process where the intensity of photoluminescence emission is decreased. It is categorized into dynamic and static quenching and occurs via variety of mechanisms like intersystem crossing, dexter interaction, FRET, and photoinduced electron transfer (PET). During this chapter, the differences between the two quenching categories are considered along with two examples of dynamic quenching: FRET and the quenching effect of water, as these mechanisms are important background in this thesis for the method development.

Photoluminescence quenching can be categorized into two types: dynamic and static quenching (**Figure 6**).[17] Dynamic quenching is caused by collision of excited luminescent molecule and the quencher. During dynamic quenching, the excited luminescent molecule returns to the ground state without photon emission as a result of molecular collision and interaction with the quencher. This interaction can be e.g. electron or energy transfer. In static quenching, a complex is formed between a luminophore and a quencher before the excitation occurs. This complex is non-luminescent as the energy of the excited state is completely released in non-radiative forms, when the quencher is bound to the luminophore.[17,22]

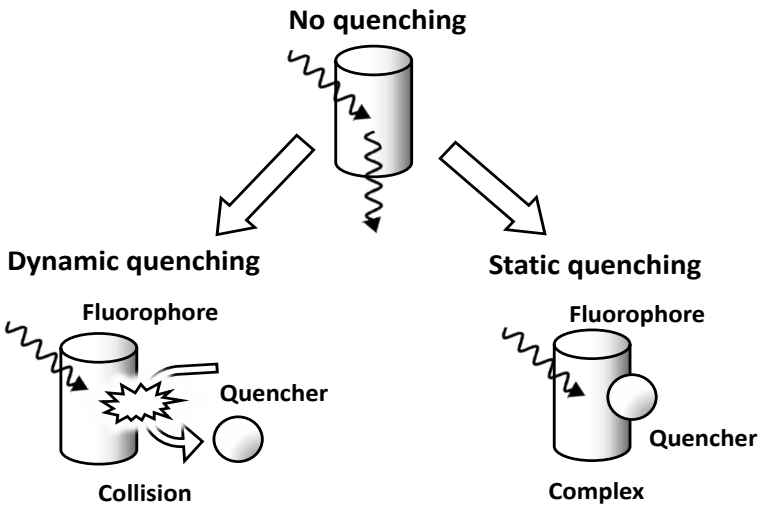

Figure 6. Principles of the dynamic and static quenching. Dynamic quenching occurs through molecular collision of the fluorophore and quencher after excitation, and excitation energy is transferred to the quencher. The collision results in the fluorophore returning to ground state without photon emission. In static quenching a complex of fluorophore and quencher is formed before excitation. This complex is non-luminescent and has unique absorption spectrum. The excitation energy absorbed by the complex is released in non-radiative forms such as heat.

Multiple mechanisms of quenching exist, such as intersystem crossing, electron exchange or dexter interaction, FRET, and photoinduced electron transfer (PET). These mechanisms can be roughly categorized into dynamic type intersystem crossing, dexter interaction, and FRET and static quenching type PET.[17] Intersystem crossing occurs when the luminophore encounters a heavy atom, such as a halogen or triplet oxygen molecule, which causes the transition from singlet state to a triplet state. The long lived triplet state is quenched by the same quencher or relaxes to the ground state by non-radiative decay.[17] Quenching by dexter interaction occurs between donor and acceptor when the excited electron in the lowest unoccupied molecular orbital (LUMO) of the donor is transferred to the acceptor. Simultaneously another electron is transferred from the highest occupied molecular orbital (HOMO) to the donor. This electron exchange process results in transferred energy from the donor to acceptor thus quenching the donor. The electron exchange depends on the spectrum overlap and short distance, generally under 10 Å ,between donor and acceptor.[17] FRET functions similarly to dexter interaction between donor and acceptor but energy is transferred instead of an electron. As energy is transferred the excited donor returns to HOMO from LUMO and an electron of acceptor is excited to LUMO from HOMO.[17] In PET the electron donor and acceptor form a complex that can return to ground state through non-radiative relaxation. During the complex formation, an electron from the donor is transferred to the acceptor and returns after relaxation and the complex is disrupted. The molecule excited in PET can either be the electron donor or acceptor, but the latter is more common.[17] These quenching mechanisms are often difficult to distinguish and they are not mutually exclusive.[17]

The Stern–Volmer equation describes the process of quenching (**7**). In the equation, F_0 and F describe the fluorescence intensity in the absence and presence of quencher, respectively. The Stern–Volmer quenching constant, $K_{SV,}$ indicates the sensitivity of luminophore towards the quencher, whereas the bimolecular quenching constant k_q refers to the accessibility of luminophores to the quencher, which affects the efficiency of the quenching. In the case of dynamic quenching, the K_{SV} is replaced by K_D. The [Q] reports the concentration of the quencher and τ_0 indicates the lifetime of the luminophore without quencher. When plotted the equation yields a linear plot as the effect of quencher is concentration dependent.[17,108–110]

$$\frac{F_0}{F} = 1 + k_q\tau_0[Q] = 1 + K_{SV}[Q] \quad (7)$$

The Stern–Volmer plot is not suitable for differentiating between dynamic and static quenching, since both types yield linear plots. Instead, these two quenching types are distinguished by the lifetime of the excited state of luminophore. Only dynamic quenching increases the decay of the observed luminescence, since it is a rate

process, which affects the whole population of excited luminophores. This is observed as shortening of lifetime. With static quenching this cannot be observed, since only the lifetime of non-quenched luminophores is measured as the complex formation prevents all emission from quenched luminophores. Static and dynamic quenching can also be differentiated by the absorption spectrum of the luminophore. Static quenching perturbs the luminophore spectrum when dynamic quenching has no effect on it (**Figure 7**). It is also possible for a single quencher to affect the luminophore by both quenching mechanisms. In such a case, the dynamic quenching can still be monitored and differentiated by lifetime measurements.[17,23]

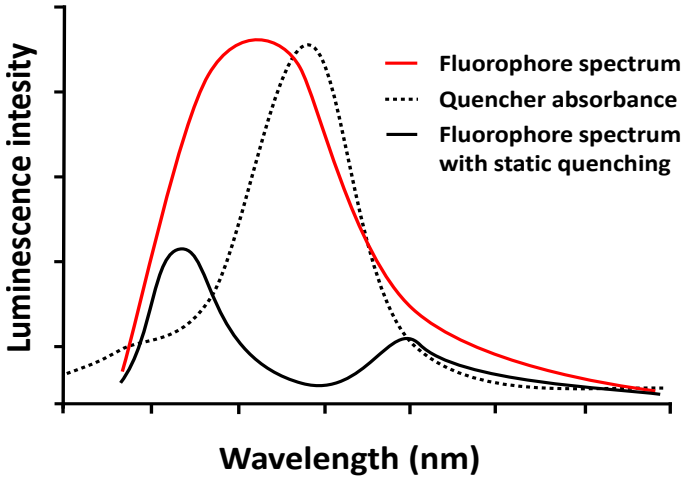

Figure 7. Static quenching complex formation affects the spectrum of the quenched luminophore. The spectrum of luminophore is affected by the complex formation with the quencher during static quenching. The spectrum of the complex becomes perturbed as the monitored maximum intensity peaks decrease and shift. Such disturbance is not present in spectrum during dynamic quenching and can be utilized to distinguish between dynamic and static quenching.

Most quenchers release the energy that they have received from the luminophore as light and thus are luminescent. Some quenchers are non-fluorescent and release the excitation energy through other means such as heat. These dark quenchers can be utilized in assays where the fluorescence of conventional quenchers interferes with the emission of other molecules. Dabcyl is an example of a dark quencher with an absorption maximum at 454 nm without measurable emission. As a quencher Dabcyl has high efficiency but requires close contact (**Table 1**).[111] Black hole quenchers, which are capable of quenching across the whole visible spectrum, are especially common in assays. The black hole quencher BHQ-1 has similar functionality with Dabcyl but requires even closer contact with the quenched luminophore. Both these quenchers utilize a static quenching mechanism.[112] Quenchers that release their

excess energy as a photon are more common. For example, the dyes Cy5 and Alexa Fluor 680 absorb energy through FRET from the donor simultaneously quenching it. Compared to Dabcyl and BHQ-1, the Cy5 and Alexa Fluor 680 are less efficient quenchers but function from longer distances from the luminophore as they utilize FRET based quenching (**Table 1**).[17,113–115] All the mentioned quencher examples are organic molecules but inorganic quenchers, such as quantum dots (Qdot), graphene, and carbon nanotubes also exist and are applicable.[116–119]

Table 1. The structure and specifications of four organic quenchers: Dabcyl, BHQ-1, Cy5 and Alexa Fluor 680.[120,121]

Name	MW (Da)	Absorption maximum (nm)	Emission maximum (nm)	Quenching efficiency (%)	Förster radii (Å)
Dabcyl	366	454	No emission	90[a]	9.3[a]
BHQ-1	554	534	No emission	96[b]	2.6[b]
Cy5	792	646	670	67[a]	56[a]
Alexa Fluor 680	643	679	702	78[a]	57[a]

Dabcyl **Black Hole Quencher 1**

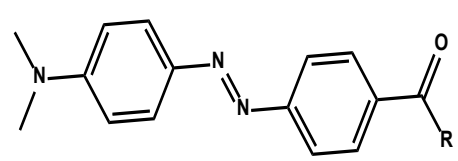

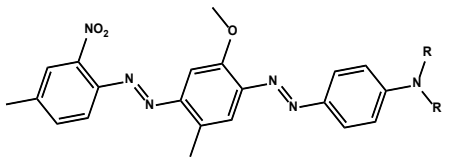

Cy5 **AlexaFluor 680**

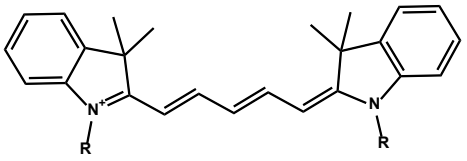

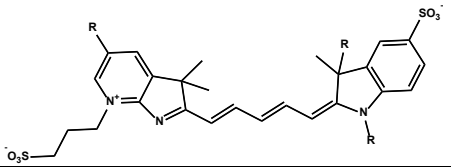

a The values were obtained with Eu^{3+}-chelate as donor.
b The values were obtained with fluorescein as donor.
* The R of the molecular structure refers to different structures depending on the quencher. The structure is employed for reactions e.g. conjugation.

Photoluminescence quenching via energy transfer: Another dynamic quenching mechanism called FRET depends on the proximity of the donor luminophore and acceptor quencher, their spectral overlap, and dipole orientation.[17] Typically, most quenching methods are dependent on the close distance (generally 10 Å) between the luminophore and quencher. This molecular contact may be in the form of either complex formation, as in static quenching, or diffusive encounter, as in dynamic quenching. The quenching efficiency is thus affected by factors influencing the

molecular contact probability, such as steric shielding and solvent viscosity. FRET is a dynamic method that functions over longer distances of generally 10-100 Å between the luminophore donor and quencher acceptor. This effect is observed in the differences between the Förster radii of static quenchers Dabcyl and BHQ-1 and FRET acceptors Cy5 and Alexa680 (**Table 1**). The distance between the donor and acceptor (r) affects the efficiency of FRET (E) with an inverse 6th-power law, where R_0 refers to the distance of donor-acceptor pair at 50 % efficiency (**Equation 8**).[17,24–26]

$$E = \frac{1}{(1+r/R_0)^6} \quad \textbf{(8)}$$

For FRET to occur the emission spectrum of the donor must typically overlap with the absorption spectrum of the acceptor and an increased overlap leads to a higher likelihood of FRET. FRET occurs after excitation of the donor has elevated an electron of the donor from HOMO to LUMO. The energy transfer leads to the return of this electron to the HOMO along with the elevation of an acceptor electron to excited state. When the excited electron of the acceptor returns to the ground state, the energy is released as non-radiative heat or measurable emission. Since the energy of the donor is transferred to the acceptor, the luminescence intensity of donor decreases and quenching occurs.[17]

The properties of the donor and acceptor affect the emission spectra obtained after FRET has occurred. If FRET is prevented, e.g. with an increased distance between the donor and acceptor, only donor emission is monitored regardless of acceptor properties (**Figure 8**). Low emission is also monitored from both donor and acceptor when dark quenchers function as acceptors. In situations like this, the excess energy initially absorbed by donor and transferred to acceptor is released in non-radiative forms. FRET generally results in high acceptor emission and lowered emission of the donor, as most acceptors are luminescent. FRET is also suitable for donors with long emission life-times enabling time-resolved FRET (TR-FRET) measurements. Long-lived excitation properties of donor lead to energy transfer to the acceptor thus resulting in long-lived emission.[17,24–26]

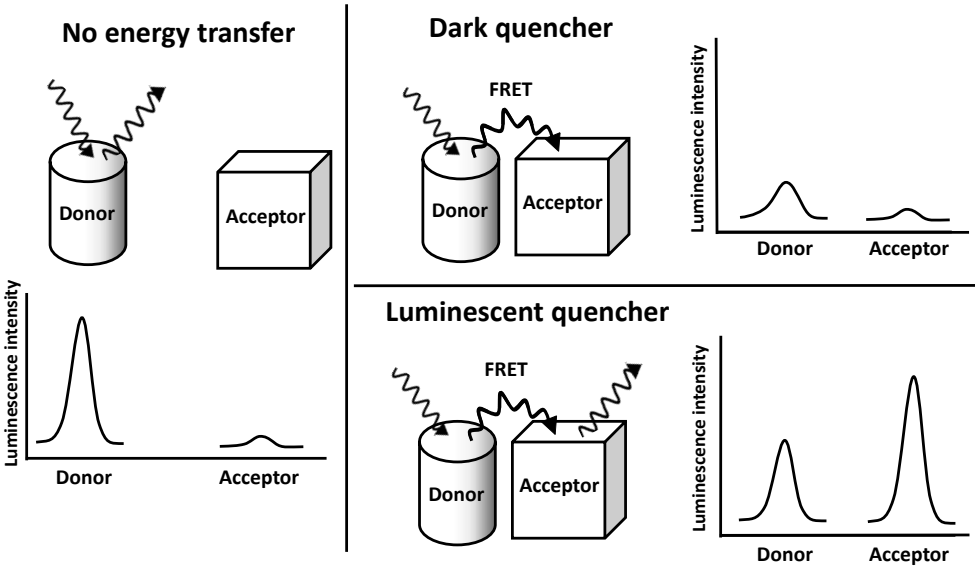

Figure 8. Types of FRET mechanisms. Energy transfer between the donor luminophore and acceptor quencher is the basis of dynamic quenching, FRET. The energy transfer between donor and acceptor requires close molecular contact of generally 10-100 Å. The acceptor of the energy transfer functions either as a non-luminescent dark quencher or a luminescent quencher. In the case of a dark quencher, the energy transfer is monitored as the emission decrease of the donor luminophore, whereas energy transfer to the luminescent quencher is measured as the emission increase of the acceptor. Most methods rely on the latter acceptor monitoring as the emission increase is often more distinct than the decrease of the donor emission.

Photoluminescence quenching via water: The quenching properties of water were first discovered with fluorescent dyes containing aromatic amino groups. Such fluorescent dyes, e.g. SYPRO Orange, 1-anilinonaphthalene-8-sulfonate (1,8-ANS), and 2-toluidinonaphthalene-6-sulfonate (2,6-TNS), have low fluorescence yields in aqueous solutions, which are greatly increased when proteins were added to the solution (**Figure 9**).[122] It has been shown that 42 of the recommended common organic labelling fluorophores are quenched by water.[32] This increase in fluorescence was affected by the concentration of added protein and its structural changes, such as denaturation, which enabled the use of water quenched fluorescence probes for studying structural properties. In addition to extrinsic dyes, the intrinsic fluorescence of many proteins, such as green fluorescent protein (GFP) and proteins containing L-tryptophan, are quenched when they come into contact with water. Additionally, fluorescent labels such as Mant and BODIPY, which are used for ATP and GTP labeling, are sensitive to the environmental quenching in aqueous solutions.[123–125] The exact mechanisms of the quenching properties of water are still debated but have been attributed to the effects of solvent polarity and transfer of electrons and protons.[31,32]

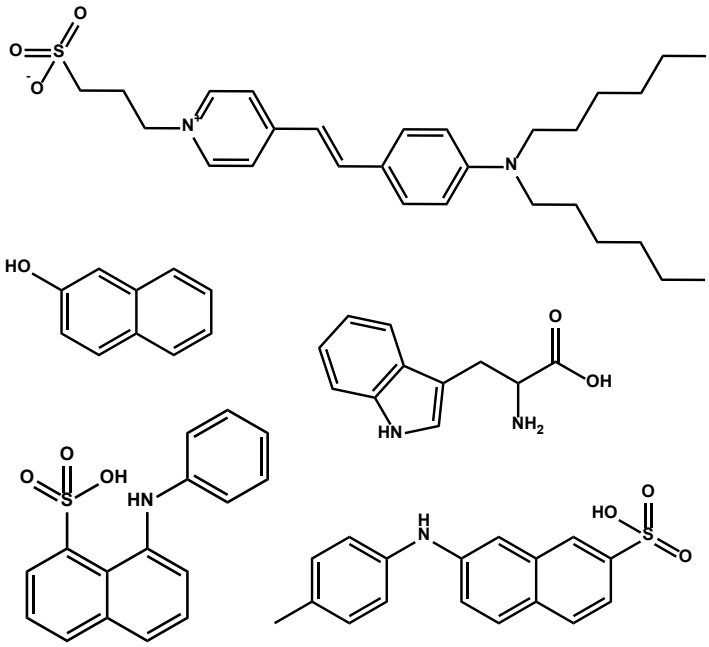

Figure 9. Examples of fluorescence dyes quenched by water. The principle of fluorescent dye quenching via water is debated to occur due to the polarity of aqueous solution or electron or photon transfer. The quenching occurs via interaction of water with either the aromatic amine group, e.g. in SYPRO Orange, 2,6-TNS and 1,8-ANS, leading to electron transfer or aromatic hydroxyl group, like in the case of 2-Napthol leading to proton transfer. Additionally to these extrinsic fluorescence dyes, the intrinsic fluorescence of L-Tryptophan residues is quenched in aqueous solution.

The high polarity of water facilitates an intramolecular charge transfer, which lowers the energy of singlet excited state and thus alleviates the transition to triplet state for quenching. This transition is likely a result of an aromatic acid group turning out from the plane of an aromatic ring, called the twist-conformation.[126] For example, the dye 1,8-ANS has a low emission in water, which increases in aprotic organic solvents and alcohol. The polarity offers only a partial explanation as the organic solvents and alcohol should have sufficient polarity for the intramolecular charge transfer.[31]

Another hypothesis for the mechanism of water quenching relies on electron or proton transfer from the fluorescent dye to water. In the case of electron transfer, the aromatic amino group of the dye is surrounded by cluster of three or four water molecules. Formation of the water molecule cluster is enabled by hydrogen bonding. The bonds are strengthened by the transition of the fluorescent dye to an excited state, which leads to electron transfer from the amino group to the water molecule cluster and quenching.[31,126] The second potential mechanism, proton transfer, requires transfer of an aromatic hydroxyl group, like that present in 2-napthol, **(Figure 9**). The excited state of 2-napthol results in proton transfer from the hydroxyl

group to a water molecule, which results in quenching of the 2-napthol emission.[17,31,127]

2.3 Application of photoluminescence quenchers in homogenous assay formats for protein investigation

Photoluminescence based methods are common in drug discovery processes, as their detection principles are simple, reliable, sensitive and applicable to HTS format. In many of these methods, quenching has an important role for improving detectability and minimizing false positives. Additionally, some methods monitor the emission of the quencher instead of the emission decrease of the quenched luminophore. The methods discussed in this section are of importance in the context of the methods developed during the studies presented in this thesis. The methods utilize FRET and the quenching effects of water for investigating proteins and their interactions and digestion in a homogenous microtiter well-plate format. Luminescence emission monitoring with standard plate readers is adequate for typical measurements, but increased performance may be obtained with more specific instrumentation.

2.3.1 Assays utilizing FRET

Assays utilizing the dynamic quenching mechanism of FRET between the luminophore donor and the quencher acceptor are one of the most popular and well-established methods in drug discovery nowadays. Methods monitoring the emission of the quencher acceptor are more popular than those monitoring donor luminophore emission. Depending on the type of donor and acceptor labels, FRET methods are performed with either steady-state or time-resolved measurements. Time-resolved FRET methods are significantly more popular due to their higher sensitivity and robustness. There are many commercial FRET methods available for variety of purposes, some of which are discussed in this chapter.

Steady-state FRET assays usually monitor the signal of extrinsic labels that are conjugated to the biomolecule analyte. In most cases the monitored signal is obtained from the luminescence emitted by quenchers acting as acceptors. Z'-LYTE monitors the extrinsic fluorescence of the acceptor and donor at different wavelengths thus providing the ratio between phosphorylated and non-phosphorylated molecules.[128–130] Exceptions to the extrinsic acceptor monitoring, such as monitoring the decrease of intrinsic emission of protein acting as donor, have also been employed. For example, donor protein tryptophan residues have been utilized for studying the conformation distribution of the prion protein repeat system with acceptor dansyl group attachments.[131]

The commercial Z'-LYTE assay was developed for monitoring kinase activity for screening and profiling purposes. The Z'-LYTE assay is initiated by a kinase reaction, which results in the phosphorylation of a tyrosine or serine/threonine residue of the labelled substrate peptide. The secondary reaction occurs in the development solution containing a site-specific protease. This cleaves all the non-phosphorylated substrate peptides, while the phosphorylated substrate remains uncleaved as the phosphate group obscures the cleavage site. The intact substrate peptides retain their ability for energy transfer between their donor (coumarin) and acceptor (fluorescein) labels, and thus the fluorescence emission of acceptor is monitored at 535 nm. The FRET is prevented as cleavage separates the labels of non-phosphorylated substrate peptide thus resulting in donor emission at 460 nm (**Figure 10**). The Z'LYTE assay monitors the kinase activity as ratio of the emissions monitored at 460 nm/ 353 nm thus enabling kinase inhibitor and activator screening along with kinase profiling.[128–130] Z'LYTE has μM level sensitivity with broad coverage of kinases and quantitative capabilities. Unfortunately, since it is based on a protease caspase, the screened molecules must not influence the activity of the studied caspase. Z'-LYTE also requires hours of incubation and involves a two-step protocol, which complicates its suitability for automation.[128,130]

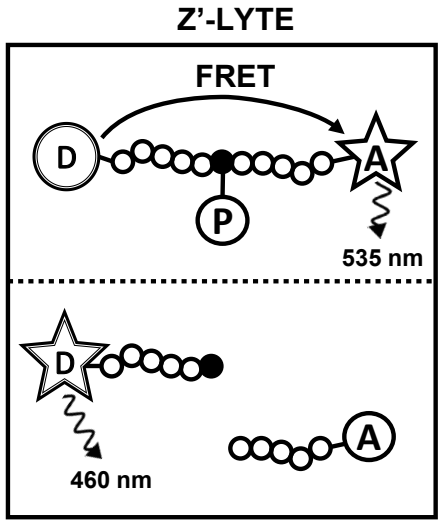

Figure 10. Principles of the steady-state FRET method, Z'-LYTE. The Z'-LYTE method provides the ratio of acceptor and donor emissions as a measure of the phosphorylation activity of a kinase. Phosphorylation of the substrate peptide linking the donor and acceptor labels prevents the peptide cleavage during the development reaction thus keeping the donor and acceptor in close proximity and resulting in FRET. The FRET increases the acceptor emission at 535 nm. In the case of an inactive kinase, no phosphate group obscures the cleavage site during development reaction and the substrate linker peptide is cleaved by a site-specific protease. This cleavage prevents FRET and results in a high donor emission at 460 nm. The activity of the kinase is then monitored as the ratio of 460nm/ 535nm.

Time-resolved monitoring is significantly more popular compared to steady state FRET assays. TR-FRET assays employ lanthanide chelates or cryptates as donors to yield acceptor emission with increased lifetime. The longer lifetime enables time-resolved monitoring, which leads to a decrease in the background luminescence, removing false-positives and improving the signal-to-noise ratio and sensitivity. The increased sensitivity enables superior miniaturization, with the requirement of less assay components improving cost effectiveness. TR-FRET assays mainly focus on monitoring the acceptor luminescence, like the commercial methods LANCE, HTRF, LanthaScreen and IMAP, but a few methods also measure donor luminescence, such as Trupoint.[132–138]

The traditional LANCE and HTRF assays require two separate antibodies labelled with a donor and acceptor, which bind to separate sites of the analyte. The binding brings the antibodies to close proximity thus enabling energy transfer between the donor and acceptor labels and resulting in measurable acceptor emission (**Figure 11A**). These TR-FRET assays are suitable for a variety of analytes, such PLIs, PPIs, antibody interactions, and enzyme substrates for activity studies of, e.g. kinases and proteases. The main difference between LANCE and HTRF is the donor label. The HTRF assay uses lanthanide cryptates instead of the lanthanide chelates used in LANCE. Compared to chelates, the cryptate structure increases the tolerance of the assay to chemical conditions, such as divalent cations (Mn^{2+}) and chelating agents, e.g. ethylenediaminetetraacetic acid (EDTA), which increase the dissociation of lanthanide chelates. Thus lanthanide cryptate emission persists longer compared to lanthanide chelates, and the HTRF assays are suitable for wider range of buffer compositions with increased sensitivity and robustness.[29,139] LANCE assay mechanism features an acceptor labelled peptide with another site for phosphorylation. When phosphorylation occurs, the donor labelled antibody is bound to the acceptor labelled peptide and energy transfer occurs. Thus, by monitoring the acceptor signal, the phosphorylation rate of the peptide can be monitored (**Figure 11B**).[137,138] The IMAP assay is designed for detecting kinase, phosphatase and phosphodiesterase activity. In the assay, the IMAP binding reagent brings the phosphate-linker, sensitizer-Tb^{3+} donor complex together with acceptor labelled phosphorylated peptide. When no phosphorylation occurs the binding reagent is unable to interact with the acceptor labelled peptide, and thus no acceptor signal is detected (**Figure 11C**).[135,136]

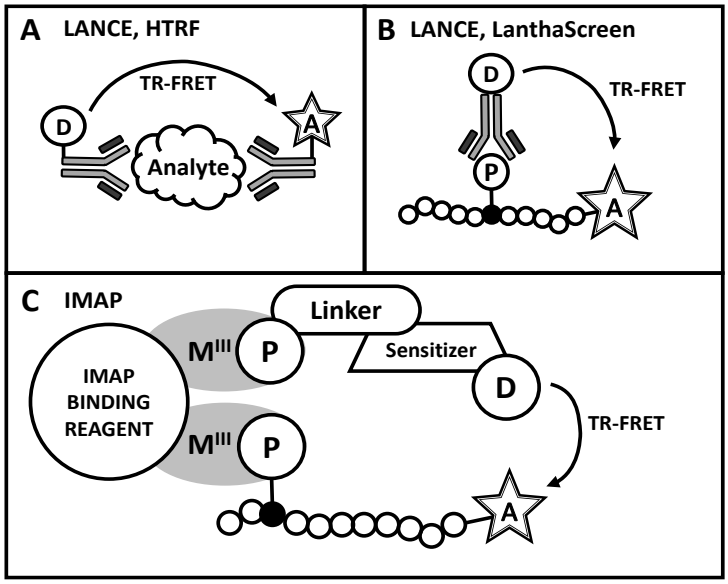

Figure 11. The principles of LANCE, HTRF, LanthaScreen, and IMAP are based on TR-FRET, i.e. the combination of TRL and FRET. **A**) The analyte, such as protein-protein interaction, is detected through two distinct antibodies labelled with a FRET donor or acceptor. Depending on the platform, these labels are different even if the principle remains the same. **B**) The LanthaScreen and some LANCE assays function by monitoring the TR-FRET between donor labelled antibody and acceptor labelled peptide. Increased TR-FRET is detected when the peptide is phosphorylated. **C)** The IMAP system monitors the phosphorylation of the acceptor labelled peptide by measuring the TR-FRET signal. The IMAP binding reagent brings the phosphate-linker-sensitizer-donor complex close to the acceptor-peptide when the peptide is phosphorylated.

These TR-FRET methods have a nanomolar level detection limit for interacting targets. They are selective and robust with low false positive and negative counts. Lance, HTRF, LanthaScreen and IMAP can study a multitude of targets, such as enzymes and protein interactions, and they are suitable for immunoassays and cell lysate samples. The main difficulties encountered by Lance, HTRF, and LanthaScreen arise from the requirement of specificity for the often used antibodies towards the chosen analyte. Additionally, assays featuring two antibodies also suffer from the hook effect. The latter occurs when a high concentration of analyte decreases the effectiveness of immune complex formation. This is due to the two antibodies not binding with the same analyte simultaneously. This mostly leads to false negatives or lower readings with single-step sandwich immunoassays.[132–138,140,141] In contrast to acceptor monitoring TR-FRET assays, the Trupoint assay monitors the decrease of donor luminescence function by the caspase activity, which cleaves the labelled substrate peptide and prevents the energy transfer between the donor and acceptor. The caspase activity thus results in increased donor emission and enables caspase ligand screening. Trupoint is also suitable for studying helicase

studies via sensory DNA. Unfortunately Trupoint requires higher µM level substrate concentrations, when compared to acceptor based TR-FRET assays [133,142]

TR-FRET assays have also been developed for studying receptor-ligand binding interactions in living cells, such as Tag-lite and quencher mediated resonance energy transfer (QRET) (**Figure 12**). Tag-lite is based on cloning the G protein-coupled receptor (GPCR) into a plasmid with a selection marker and transfecting the plasmid into a cell line. This selection marker expressed on the surface of the cell is then labelled with TR-FRET donor cryptate before addition of acceptor labelled ligand molecule. This ligand-acceptor binds to the GPCR, which brings it close to the donor. This initiates energy transfer, which allows the monitoring of acceptor signal. When the studied GPCR binding ligand is added it replaces the ligand-acceptor. This prevents the energy transfer and the acceptor signal decreases (**Figure 12**).[30,143,144] The assay has also been modified for screening ligands for ligand-gated ion channel ligands.[145] Tag-lite is suitable for kinetic studies for both rate of association and dissociation. As a TR-FRET based method, Tag-lite is sensitive and requires only small concentrations of labelled ligands. The drawbacks of Tag-lite include the required cloning and transfection, as well as modifications to the labels for each individual GPCR. [30,143,144]

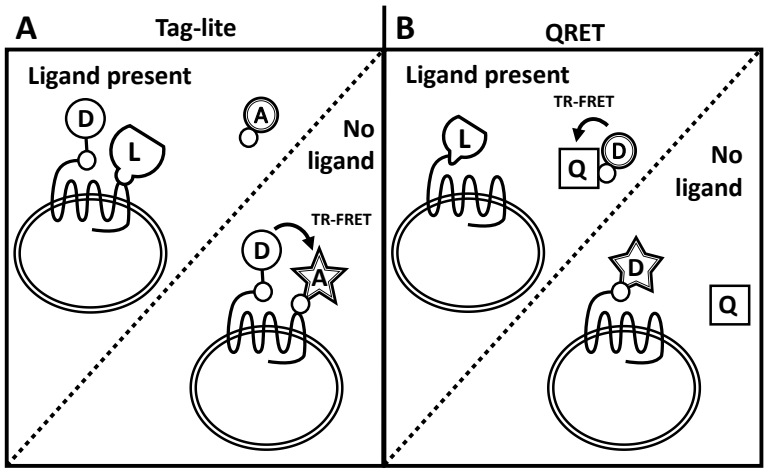

Figure 12. Tag-lite and QRET are designed to monitor ligand binding to GPCRs in living cells. **A)** The Tag-lite method initially clones selection marker containing GPCR protein into plasmid and transfects the plasmid to living cell line. The GPCR is the expressed on the cell membrane and labelled with FRET donor cryptate. In the presence of ligand the TR-FRET acceptor is unable to interact with the GPCR thus no acceptor emission is detected. When no ligand obscures the GPCR binding site for the acceptor it comes to proximity with the donor and TR-FRET occurs and increased acceptor emission can be monitored. **B)** The QRET method utilizes soluble quencher as TR-FRET acceptor. In the presence of GPCR ligand low donor emission is monitored it is quenched by the soluble quencher acting as TR-FRET acceptor. When no ligand is bound to GPCR the ligand labelled donor interacts with the membrane protein and is protected from the quenching effect of the TR-FRET acceptor.

QRET is a single label TR-FRET method that was developed for monitoring ligand binding to a GPCR called β2-adrenoreceptor (β2AR) in living cells. In the presence of the β2AR ligand, TR-FRET occurs between the pindolol bound Eu^{3+}-chelate donor and soluble quencher acceptor, resulting in a decrease of Eu^{3+}-chelate emission. When no ligand is present, the pindolol–Eu^{3+}-chelate interacts with the β2AR, which separates it from the soluble quencher thus resulting in increased donor emission. The main advantage of QRET is the single-label format enabled by the soluble quencher, which reduces costs and increases efficiency of ligand screening as fewer compromises in assay design are required. Additionally to living-cell studies, QRET is suitable for immunoassays and studying post translational modification via peptide break assay.[146,147]

2.3.2 Assays utilizing quenching by water

The quenching effect of water is convenient and simplifies photoluminescence assays as no additional quencher is required. The quenching effect can affect both the intrinsic fluorescence obtained from the investigated proteins themselves and extrinsic luminescence from the added luminescent dyes. The intrinsic fluorescence-based methods often utilize the fluorescence of tryptophan residues or the green fluorescent protein and its derivatives for detection. The extrinsic methods rely mainly on the addition of fluorescent dyes to the assay solution, such as SYPRO Orange and 1,8-ANS. The work presented in this thesis mainly focuses on extrinsic methods based on the conventional differential scanning fluorometry (DSF), which are often performed with either RT-PCR or a standard plate reader. DSF is mainly utilized for observing the thermal profiles of proteins and optimizing protein storage condition along with PLI screening.[148–150]

The main principle of the use of DSF with extrinsic dyes relies on the disruption of the structure of the investigated target protein. The disruption reveals the hydrophobic regions of the target protein for fluorescence dye binding. The hydrophobic environment shields the dye from water thus decreasing the quenching effect and resulting in an increased emission. The structure of the target protein can be affected by variety of conditions, such as protein denaturation, aggregation and digestion or freeze-induced perturbations. In the case of heat denaturation, the emission increases as the hydrophobic regions are unveiled at increasing temperatures thus enabling fluorescent dye binding (**Figure 13**).[32,151–153] Further heating to higher temperatures results in an emission decrease due to breakage of the hydrophobic regions. The monitored emissions can be plotted as a thermal profile curve, and the denaturation temperature (T_m) can be calculated from a sigmoidal fitting curve. The most popular use of DSF relates to the thermal shift assays (TSA) where an additional molecule, e.g. ligand or other protein, interacts with the target

protein and affects its thermal stability. In most cases, the molecule stabilizes the target protein thus resulting in a higher T_m as more energy is required for the denaturation of the interaction complex. TSAs are popular methods for screening potential ligand molecules and proteins binding to target proteins.[32,151–153] The information obtained from DSF can be further used for a range of purposes, such as optimizing protein storage conditions, protein quantitation and aggregation.

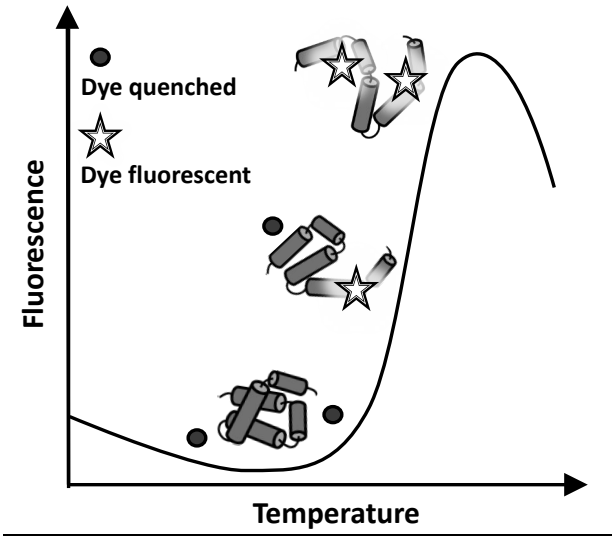

Figure 13. The basic principle of the DSF method developed for monitoring the thermal stability of a target protein. The emission of the unbound fluorescent dye, e.g. SYPRO Orange, is quenched by the water in the assay solution in presence of the native target protein. During the assay, the sample is heated leading to the denaturation of target protein. The denaturation reveals the hydrophobic inner regions of the target protein thus enabling fluorescent dye binding. This binding protects the fluorescent dye from the quenching effect of water and thus the fluorescence emission of the dye increases.

The thermal stability information obtained by DSF is suitable for optimizing protein storage conditions, especially in terms of solubility and stability. DSF screening of buffer conditions related to pH, component concentrations, and additives has alleviated problems with protein stability and aggregation and increased the success of crystallisation.[154–156] Protein quantitation methods based on DSF determine the concentration of a target protein sample by comparing it to the standard curve typically assayed with BSA. The comparison utilizes samples heated at high temperatures to obtain emission from such commercial fluorescent dyes as AccuOrange and NanoOrange.[157] At high temperatures, the dye interacts with the unfolded target and standard proteins, and is protected from the quenching effect of water. The emission of the dye reports the concentration of the target protein in

relation to the standard curve thus enabling DSF based quantitation. DSF is also utilized for studying the aggregation and fibril formation of proteins.[158–160] The T_m obtained from the temperature profiles produced with conventional water quenched fluorescent dyes provides information on the aggregation likelihood of the sample when combined with size based assays.[161] Dyes quenched by the rotation of a dye molecule such as Thioflavin T and ProteoSTAT are utilized in DSF for protein aggregation studies, even in non-thermal induced aggregation. The rotation of the dye molecule in aqueous solution prevents emission but aggregate formation immobilizes the rotation thus increasing emission. Thioflavin T is mainly used for detection of amyloid fibrils, whereas ProteoSTAT is suitable to variety of proteins.[161]

The main strengths of extrinsic dyes in DFS are robustness and simplicity. DSF is suitable for variety of protein studies without requiring labelling or production of recombinant proteins. DFS is economical and accessible, requiring only RT-qPCR machinery suitable also for HTS.[33,34] There are also limitations to extrinsic DSF, like its μM range sensitivity. Also, the chosen target protein must contain hydrophobic regions for fluorescence dye interaction during denaturation. Targets with hydrophobic regions available at room temperature lead to high initial emission and background, which can partially or completely mask the denaturation induced emission increase. Additionally, the target protein structure may affect the clarity of the obtained thermal profile. For example, some domains may have distinct thermal stability properties, and structural rearrangements during denaturation may perturb the thermal curve. Measurements of protein mixtures are also impossible since the observed denaturation curves cannot be related to their respective proteins.[33] The choice of assay buffer is also limited as none of the components of the buffer can interact with the target protein or fluorescent dye. This includes detergents such as EDTA, which may interact with the fluorescent dyes and result in an emission increase at significantly lower temperatures.[33,162]

In addition to extrinsic DSF methods, an intrinsic type of DSF named NanoDSF has been developed based on the fluorescence of tryptophan residues. The NanoDSF method is mainly performed with a specific instrument, such as the Prometheus NT.48 (designed by NanoTemper), and seldom with standard plate readers.[163] Another intrinsic DSF method called GFP-Basta is a heterogeneous assay based on a GFP tag fused to the target protein and reports its denaturation and subsequent aggregation after denatured, and folded complexes have been separated by centrifugation.[148]

Additional protein quantitation method, named FluoroProfile, features eppicocconone, a compound with a low fluorescence emission in water. The FluoroProfile method monitors the increase of eppicocconone emission when the compound comes into contact with target protein. In contrast to DSF, thermal denaturation has no effect on the eppicocconone emission and heating is not required

for detection.[164,165] In addition to protein quantification, the eppicocconone compound has also been utilized for real-time monitoring of protein digestion by trypsin. As the substrate protein was digested by the protease, the emission of eppicocconone decreased as it was no longer in contact with substrate protein. The method is compatible with natural substrate proteins and enables the removal of tags from recombinant proteins.[166]

2.4 Summary

Drug discovery is initiated with hit compound screening against the selected target biomolecule important for the disease function. The results of this primary screening have to be verified by secondary methods to ensure the effectiveness and safety of the chosen candidate drugs. The orthogonal secondary screening methods also investigate the absorption, distribution, metabolism and excretion of the compounds, and are important for optimizing the compound specificity, selectivity and stability. Thus a successful drug discovery process requires a multitude of methods with a variety of usages to avoid dead-ends resulting in an unsuitable compound in the later phases. The requirements for drug discovery suitable assays include cost- and time-effectiveness with high reliability and robustness. Cost-effectiveness relies mainly on the sensitivity of the assay, as the biomolecules, such as enzymes and interacting proteins, are often the most expensive assay components along with the reporter molecules. Both cost- and time-effectiveness depend on the simplicity of the assay as less steps and components lead to less material consumption and a more rapid assay format. Automation and miniaturization also decrease costs and time requirements and have higher potential with simpler assay formats. The optimal assay is balanced between efficiency and reliability. Most often the cheapest assay may result in unreliable results, such as false positives and negatives thus requiring intensified secondary screening. High robustness of the assays enables minor changes to optimize productivity and efficiency without sacrificing assay reliability. Photoluminescence based methods often achieve desirable assay properties and have become one of the most useful tools for drug discovery, especially due to their homogenous format. Photoluminescence quenching is often useful for improving the signal-to-noise ratio of the assays and was used in the work presented in this thesis for developing new protein interaction and digestion assays. These novel assays were developed with the aim to function as secondary screening methods but also have potential to be used for primary screening.

FRET methods are one of the most popular photoluminescence assays used in both cellular and biochemical assays for drug discovery. FRET based methods monitor the dynamic quenching mechanism FRET between the luminophore donor, and the quencher acceptor. FRET methods study the interactions of the donor and

acceptor label conjugated biomolecules by monitoring the increased rate of FRET when the labels come in close contact (10-100 Å). Their proximity initiates energy transfer from the excited donor to acceptor, which then emits the excess energy, mostly as luminescence. This property can be utilized for numerous purposes, such as investigating protein interactions with ligands or other proteins, e.g. with TruPoint or enzyme activity, like the phosphorylation by kinases with Z'-LYTE. Depending on the properties of the donor and acceptor, FRET is suitable for steady-state and time-resolved measurements. Methods utilizing time resolved monitoring, TR-FRET, are especially popular due to their increased sensitivity and diminished false negatives and positives, when compared to steady-state FRET. For TR-FRET purposes, the commercial methods LANCE and LanthaScreen utilize lanthanide chelates as donor, whereas in case of HTRF more stable lanthanide cryptates are preferred.

The FRET and TR-FRET methods are highly sensitive at the pM range and homogenous with simple mix and measure type protocols. With a slightly more complicated assay design, TR-FRET is also suitable for screening membrane protein ligands in viable cells. Unfortunately, FRET based methods require dual labelling of both donor and acceptor and often utilize antibodies, which require target specific design. In high donor concentration, the emission of especially non-quenched donor molecules may interfere in the acceptor channel and lead to false positives. The multiplexing possibilities of FRET and TR-FRET are generally quite low as the methods are designed for studying specific interactions (**Table 2**).

The properties of luminescence quenching by water have been utilized for developing DSF methods. DSF is based on monitoring the increased emission of external fluorescent dye when the dye interacts with the hydrophobic regions of a target protein unveiled by thermal denaturation. This property enables the monitoring of protein thermal profiles and stability with DSF, in addition to protein aggregation and quantitation and storage optimization. Since ligand binding has an effect on the thermal stability of proteins, DSF can be utilized for ligand screening by monitoring the Tm of the target protein. The main advantage of DSF methods is the simplicity of the label-free format, since they rely on external dyes quenched by the water in the assay solution. The DSF method requires no specific labels or dyes for every target protein, which increases the assay versatility significantly but also complicates to study protein mixtures. DSF methods are suitable for studying low affinity interactions as a high ligand concentration has little effect on the quenching of fluorescent dye in aqueous solution. Alas, the simplicity leads to lower µM range sensitivity when compared to FRET based assays. Additionally, the DSF methods are unsuitable for investigation of membrane proteins and their ligands (**Table 2**).

Table 2. Comparison between commercial methods and the methods developed during this doctoral thesis.

	Energy transfer	**Quenching via water**	**Methods developed during thesis**	
Method	FRET or TR-FRET	DSF	QRET and QTR-FRET	DSF
Name	Trupoint, HTRF, LANCE	NanoOrange, NanoDSF	QTR-FRET (Pub. **I** & **II**)	The Protein-Probe (**III** & **IV**)
Luminophore monitored	Donor or acceptor	Fluorescent dye	Donor and acceptor	External Eu^{3+}-probe
Sensitivity	pM	µM	nM	nM
Labels	Dual label	Label-free	Dual label	Label-free
Steps	Single	Single	Single	Double
Multiplexing	Yes	No	Yes	No
Quantitative	Yes	Yes	Yes	Yes
Targets	Specific	Non-specific	Specific	Non-specific
Membrane proteins	Yes	No	No*	No

* Utilizes QRET, which has capability for GPCR membrane PLI monitoring.

3 Aims

The aim of this doctoral project was to develop two methods based on photoluminescence quenching. Both methods, QTR-FRET and the Protein-Probe, were developed with the view for suitability in drug discovery purposes, especially during secondary screening. The methods were thus developed to be performed in a homogenous multi-well plate format with simple design and high robustness. These methods are the basis of four scientific publications with two articles written about each. Both the QTR-FRET and the Protein-Probe were developed to be suitable for drug discovery purposes especially during secondary screening. Thus, the methods were developed to be performed in a homogenous multi-well plate format with simple design and high robustness.

Specific aims of each publication:

I The development of the QTR-FRET as combination of TR-FRET and QRET to enable low affinity PLI studies requiring high donor concentrations.

II To enable single well detection for PLI and subsequent PPI with the QTR-FRET method.

III Development of a label-free Protein-Probe method for PLI screening with increased sensitivity compared to conventional DSF SYPRO Orange.

IV To enable the Protein-Probe method for monitoring protease activity via variety of unmodified substrate proteins.

4 Materials and Methods

In this chapter a summary of materials and methods used in is doctoral project are presented. Detailed descriptions can be found from original publications **I**–**IV** and their supplementary information.

4.1 Luminescent probes and quenchers

Fluorescent dye label conjugations: In the publications the luminescent probes with fluorescent dye labels: Cy5-SA (**I**), Alexa680-SA (**I** and **II**), and Alexa680-RAF-RBD (**II**), were prepared by conjugation. The SA conjugations were performed by labelling SA with two-fold molar excess of Cy5 N-hydroxysuccinimide ester in 50 µL (**I**) or with Alexa680 N-hydroxysuccinimide ester in 100 µL (**II**). The Ras binding domain of the c-Raf kinase protein (RAF-RBD) was labelled with two-fold molar excess of Alexa680 N-hydroxysuccinimide ester in 175 µL (**II**). The reactions were performed in 50 mM carbonate buffer (pH 8.3) and purified with NAP-5 columns in 50 mM HEPES pH 7, and the degree of labeling was monitored by UV absorbance.

Luminescent Eu^{3+}-chelate complex conjugations: The Eu^{3+}-chelate based probes, Eu^{3+}-biotin (**I**), GTP-Eu^{3+} (**I**), γ-GTP-Eu^{3+} (**II**), and Eu^{3+}-probe (**II** and **IV**) were conjugated by isothiocyanate (ITC) chemistry. In publication **I**, three Eu^{3+}-biotin complexes containing 7-, 9-, and 11-dentate Eu^{3+}-chelates and two 2'/3'-GTP-Eu^{3+} complexes containing 7- and 9-dentate Eu^{3+}-chelates were prepared. The γ-GTP-Eu^{3+} in publication **II** was synthesized from GDP to GTP-ethanolamine, which was then conjugated with excess of ITC-activated Eu^{3+}-chelate. The Eu^{3+}-probe in publications **III** and **IV** was prepared by conjugating ITC-activated Eu^{3+}-chelate to the N-terminus of peptide sequence (NH2-EYEEEEEVEEEVEEE). The conjugations in all publications were performed by dissolving 1 mg Eu^{3+}-chelate in water (100 µl) and mixing with the target, such as biotin, GTP, or peptide (0.5 mg), in 100 µl label buffer containing pyridine/H_2O/triethylamine in a 9:1.5:0.1 ratio. After 18 h incubation at room temperature the product was purified with reverse-phase liquid chromatography. The product concentration was determined by comparing the luminescence signal of the dissociated Eu^{3+}-ion of the conjugation complex to commercially available Eu^{3+}-standard in development solution.

Soluble luminescence quenchers: Several different quenchers were used in the publications, such as MT2 (**I**), MG (**I** and **II**) and 1,1,3,3,3′,3′-hexamethylindodicarbocyanine iodide (**III** and **IV**). In publication **I**, MT2 acted as quencher for Eu^{3+}-biotin conjugates, in addition to MG which quenched Eu^{3+}-biotin and GTP-Eu^{3+} conjugates. In publication **II**, MG quenched both GTP-Eu^{3+} and γ-GTP-Eu^{3+}. In publication **III** and **IV,** 1,1,3,3,3′,3′-hexamethylindodicarbocyanine iodide quenched the emission of the Eu^{3+}-probe.

4.2 Instruments and measurement settings

The luminescence emissions (TRL, QRET, TR-FRET, QTR-FRET and fluorescence) were measured with a Victor 1420 multilabel counter (**I**), plate reader from Labrox Ltd (**II**), and a Tecan Life Sciences Spark 20M plate reader (**I**–**IV**). The TRL and QRET emissions of Eu^{3+}-chelates were measured at 615 nm (**I**–**III)** or 620 nm (**IV**) with excitation at 340 nm using a delay time of 400 (**I** and **III**), 600 (**II**) and 800 µs (**IV),** and an integration time of 400 µs. For the TR-FRET and QTR-FRET measurements of Cy5 (**I**), 340 nm excitation with 665 nm emission wavelengths and 75 µs delay and integration times were used. The TR-FRET emission of Alexa680 (**I** and **II**) was monitored with 340 nm excitation and 730 nm emission wavelengths, with 75 µs delay and 400 µs integration times. In publication **III,** SYPRO Orange fluorescence was measured with 485 nm excitation and 590 nm emission wavelengths.

Several different instruments were used throughout the publications for purifications, thermal controlling, lifetime monitoring and quantification. The Eu^{3+}-chelate complex purifications were performed by reverse-phase liquid chromatography with a Dionex Ultimate 3000 LC –system and Ascentis RP-amide C18 column. The thermal denaturation (**III** and **IV**) was performed with a PTC-100 Programmable Thermal Controller. The concentration of proteins and their labeling degrees were monitored with a Nanodrop 2000C spectrophotometer at A_{280} and A_{680} (**II**).

4.3 Assay buffers

The composition of the buffers, HEPES and PBS, were varied on the basis of the requirements of the enzymes present in the assays. The main buffers for each publication are listed in the **Table 3.**

Table 3. Buffer compositions in publications **I**–**IV**.

Pub	Sample buffer	Usage
I	**1.** 50 mM HEPES pH 7, 0.05 % Triton (w/v), 150 mM NaCl, 0.05 % BSA	Eu^{3+}-biotin–SA-Cy5
I	**2.** 25 mM HEPES pH 7, 0.01 % Triton (w/v), 1 mM $MgCl_2$, 10 mM NaCl, 0.005 % γ-globulin	AVI-KRAS–SA-Alexa680
II	**3.** 20 mM HEPES pH 7.5, 0.01 % Triton (w/v), 1 mM $MgCl_2$, 10 mM NaCl, 0.005 % γ-globulin	Eu^{3+}-GTP–KRAS–RBD-Alexa680
II	**4.** 20 mM HEPES (pH 7.5), 0.01% Triton (w/v), 1 mM $MgCl_2$, 0.4 mM $MnCl_2$, and 0.005% γ-globulins	KRAS glycosylation by TpeL
II	**5.** 20 mM HEPES pH 7.5, 0.01 % Triton (w/v), 5 mM NaCl, 5 mM EDTA	G(i)α $MgCl_2$ unloading buffer
II	**6.** 20 mM HEPES (pH 7.5), 0.01% Triton (w/v), 20 mM $MgCl_2$, 5 mM $MnCl_2$, and 0.005% γ-globulins	γ-GTP-Eu^{3+}-G(i)α–biotin-NAD^+–SA-Alexa680
III	**7.** 0.1x PBS pH 7.5, 0.001 % Triton (w/v),	Protein denaturation curves, SA–biotin, CA–AZA
IV	**8.** 10 mM HEPES pH 7.5, 0.001 % Triton (w/v)	Pronase digestion activity
IV	**9.** 10 mM HEPES pH 7.5, 0.001 % Triton (w/v)	Papain digestion activity and inhibition by E-64
IV	**10.** 0.1x McIlvaine pH 3*, 0.001 % Triton (w/v)	Pepsin digestion activity and inhibition by Pepstatin A
III IV	**11.** 0.1x McIlvaine pH 4*, 0.001 % Triton (w/v)	Modulation solution buffer for detection

* 1x McIlvaine buffer was prepared by combining 0.2 M Na_2HPO_4 and 0.1 M citric acid in ratio 1:3.9 and 1:1.6 for pH 3 and pH 4, respectively.

4.4 Assay proteins

The PLI, PLI/PPI and digestion substrate proteins studied during the doctoral thesis were purchased or obtained as kind gifts from collaborators. Avi-tagged KRAS was received from Jonas Kapp (University of Zurich, Switzerland), SOS^{cat}, RAS, and TpeL from Dr. William Gillette (Frederick National Laboratory, USA), eIF4A1 from John Le Quesne and Martin Bushell (University of Glasgow, UK), p120GAP from Stefan Veltel (Hochschule Bremen, Germany), PTX and G(i)α proteins from Moona Miettinen and Arto Pulliainen (University of Turku, Finland).

4.5 Assay protocols

4.5.1 QTR-FRET (**I** & **II**)

*QTR-FRET was developed as a combination of TR-FRET and QRET (**I**):* In publication **I** the SA binding assays were performed in a final volume of 50 µL of buffer 1 (**Table 3**) in triplicates. First the three Eu^{3+}-biotin complexes containing 7-, 9-, or 11-dentate Eu^{3+}-chelates were compared in QRET, TR-FRET and QTR-FRET assays. The comparison was performed by competitive biotin titration (0.050-200 nM) in 1 nM of Cy5-SA for TR-FRET and QTR-FRET and 1 nM of SA for QRET. The biotin and Cy5-SA/SA were combined before addition of Eu^{3+}-biotin (4 nM) and 30 min incubation in room temperature. Then the QRET, TR-FRET, and QTR-FRET signals were monitored according to 4.2 and thereafter the quenchers MT2 and MG (20 µM) were added for QRET and QTR-FRET, respectively. After quencher addition the plates were incubated for 10 min at room temperature and QRET and QTR-FRET signals were measured.

In publication **I,** Cy5-SA (10 nM) was incubated with and without biotin (3 µM) for 5 min and titration of the chosen Eu^{3+}-biotin (9-denate Eu^{3+}-chelate, 4-972 nM) was performed. Then 20 min incubation at room temperature took place and TR-FRET signals were monitored before addition of soluble quencher MG, (0-120 µM). Thereafter the plate was incubated for 10 min and the QTR-FRET signals were monitored at 665 nm.

The other interaction model assay in publication **I,** featuring Avi-KRAS–SA-Alexa680, was performed in a final volume of 10 µL of buffer 2 (**Table 3**). 20 nM SA-Alexa680 and Eu^{3+}-GTP (5 nM, 20 nM, or 80 nM) were combined in the Biotin-KRAS titration (0–1200 nM) before initiating the nucleotide exchange with 10 nM SOS^{cat}. After 20 min incubation, the TR-FRET signals were measured before adding MG in a Eu^{3+}-GTP concentration dependent manner (10 µM, 15 µM or 20 µM). After 15 min incubation, the QRET signals reporting PLI and QTR-FRET signals reporting PPI were measured as detailed in **4.2**.

*Dual parametric monitoring of PLI and PPI with QTR-FRET (**II**):* In publication **II,** the designed ankyrin repeat proteins (DARPins) K27 and K55 were utilized for blocking the PLI and PPI reactions between PLI KRAS–Eu^{3+}-GTP and KRAS–RAF-RBD, respectively. The KRAS (200 nM) was combined with the DARPins K27 (500 nM) and K55 (5 µM) in 7 µl of buffer 3 (**Table 3**) and incubated for 10 min at RT. Then 6 µl of detection solution (Eu^{3+}-GTP 25 nM, MQ 24 µM and RBD-Alexa680 25 nM) was added and QRET, TR-FRET, and QTR-FRET signals were measured. Afterwards, SOS^{cat} (10 nM, 2 µl) was added to induce the nucleotide exchange to produce KRAS–Eu^{3+}-GTP and result in subsequent KRAS/RAF-RBD interaction.

The QRET, TR-FRET, and QTR-FRET signals were monitored in intervals during 60 min incubation at room temperature.

For publication **II,** the Eu^{3+}-GTP or Eu^{3+}-GDP (25 nM) nucleotide exchange reaction of KRAS (200 nM) was performed with SOS^{cat} (10 nM) in 5 µL of buffer 3 (**Table 3**) containing MG (15 µM) and incubated for 15 min at room temperature. Thereafter TpeL toxin (0-50 nM) and UDP-GlcNAc (25 µM) were added in 4 µL of buffer 4 (**Table 3**) to initiate the glycosylation reaction. Plates were incubated for 20 min at room temperature before adding RBD-Alexa680 (25 nM) in 6 µL of buffer 3 (**Table 3**) and monitoring QRET and QTR-FRET signals.

The ADP-ribosylation reaction in publication **II** was performed with G(i)α (150 nM), Pertussis toxin (PTX) (0-600 nM), and bio-NAD^+ (25 nM) in buffer 5 (**Table 3**). To unload the GDP from G(i)α, γ-GTP-Eu^{3+} (25 or 50 nM) was added with GTP (0 or 10 µM) in buffer 3 (**Table 3**) to enable γ-GTP-Eu^{3+} loading. The loading was monitored at 615 and 730 nm with 340 nm excitation for 30 min at room temperature before adding SA-Alexa680 to 15 µl total volume. The QRET and QTR-FRET signals were monitored for 90 min before adding 2 µl MG (20 or 35 µM) and monitoring signals after 30 min in room temperature.

4.5.2 The Protein-Probe (**III** & **IV**)

All Protein-Probe assays in publication **III** and **IV** were performed in two-steps by combining 8 µl of buffer 7 (**Table 3**) containing the studied protein of interest, ligands, and enzymes with 65 µl of the modulation solution (buffer 11 (**Table 3**), 3.5 µM 1,1,3,3,3′,3′-hexamethylindodicarbocyanine iodide, and 1 nM Eu^{3+}-probe). Thereafter the plates were incubated for 5 min at room temperature and the TRL signals were monitored as described in **4.2**.

*Monitoring thermal denaturation of proteins and the effect of PLI with the Protein-Probe (**III**):* In publication **III**, the thermal denaturation curve of IgG_1 (80 nM and 2 µM) was assayed with the Protein-Probe and SYPRO Orange methods, respectively. IgG_1 samples were heated in 8 µL for 3 min with 5 °C temperature increments from 55 to 80 °C before addition of the Protein-Probe modulation solution or 2 µL SYPRO Orange (x1). After 5 min incubation at RT, the TRL and fluorescence signals were monitored as indicated in 4.2. Next the sensitivities of the Protein-Probe and SYPRO Orange were compared with titration of heat denatured (3 min, 80 °C) IgG_1 (0-5 µM). After denaturation, modulation solution or SYPRO Orange was added, and signals were measured as previously. In addition to IgG_1 the denaturation curves of three proteins, CA (200 nM), SA (400 nM), and MDH (100 nM) were monitored with the Protein-Probe in thermal intervals 2-5 °C from 25 to 90 °C.

Biotin (0-20 µM) and acetazolamide (AZA, 0-90 µM) were titrated in publication **III** with SA (400 nM) and CA (200 nM), respectively. The PLI combinations SA–biotin and CA–AZA were heated 3 min at 70 °C or 90 °C, respectively. Thereafter the modulation solution was added and TRL signals were monitored as stated in 4.2. Thereafter the thermal shifts initiated by the PLI interactions, SA–biotin and CA–AZA, were investigated by monitoring their denaturation curves with the Protein-Probe. SA (400 nM) and CA (200 nM) were heated for 3 min in intervals of 2-5 °C from 55 to 90 °C with and without biotin (10 µM) and AZA (5 µM), respectively. The denaturation was monitored with the TRL signals of the Protein-Probe modulation solution as previously.

*The Protein-Probe methods for monitoring protease activity via the digestion of unmodified substrate proteins (**IV**):* In publication **IV,** papain (0–16 µM) was titrated with intact (100 nM) and heat denatured (3 nM) CA (3 min at 75 °C) as a digested substrate. The titrations were performed with the substrate and protease in buffer 9 (**Table 3**) by incubating the digestion reaction for 30 min at 37 °C before adding the modulation solution in buffer 1 (**Table 3**) and measuring TRL-signals. The inhibitor titration followed the same protocol by combining papain (1 or 100 nM for denatured and native CA, respectively) and E-64 inhibitor (0-400 nM) prior addition of the substrate, native (100 nM) or heat denatured (3 nM) CA. The samples were incubated for 30 min at 37 °C before the Protein-Probe addition and TRL-signal monitoring, as previously described.

During the studies presented in publication **IV**, nine native substrate proteins (eIF4A1, PTX, MDH, SOS^{cat}, BSA, CA, KRAS, Gαi, p120GAP) at 25 and 50 nM concentrations were digested with pronase and papain (12.5, 25, 50 and 100 nM) in buffers 8 and 9 (**Table 3**), respectively. The digestion reactions were incubated for 10 min at 37 °C, followed by potential post-digestion denaturation performed by 3 min heating at 60 °C (p120GAP, PTX, MDH, eIF4A1, SOS^{cat}, Gαi, and BSA) or 70 °C (KRAS, and CA). The Protein-Probe detection was then performed with both native and post-digestion denatured substrates.

5 Results and discussion

The work presented in this doctoral thesis was focused on the development of two luminescence assays, i.e. the quencher modulated Time-Resolved Förster Resonance Energy Transfer (QTR-FRET) and the Protein-Probe. These assays utilized soluble quencher addition for decreasing the luminescence of unbound reporter molecules to increase the change in emission monitored after reporter binding. The main advantages of these assays are simplicity, high sensitivity, robustness, and versatility. These are important assay qualities, e.g. for drug discovery, which has a growing need for novel assays.

During the first phase of the thesis, the QTR-FRET assay was developed based on QRET and TR-FRET (**I** and **II**). QTR-FRET was introduced in publication **I** as an improvement of conventional TR-FRET with increased S/B-ratio and enhanced functionality for studying low affinity interactions. The full potential of QTR-FRET was presented in publication **II** with two model assays for dual parametric monitoring of the PLI and subsequent PPI or post translational modification (PTM) in a single well format.

In the second phase of the thesis a new Protein-Probe assay was developed utilizing external luminescent probe and soluble quencher (**III** and **IV**). In publication **III**, the Protein-Probe was used to monitor the changes in the target protein thermal profile affected by PLI. In publication **IV**, the ability of the Protein-Probe to observe the activity of proteases by monitoring the digestion of unmodified protein substrates was investigated. The Protein-Probe assay successfully monitored molecular inhibition of proteases, and digestion activity in vide range of substrate-protein screens.

The main results of publications **I-IV** are summarized in the following chapter. More detailed results and discussion can be found in the original publications.

5.1 QTR-FRET

The QTR-FRET assay combines the soluble quencher addition utilized in QRET and the time-resolved energy transfer properties of TR-FRET. QTR-FRET delivers a method with a reduced background signal of donor luminescence observed in the acceptor measurement window (**I**) and a simple approach for dual parametric

monitoring of PLI and the subsequent PPI or PMT from a single well (**II**). The QTR-FRET method is readily modifiable for studying different PLI and PPI or PMT combinations which will be demonstrated during following chapter.

5.1.1 Protein-ligand interaction studies (I)

In publication **I** the improvements of QTR-FRET functionality over QRET and TR-FRET were demonstrated with two model PLI interactions between SA-Cy5 and Eu^{3+}-biotin, and SA-Cy5/Avi-KRAS and Eu^{3+}-GTP.

The SA-biotin interaction model was chosen due to its femtomolar affinity, which enables more reliable comparison between QRET, TR-FRET, and QTR-FRET, as full binding is expected in all three assays (**Figure 14**).[167,168] With QRET the changes of Eu^{3+}-biotin emission are monitored. In the presence of competing non-labelled biotin, the Eu^{3+}-biotin is unable to interact with SA and its TRL emission is quenched by the soluble quencher (**Figure 14A**). When no competing biotin is present, the Eu^{3+}-biotin interaction with SA reduces the local concentration of quencher in proximity of the Eu^{3+}-biotin. Thus, the TRL emission of Eu^{3+}-biotin is greatly increased. In TR-FRET, the interaction of Eu^{3+}-biotin donor with SA-Cy5 acceptor leads to energy transfer between the labels and TR-FRET signal emission by Cy5 (**Figure 14B**). The competing non-labelled biotin blocks this interaction and the energy transfer, thus preventing TR-FRET emission. In the TR-FRET assay, the unbound Eu^{3+}-biotin emits TRL signal whether or not the energy transfer occurs. In QTR-FRET, the TRL signal of the unbound Eu^{3+}-biotin is diminished by soluble quencher, like in the case of QRET (**Figure 14B**). The QTR-FRET monitors the interaction of Eu^{3+}-biotin and SA-Cy5 through the Cy5 emission akin to TR-FRET. Thus the QTR-FRET assay functions as the combination of QRET and TR-FRET to prevent the TRL emission of Eu^{3+}-biotin donor from interfering in the acceptor channel.

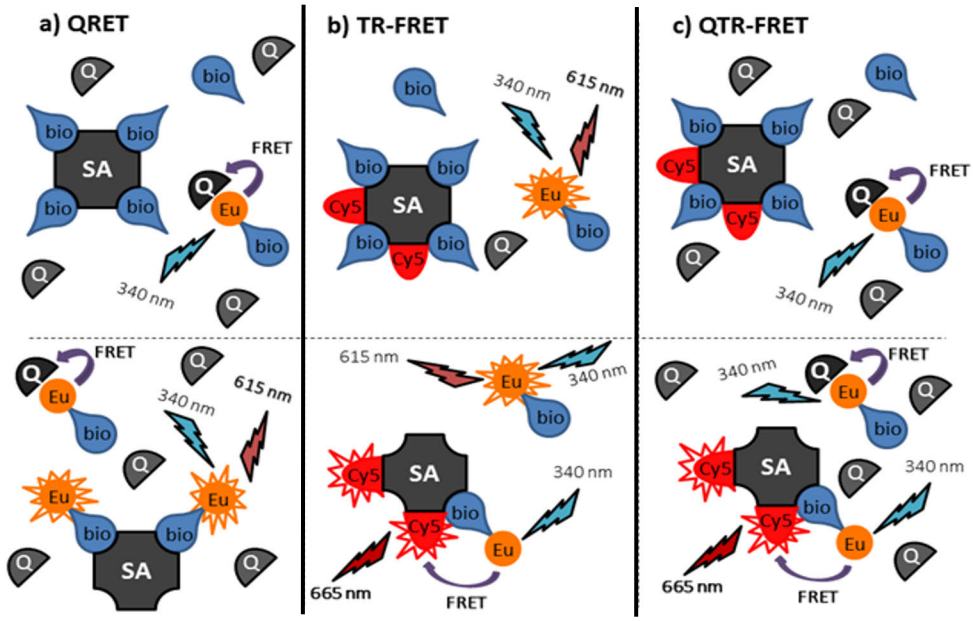

Figure 14. The detection mechanisms of three homogenous energy transfer systems used for SA-biotin model assays. **A**) In the QRET assay the binding of Eu^{3+}-biotin to SA is detected as the increase of TRL-signal. In the presence of competing biotin the Eu^{3+}-biotin no longer interacts with SA but with soluble quencher, which prevents TRL emission. **B**) The TR-FRET assay monitors the energy transfer between the donor Eu^{3+}-biotin and acceptor Cy5-SA when they are in close proximity by monitoring the TR-FRET emission of the Cy5 label. Additionally the unbound Eu^{3+}-biotin emits TRL signal, which can interfere with the measurements in the TR-FRET acceptor channel. **C)** The QTR-FRET also monitors the TR-FRET emission of Cy5 label upon energy transfer from the Eu^{3+}-biotin. The TRL emission of the unbound Eu^{3+}-biotin is reduced by quencher acting as second acceptor.

For the SA-biotin interaction model, three Eu^{3+}-biotin complexes named bio7, bio9, and bio11 were prepared with different Eu^{3+}-chelate structures: 7-, 9-, and 11-dentate Eu^{3+}-chelates, respectively. The Eu^{3+}-chelates have a similar basic structure but have additional iminodiacetate coordinating arms.[169] These Eu^{3+}-chelates all have an excitation peak at 320–325 nm and dual emission peaks: the main at 615–620 nm and secondary at 695–700 nm. Both SA-Cy5 and MG excitation and absorption overlap with the Eu^{3+}-chelate emission at 655 nm and 616 nm, respectively. The MT2 quencher utilized in QRET is unsuitable for QTR-FRET since the MT2 emission maximum is at 665 nm where QTR-FRET emission of SA-Cy5 is monitored. The functionality of the three Eu^{3+}-biotins (4 nM) were compared in QRET, TR-FRET and QTR-FRET as competitive biotin titrations (0.050-200 nM) with 1 nM SA-Cy5 or SA. The QRET and QTR-FRET utilized MT2 and MG (20 µM) as quenchers. The S/B ratios were calculated by dividing the signals measured without including competing biotin with signals measured

including the biotin. The bio7 was most optimal for TR-FRET with an S/B ratio of 14 and bio9 for QRET with an S/B ratio of 8. The quencher addition to TR-FRET to perform QTR-FRET did not have an effect on the bio7 S/B ratio but with bio9 it resulted in the highest increase of the S/B ratio from 12 to 18. Thus the bio9, which was optimal for both QRET and QTR-FRET, was selected for further characterization of QTR-FRET.

The high affinity of SA-biotin interaction resulted in full binding of SA with the low concentration of Eu^{3+}-biotin (4 nM) in the initial assays. Under these conditions great improvements of QTR-FRET over TR-FRET are not expected. However, full binding of ligand to protein is seldom the case in more biologically relevant cases. Thus, the QTR-FRET functionality was demonstrated in increasing concentrations of Eu^{3+}-biotin. Excess Eu^{3+}-biotin, bio9, (4–972 nM) was titrated with increasing quencher (MG) concentrations (0–120 µM) with or without competing 3 µM biotin in Cy5-SA binding assay (**Figure 15A**). The assay was monitored with TR-FRET and QTR-FRET. In the TR-FRET assay, the Eu^{3+}-biotin concentrations of 36 nM and below gave nearly identical S/B ratios (12–13). The ratio decreased significantly as Eu^{3+}-biotin concentration increased due to the Eu^{3+}-chelate derived background signal at the 665 nm measurement channel. The effect was reduced by the quencher in the QTR-FRET measurements at all Eu^{3+}-biotin concentrations and provided increased S/B ratios. The optimal S/B ratio was detected with approximately 60 µM MG, except when using lowest Eu^{3+}-biotin concentration (4 nM). Higher MG concentrations reduced also the specific signal obtained from samples thus lowering the S/B ratio. The highest S/B ratio increase of 7-fold compared to TR-FRET S/B ratios was detected with 330 nM Eu^{3+}-biotin and 60 µM MG. The optimal quencher concentration decreased the Eu^{3+}-biotin signal near the background level without decreasing the specific signal. The quenching of unbound Eu^{3+}-biotin was intensified compared to the quenching of unbound Eu^{3+}-biotin, which had linear signal repression in increasing MG concentrations (**Figure 15B**).

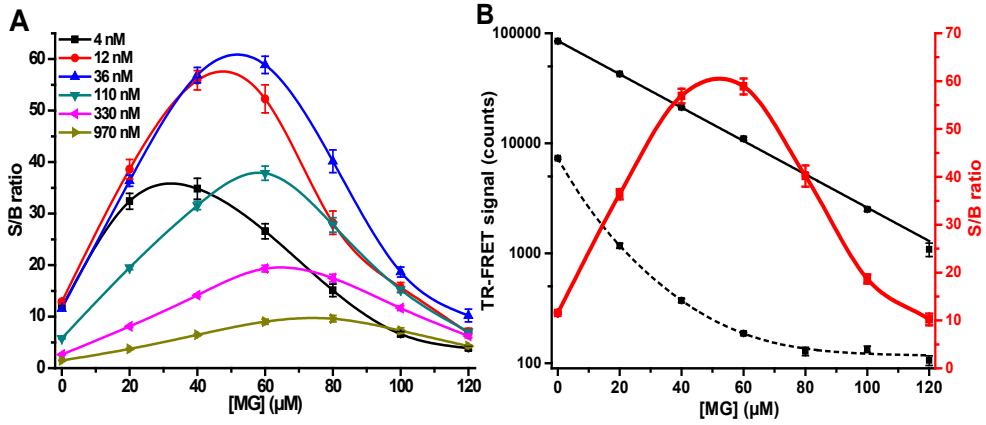

Figure 15. QTR-FRET provided an increased S/B ratio compared to TR-FRET. The Cy5-SA (10 nM) Eu^{3+}-biotin (4-972 nM) interaction model monitored the S/B ratio improvement during MG (0-120 µM) titration with and without competing biotin (3 µM). **A**) Compared to the TR-FRET monitoring at 0 µM MG the QTR-FRET with soluble quencher delivers improved S/B ratio in all Eu^{3+}-biotin concentrations. TR-FRET S/B ratio is improved by additional Eu^{3+}-biotin until a concentration of 36 nM, thereafter no S/B ratio increase was achieved. **B**) Increasing MG concentration lead to a decrease in the signal level when assayed with 36 nM Eu^{3+}-biotin. With the added competing biotin (black, dashed) the decrease was enhanced compared to the linear decrease without it (black, solid). S/B ratio (red) increases until the sample containing competing biotin reaches background signal level. Data represent mean ± SD (n = 3).

To demonstrate further applicability of QTR-FRET, a second model assay featuring Eu^{3+}-GTP–Avi-KRAS and SA-Alexa680 interaction was designed. In the designed assay, the SOS^{cat} (10 nM) catalyzed the nucleotide exchange reaction of Avi-KRAS (0-1200 nM) with Eu^{3+}-GTP (5 nM, 20 nM, and 80 nM). This nucleotide exchange was monitored with QRET as the Eu^{3+}-GTP–Avi-KRAS interaction protects the Eu^{3+}-GTP from the soluble quencher, thus resulting in increase of TRL-signal. The following interaction of biotinylated Avi-KRAS with SA-Alexa680 (20 nM) enabled the energy transfer from the Eu^{3+}-GTP donor to SA-Alexa680, thus facilitating TR-FRET and QTR-FRET monitoring. The TR-FRET signals were monitored before addition of the quencher MG and monitoring QRET and QTR-FRET signals. The QTR-FRET improved the S/B ratio 3-fold compared to TR-FRET at highest Eu^{3+}-GTP concentration (**Figure 16A**). This improvement was likely due to the increasing concentrations of non-bound Eu^{3+}-GTP–Avi-KRAS complexes in the solution since the 20 nM SA-Alexa680 is inadequate for full binding. In this situation, the concentration of free Eu^{3+}-GTP–Avi-KRAS increases the non-specific TR-FRET signal, whereas the specific signal stays constant. Thus, decreasing the Eu^{3+}-GTP–Avi-KRAS emission by quencher leads to higher S/B ratio of QTR-FRET compared to TR-FRET (**Figure 16A**). In addition to an S/B ratio increase, the QTR-FRET enabled

monitoring the Eu^{3+}-GTP interaction with Avi-KRAS through QRET as presented in the **Figure 16B**. This highlights the possibility of measuring two wavelengths in coupled assays of multiple analytes for monitoring separate binding events.

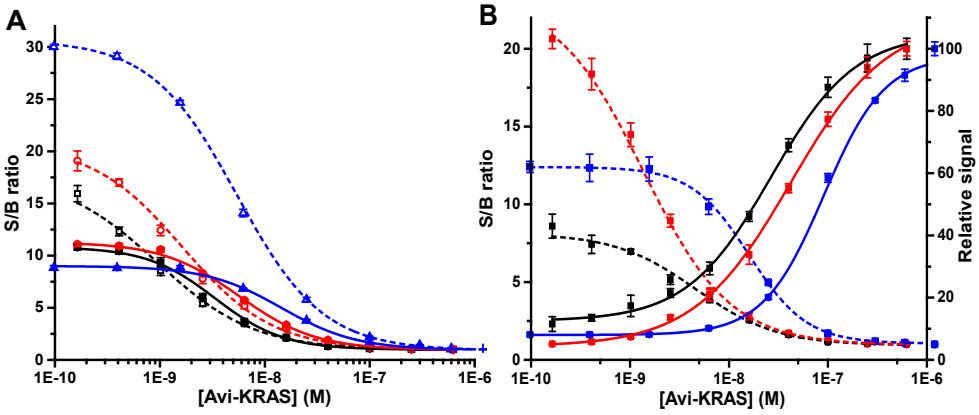

Figure 16. The QTR-FRET method improved the S/B ratio and enabled monitoring of dual interactions. Avi-KRAS titrations monitored with TR-FRET, QTR-FRET, and QRET were performed with 5 nM (black), 20 nM (red), and 80 nM (blue) Eu^{3+}-GTP in presence of SOS^{cat} (10 nM) and SA-Alexa680 (20 nM). **A**) TR-FRET (solid) monitoring in low Avi-KRAS concentrations reported S/B ratios between 9 and 12, which decreased as Avi-KRAS concentration increased. After MG (10-20 µM) addition, the QTR-FRET (dashed) monitored 3-fold improved S/B ratios. **B**) MG addition enabled QRET (solid) monitoring of SOS^{cat} catalyzed nucleotide exchange of Avi-KRAS with Eu^{3+}-GTP from the same well together with QTR-FRET (dashed). Data represent mean ± SD (n = 3).

The new QTR-FRET assay was compared to TR-FRET and QRET assays in two model PLI assays. In the QTR-FRET the background luminescence of non-bound Eu^{3+}-ligand was efficiently reduced with the addition of the soluble quencher. This functionality enables the use of increased Eu^{3+}-ligand concentrations, which is especially beneficial for studying low affinity interactions. The QTR-FRET assay also has the potential for monitoring dual-binding assays at different wavelengths. Firstly, the binding of Eu^{3+}-ligand to its target is monitored with QRET at 615 nm and secondly the following energy transfer with QTR-FRET at the acceptor emission window. This was further investigated in the publication **II** and discussed in the following paragraph.

5.1.2 Protein-ligand and subsequent protein-protein interaction studies (II)

In publication **II** the potential of the QTR-FRET assay for monitoring PLI and subsequent PPI was investigated with two model assays. The first model monitored the nucleotide exchange of RAS with Eu^{3+}-GTP association (PLI) followed PPI with

RAF-RBD-Alexa680. In the second model, the γ-GTP-Eu^{3+} association to G(i)α (PLI) and the following the post-translational modification (PTM) of ADP-ribosylation of G(i)α catalyzed by PTX were measured.

In the RAS model, the initial nucleotide exchange of GDP to Eu^{3+}-GTP was performed by SOS^{cat} and monitored from increased TRL emission of Eu^{3+}-GTP (**Figure 17**). If the nucleotide exchange is blocked and the Eu^{3+}-GTP remains unbound, its TRL emission is quenched by the soluble quencher MG in the assay. Following the nucleotide exchange and PLI, the Eu^{3+}-GTP–RAS complex binds to RBD-RAF-Alexa680 (PPI), which leads to energy transfer from Eu^{3+}-chelate to the Alexa680 label, which then emits the TR-FRET signal. It was hypothesized that both the SOS^{cat} induced nucleotide exchange and the following RAS-GTP–RAF-RBD interaction and their inhibition can be monitored simultaneously, and this was demonstrated by two inhibitor molecules, DARPins.

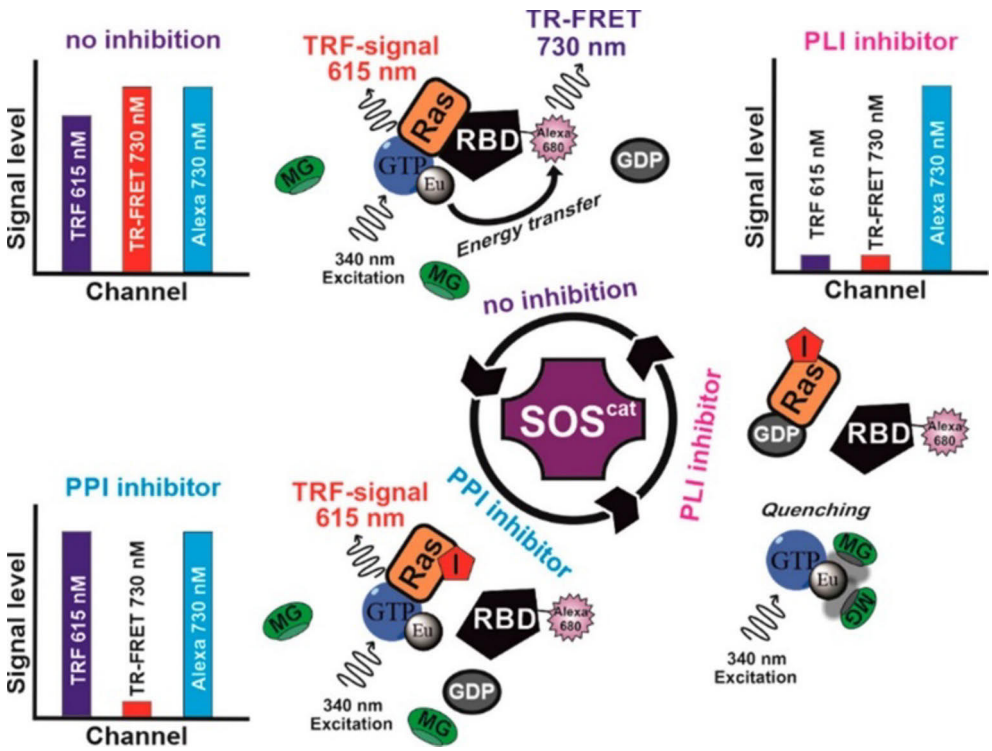

Figure 17. QTR-FRET is suitable for studying both nucleotide exchange (PLI) by SOS and the following RAS/RBD-RAF interaction (PPI) simultaneously in dual-parametric form. In the nucleotide exchange the GDP dissociation from RAS is initiated by SOS^{cat} thus enabling Eu^{3+}-GTP association to RAS (PLI). The binding protects the Eu^{3+}-GTP from the soluble quencher MG thus leading to increased TRL-signal. The Eu^{3+}-GTP–RAS interaction facilitates binding of the complex to RBD-RAF-Alexa680 (PPI), which leads to energy transfer from Eu^{3+}-chelate to Alexa680. Thereafter TR-emission of Alexa680 can be monitored to observe the PPI.

The QTR-FRET performance as a kinetic single well method was evaluated by investigating inhibition of KRAS nucleotide exchange and PLI with the DARPin K27 (500 nM) and RAS/RBD-RAF interaction using DARPin K55 (5 µM). These inhibitors were combined with Eu^{3+}-GTP (25 nM), MG (25 µM), KRAS (200 nM), and RBD-Alexa680 (25 nM) before addition of SOS^{cat} (10 nM). When no inhibitor was present, QTR-FRET successfully distinguished the addition of SOS^{cat} and the nucleotide exchange of KRAS (PLI) as increasing TRL emission of Eu^{3+}-GTP (**Figure 18A**). QTR-FRET also monitored the subsequent RAS–RAF-RBD interaction as TR-FRET emission of Alexa680 (**Figure 18B**). The addition of DARPin K27 inhibits the nucleotide exchange and subsequent RAS–RAF-RBD interaction and resulted in decrease of both TRL signal in **Figure 18A** and TR-FRET in **Figure 18B**. The K55 addition only reduced the TR-FRET signal in **Figure 18B** thus visualizing how K55 only blocks the RAS–RAF-RBD interaction. This difference in the inhibition effect is due to the different bindings sites of K27 and K55 to the RAS protein.

The QTR-FRET capability for monitoring RAS regulation through glycosylation was also evaluated. The glycosylation of RAS is an example of a PTM that blocks the RAS–RAF-RBD interaction by inhibiting the nucleotide exchange, which was performed by *bacterial clostridium perfringes* lethal toxin (TpeL). In this assay, a nucleotide exchange with either Eu^{3+}-GTP or Eu^{3+}-GDP (25 nM) was performed before adding TpeL in increasing concentrations with UDP-GlcNAc (25 µM) sugar. The effect of KRAS glycosylation in increasing TpeL concentrations resulted in decreasing TR-FRET emission (**Figure 18C**). Additionally, this assay demonstrated the correct functionality of QTR-FRET as no TR-FRET signal was observed when Eu^{3+}-GDP was loaded into KRAS, as KRAS-GDP does not interact with RAS–RAF-RBD (**Figure 18C**). These results indicate that the QTR-FRET assay is suitable for single well monitoring of nucleotide exchange and RAS/RAF-RBD interaction along with their inhibition. QTR-FRET also has potential for investigation of PTMs.

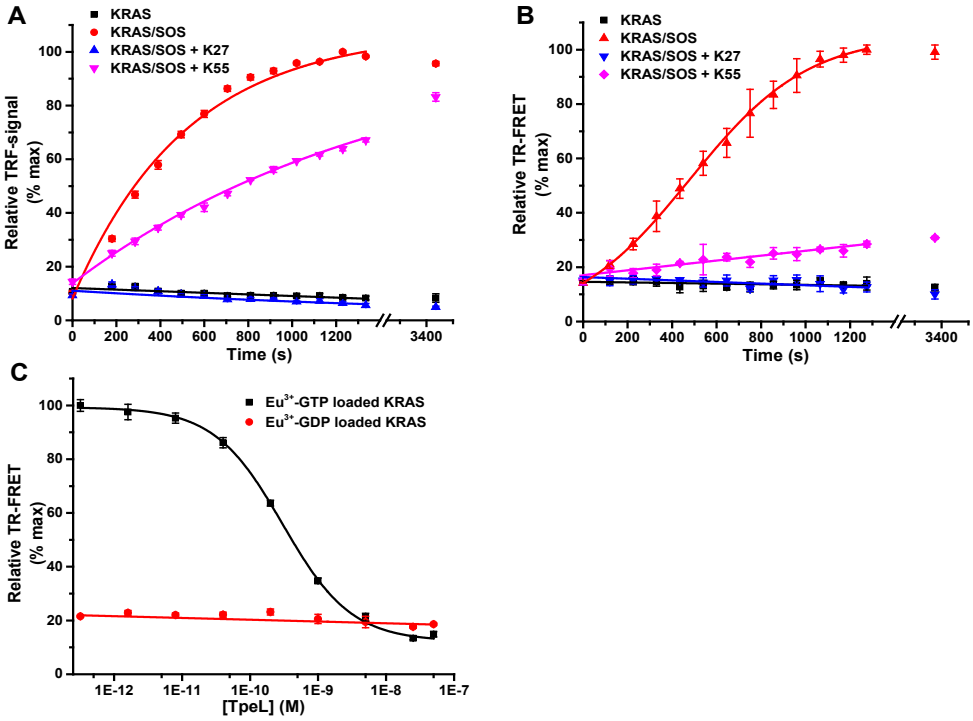

Figure 18. QTR-FRET monitoring of nucleotide exchange (PLI) and KRAS/RAF-RBD (PPI) in a single-well format. Eu^{3+}-GTP (25 nM) association facilitated by SOS^{cat} (10 nM) to KRAS (200 nM) was monitored at 340/615 nm (**A**) and the subsequent KRAS–RAF-RBD (25 nM) interaction at 340/730 nm (**B**). Excluding SOS^{cat} (black) resulted in low TRF and TR-FRET signals, while including SOS^{cat} (red) led to a rapid increase of TRL-signal and slightly delayed TR-FRET signal increase. The Eu^{3+}-GTP exchange and subsequent PPI are blocked by the inhibitor K27 (blue) thus low TRF and TR-FRET were observed. The KRAS/RAF-RBD interaction is interrupted by the K55 (magenta), which leads to a slight decrease of TRF and significant reduction of TR-FRET. All tests were performed with 24 µM MG. **C**) The Eu^{3+}-GTP or Eu^{3+}-GDP loaded KRAS was glycosylated by increasing TpeL concentrations with UDP-GlcNAc sugar. This blocks the KRAS–RAF-RBD interaction, which was monitored as clear decrease of TR-FRET signal at 730 nm with the Eu^{3+}-GTP loaded KRAS. No TR-FRET signal was monitored with Eu^{3+}-GDP-KRAS as it does not enable KRAS–RAF-RBD interaction. Data represent mean ± SD (n = 3).

The dual parametric assay format of QTR-FRET was next modelled with ADP-ribosylation of GTP-binding G(i)α catalyzed by PTX. In the assay, the ADP-ribosylation of G(i)α (150 nM) was performed with bio-NAD^+ (25 nM) with increasing concentrations of PTX, before γ-GTP-Eu^{3+} (25 or 50 nM) loading in the presence and absence of GTP (10 µM). The previously utilized Eu^{3+}-GTP lacked the required affinity with the G(i)α protein the new γ-GTP-Eu^{3+} had to be prepared. The G(i)α was loaded with γ-GTP-Eu^{3+} by $MgCl_2$/EDTA exchange, where the EDTA chelates $MgCl_2$ and unloads the GDP from G(i)α. The excess $MgCl_2$ is then utilized

to load the γ-GTP-Eu^{3+} to G(i)α. ADP-ribosylation was monitored by adding SA-Alexa680 (25 nM) and MG (20 or 35 µM) and higher TR-FRET and QTR-FRET signals were monitored as the PTX concentration increased (**Figure 19A**). MG addition increased the S/B ratios, which were calculated by comparing the signal of the GTP-blocked reaction to successful γ-GTP-Eu^{3+} loading. Additional TRL signal monitoring at 615 nm ensured that the PTX had no effect on the γ-GTP-Eu^{3+} loading (**Figure 19B**). At 615 nm the difference in S/B ratios were due to more complete G(i)α loading with increased γ-GTP-Eu^{3+} concentration.

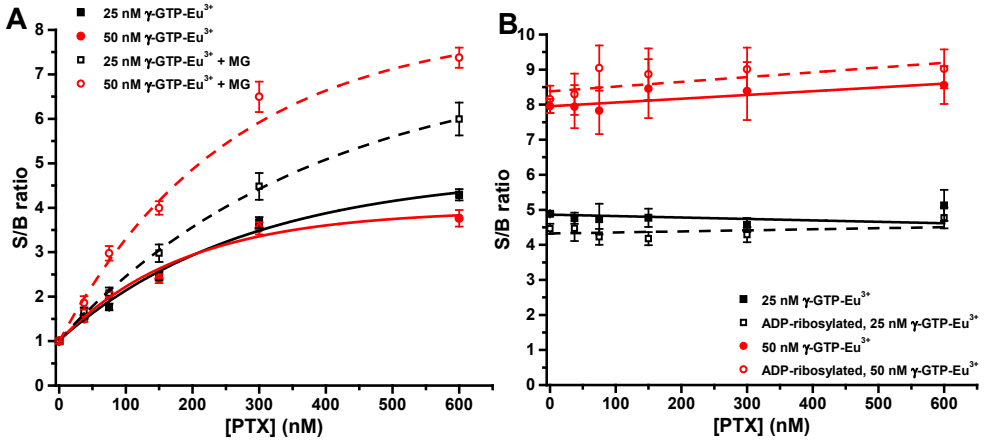

Figure 19. QTR-FRET dual-parametric monitoring of G(i)α γ-GTP-Eu^{3+} association and ADP-ribosylation. The G(i)α (150 nM) ADP-ribosylation with biotin-NAD^+ (25 nM) catalyzed by PTX (0–600 nM) was monitored by TR-FRET with additional SA-Alexa680 as acceptor and QRET. The signals of the γ-GTP-Eu^{3+} (25 or 50 nM) loaded G(i)α were divided by those with GTP to obtain S/B ratios. **A**) Additional MG (dashed vs. solid) improved the S/B ratios significantly especially with higher γ-GTP-Eu^{3+} concentration. **B**) The QRET signals were unaffected by ADP-ribosylation (dashed vs. solid) and only increased γ-GTP-Eu^{3+} association in higher concentration increased the S/B ratios. Data represent mean ± SD (n = 3).

In summary, the QTR-FRET combines the single-label QRET and dual-label TR-FRET techniques to provide a single well kinetic method for monitoring two interactions with high sensitivity. The method is also suitable for studying molecular inhibitors or modifications of interacting targets that affect the interactions. In addition it provides increased S/B ratio compared to the conventional TR-FRET since the background signal of donor emission is greatly reduced. Based on the results obtained with the model assays, QTR-FRET can be converted for new targets and inhibitors.

5.2 The Protein-Probe

During the work presented in this thesis, a new assay, the Protein-Probe, was developed as a label free method based on an external Eu^{3+}-probe reporter for investigating PLIs and protease activity. The Eu^{3+}-probe has a peptide sequence that enables binding to proteins and especially their hydrophobic regions. During these studies, the Protein-Probe method has been applied for monitoring PLI through thermal stability of a target protein (**III**) and observing the digestion activity of proteases (**IV**). These approaches will be discussed during the rest of this chapter.

5.2.1 Thermal profile and protein-ligand interaction studies (III)

The Protein-Probe method was developed as an approach to study PLI and the stabilizing effect of ligand on the target protein. The design focused on simplicity through a label-free, rapid, and homogenous format with increased sensitivity compared to conventional TSAs. The conventional TSAs rely on the quenching effect of water upon the dye, e.g. SYPRO Orange, 1,8-ANS, or 1,6-TNS. The Protein-Probe TSA is based on a modulation solution containing a soluble quencher that prevents the TRL emission from the Eu^{3+}-probe. The Eu^{3+}-probe binds especially to the hydrophobic region of the proteins. The binding divides the Eu^{3+}-probe and the quencher, and results in TRL-signal increase. Since the hydrophobic core of a protein is exposed during denaturation, the thermal stability of the target protein can be studied with the Protein-Probe via the Eu^{3+}-probe interaction. The target protein can be stabilized by interaction with a suitable ligand, which results in an increased denaturation temperature (T_m). The increased Tm results in the TRL-signal of the Protein-Probe increasing in higher temperature compared to the non-bound target protein. This principle enables the observation of PLI through thermal shift with the Protein-Probe assay **(Figure 20**).

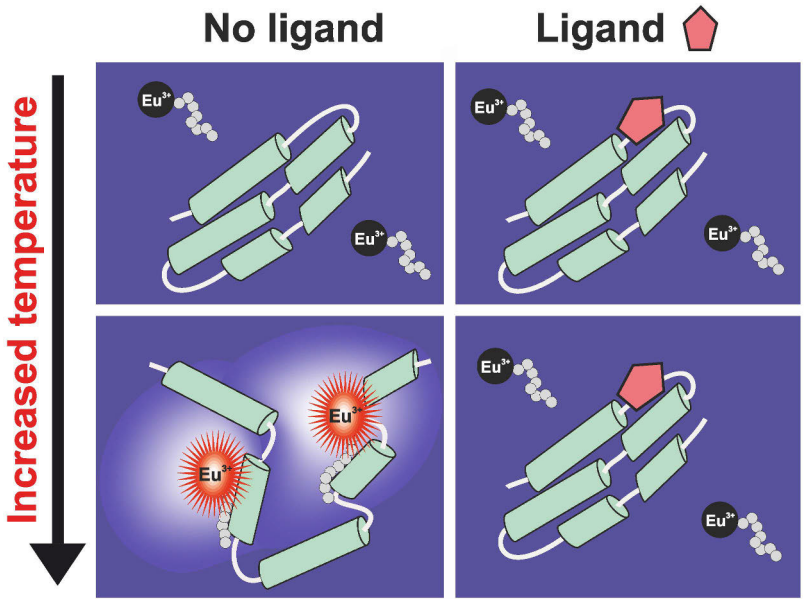

Figure 20. The principle of the Protein-Probe method for TSA. In the modulation solution with soluble quencher the TRL-signal of Eu^{3+}-probe is low in the presence of native protein. The TRL-signal increases when thermal denaturation exposes the hydrophobic core of the protein for Eu^{3+}-probe interaction. Ligand interaction stabilizes the protein and thus increases the melting temperature, which leads to thermal shift and enables protein-ligand interaction monitoring.

Initially the Protein-Probe method was compared to the conventional TSA with SYPRO Orange dye. First, the reliability of the Protein-Probe was tested by monitoring the thermal profile of IgG_1 (80 nM for Protein-Probe and 2 µM for SYPRO Orange) from 25 to 80 °C in 5 °C intervals. The assays were performed by heating IgG_1 for 3 min in the sample buffer before adding the Protein-Probe modulation solution or SYPRO Orange and monitoring the Protein-Probe TRL-signals and SYPRO Orange fluorescence. Both methods successfully observed the denaturation of IgG_1, and the T_m values calculated from the denaturation curves were virtually identical at 67.0 and 66.6 °C for the Protein-Probe and SYPRO Orange, respectively (**Figure 21A**). Secondly, the sensitivities of the methods were compared in a titration assay of IgG_1 heated to 90 °C. The Protein-Probe method resulted in a 50-fold increase in the sensitivity calculated at the S/B ratio of 3 compared to SYPRO Orange (**Figure 21B**). These results highlight the potential of the Protein-Probe as a reliable method with an increased sensitivity compared to conventional methods based on fluorescent dyes.

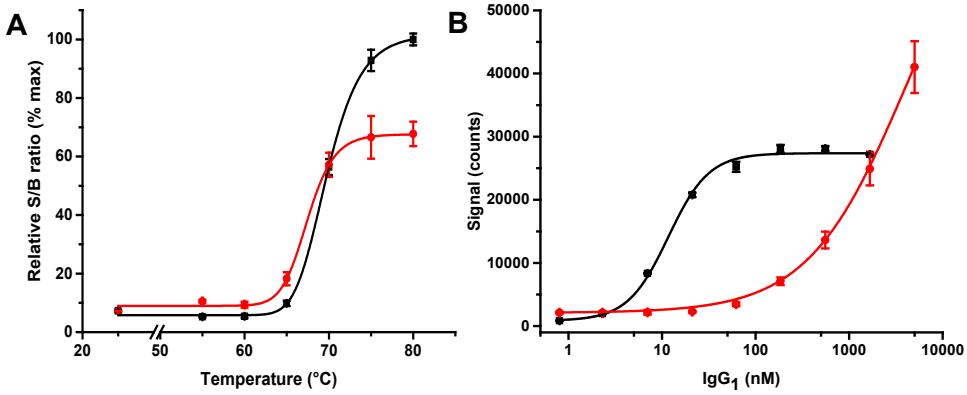

Figure 21. The Protein-Probe assay monitors the same melting temperature with increased sensitivity compared to SYPRO Orange. **A**) The melting curves of IgG_1 (80 nM, 2 µM) were monitored with the Protein-Probe containing 1 nM Eu^{3+}-probe (black) and SYPRO Orange (red), respectively. The T_m values obtained from sigmoidal fitting curves were effectively equal between methods. **B**) IgG_1 titration (0-5 µM) at 80 °C revealed a 50-fold sensitivity increase when monitored with the Protein-Probe (black) compared to SYPRO Orange (red), calculated at SB ratio of 3. Data represent mean ± SD (n = 3).

The main aim of conventional TSA methods is to investigate the effect of PLI or PPI on the T_m of the protein to obtain information on the stabilizing effect of the ligand binding to the protein. The Protein-Probe was tested with two model proteins, SA and CA, with known ligands, biotin and AZA, respectively. Firstly, ligand titrations were performed at a temperature where the ligand stabilized the protein and prevents full denaturation. The Protein-Probe assay successfully detected the stabilization effect of increasing ligand concentration on the target protein (**Figure 22A**). Based on these results, a saturating concentration of ligand was chosen to test the TSA capability of the Protein-Probe. Denaturation curves for both proteins were successfully monitored with and without ligands and thermal shifts of 2.1 and >15 °C were calculated for CA and SA, respectively (**Figure 22B**). With SA the stabilization effect of biotin resulted in a denaturation temperature above 100 °C, which was unfortunately unmeasurable.[167]

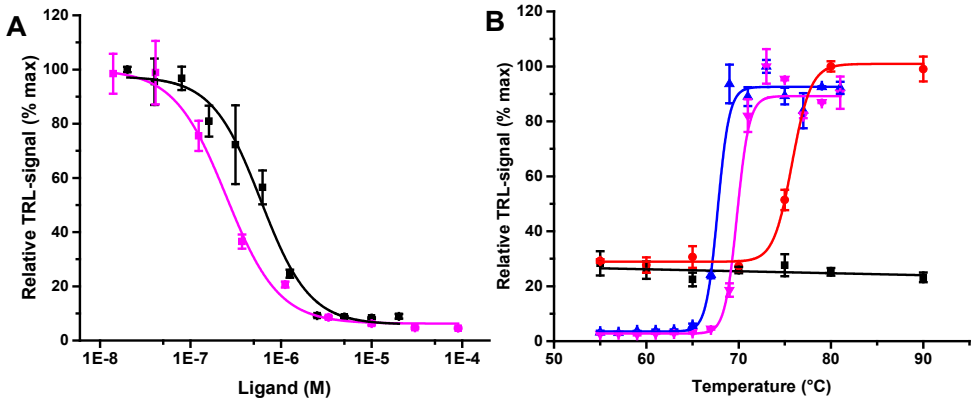

Figure 22. The Protein-Probe observed the ligand binding effect on the T_m of the studied protein. **A)** The Protein-Probe with 1 nM Eu^{3+}-probe monitored biotin (black) and AZA (magenta) titration with SA (400 nM) and CA (200 nM) at denaturation temperatures. The EC_{50} values for both ligands were in stoichiometry with their target proteins. **B)** The Protein-Probe reported T_m values for SA (red, 400 nM) and CA (blue, 200 nM) with and without their respective ligand in saturating concentration, biotin (black, 10 µM) and AZA (magenta, 5 µM). There were clear thermal shift of 2.1 and >15 °C between the T_m of CA and CA–AZA and SA and SA-biotin, respectively. Data represent mean ± SD (n = 3).

In summary, it was concluded from publication **III** that the Protein-Probe method is suitable for investigating the denaturation of proteins and the effects of ligand binding on the stability of proteins. The method is robust and highly sensitive, which enables the consumption of less proteins and ligand, minimizing the possibility of spontaneous aggregation and decreasing assay costs. As a homogeneous and label-free multiwell-plate assay the Protein-Probe method is an attractive option for drug discovery purposes.

5.2.2 Substrate independent digestion efficiency monitoring (IV)

Another important target for novel drugs are proteases. They control multiple processes in human bodies, such as digestion and the immune system, and their impaired activity plays a part in many diseases e.g. HIV and cancer. Unfortunately, developing assays for proteases is complicated as each protease cleaves specific peptide sequences of the substrate protein, which makes the development of assays requiring the labeling of protease substrates particularly problematic. As a label-free assay the Protein-Probe assay provides a highly versatile alternative since the Eu^{3+}-probe is capable of binding to numerous natural substrate proteins. When these natural substrate proteins are digested, the Eu^{3+}-probe is no longer bound to the target

substrate and protected from the soluble quencher in the Protein-Probe modulation solution. This decreases the TRL emission of the Eu^{3+}-probe (**Figure 23**). Thus the digestion efficiency of proteases can be investigated with the Protein-Probe assay.

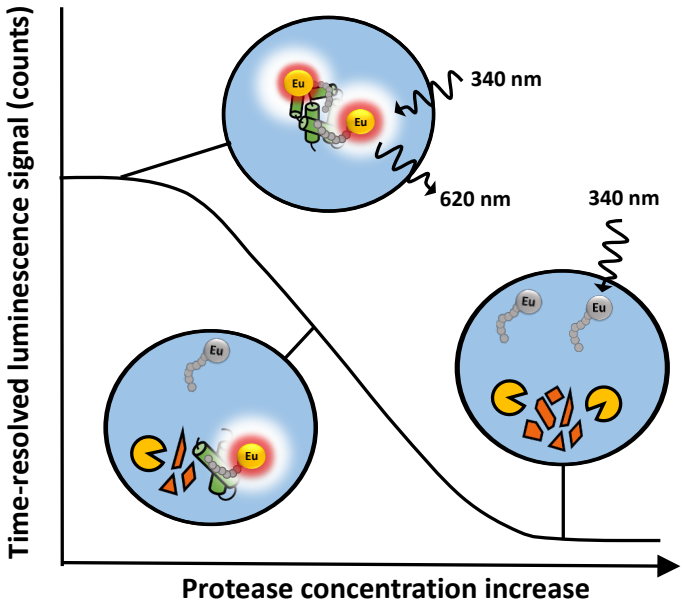

Figure 23. The principle of the Protein-Probe for studying digestion efficiency. When the Eu^{3+}-probe of the Protein-Probe interacts with the hydrophobic regions of intact substrate protein, it is separated from the soluble quencher in the modulation solution and emits TRL at 620 nm. This interaction is prevented by substrate digestion by protease thus decreasing the TRL-signal of Eu-probe due to quenching.

Concentration is known to affect the efficiency of proteases for substrate digestion. To study this with the Protein-Probe, papain was titrated with a model substrate, CA. Both heat denatured and native CA were digested, since denaturation is known to increase the TRL-signal obtained with the Protein-Probe. This assay was performed by digesting the heat denatured (3 min, 85 °C) CA (3 nM) and native CA (100 nM) with papain in 37 °C for 30 min. Modulation solution with 1 nM Eu^{3+}-probe was then added and the TRL-signals were monitored. The Protein-Probe successfully monitored the digestion of denatured and native substrate CA with the EC_{50} values of 1.9 ± 0.1 nM and 0.14 ± 0.01 nM, respectively (**Figure 24A**). The decreased substrate concentration lowered the required protease amount for effective digestion while maintaining high S/B ratio. However, this effect was not linear, which could be explained by the open structure of the denatured protein being prone to digestion. Nonetheless, the results confirmed that digestion of both denatured and native substrate can be monitored with the Protein-Probe assay.

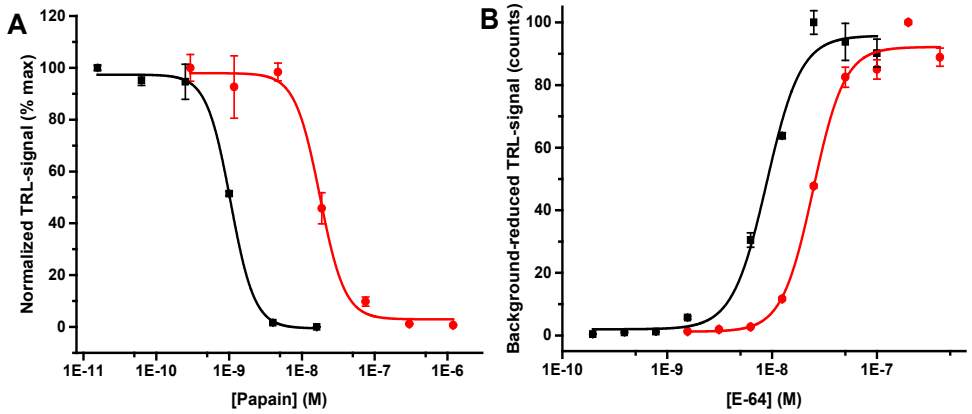

Figure 24. The Protein-Probe monitoring of heat denatured and native CA digestion by papain. In all assays the digestion were performed at 37 °C (30 min) before adding the Protein-Probe modulation solution and measuring TRL-signals. **A**) Denatured (3 nM, black) and native (100 nM, red) CA were digested with increasing amounts of papain. The EC_{50} values of 0.14 ± 0.01 nM and 1.9 ± 0.1 nM and S/B ratios of 59 and 62 were obtained with denatured and native CA, respectively. **B**) The inhibition of digestion of denatured CA (3 nM) and native CA (100 nM) by papain (1 or 100 nM, respectively) was investigated with titration of E-64. The obtained EC_{50} values were 8.9 ± 0.9 nM and 24.7 ± 1.8 nM for the denatured and native CA, respectively. Data represent mean ± SD (n=3).

Abnormal digestion activity is linked to multiple diseases and protease inhibitor drugs have been developed to combat these issues. Thus inhibitor screening is an important property of every protease activity monitoring assay. Since inhibitor E-64 blocks papain digestion, its effectiveness was investigated by E-64 titration in two papain substrate combinations; 1 nM papain with denatured CA (3 nM) and 100 nM papain with native CA (100 nM). The inhibitor and protease were combined prior to substrate addition and digestion reaction. Then the modulation solution was added, and TRL signals monitored as previously. The EC_{50} values for denatured and native CA were 8.9 ± 0.9 nM and 24.7 ± 1.8, respectively (**Figure 24B**). As expected, these values were different for each protease concentration and they were in accordance with reported literature values.[170–172] These results suggest that the Protein-Probe method holds high potential for screening of novel protease inhibitors.

To combat the problematic aspect of protease and substrate heterogeneity, the Protein-Probe assay was designed to monitor digestion activity irrespective of the substrate protein. This was demonstrated by monitoring the digestion activity of papain and pronase (0-100 nM) with nine different native model substrates, eIF4A1, PTX, MDH, SOS^{cat}, BSA, CA, KRAS, G(i)α, and p120GAP, at two concentrations,

25 and 50 nM. Since these substrates have unequal binding with the Eu^{3+}-probe, they were exposed to heat denaturation (3 min at 60 or 70 °C) after the digestion reaction (10 min at 37 °C) to guarantee their detectability. The substrates were heat denatured after digestion to ensure that no effect befalls on the protease activity. In addition, the same set of native substrates was monitored without denaturation.

The Protein-Probe assay detected digestion activity of both papain and pronase towards all substrates, calculated from the background-reduced TRL-signal decrease when the substrate was incubated with or without the protease. At the 50 nM concentration, seven of the nine substrates resulted in clear TRL-signal without post-digestion denaturation. Heat denaturation increased the maximum signal 5–95 times above the signal obtained for four of the non-digested substrates. Significantly with MDH, which was undetectable in native form, the S/B ratio increased from 2.9 to 291 (**Figure 25**). As the denaturation was carried out after digestion, it had no impact on the protease activity. However, the selection of substrate protein had a great effect on digestion efficiency, as pronase was most active with PTX and KRAS and papain with p120GAP and PTX. Both proteases required high concentrations for BSA digestion, as well as with G(i)α and CA for pronase and SOS^{cat} for papain. These results highlight the importance of substrate selection for specific protease studies. For further investigation of the results, MDH and eIF4A were chosen due to their different detectability. Native MDH resulted in low TRL-signals in both concentrations, whereas eIF4A was detectable even at 25 nM concentration. Heating increased the MDH obtained TRL-signals over 90-fold (**Figure 25A** & **25B**) but only 2.6-fold with eIF4A (**Figure 25C** & **25D**). With both substrates the digestion efficiency was mainly affected by the protease and substrate concentrations. With the lowest protease concentration the digestion efficiency increased up to 7.1 and 1.4 fold with post-digestion heated and native substrate, respectively. This effect diminished in higher protease concentrations, indicating that less protease is required to digest lower substrate concentrations.

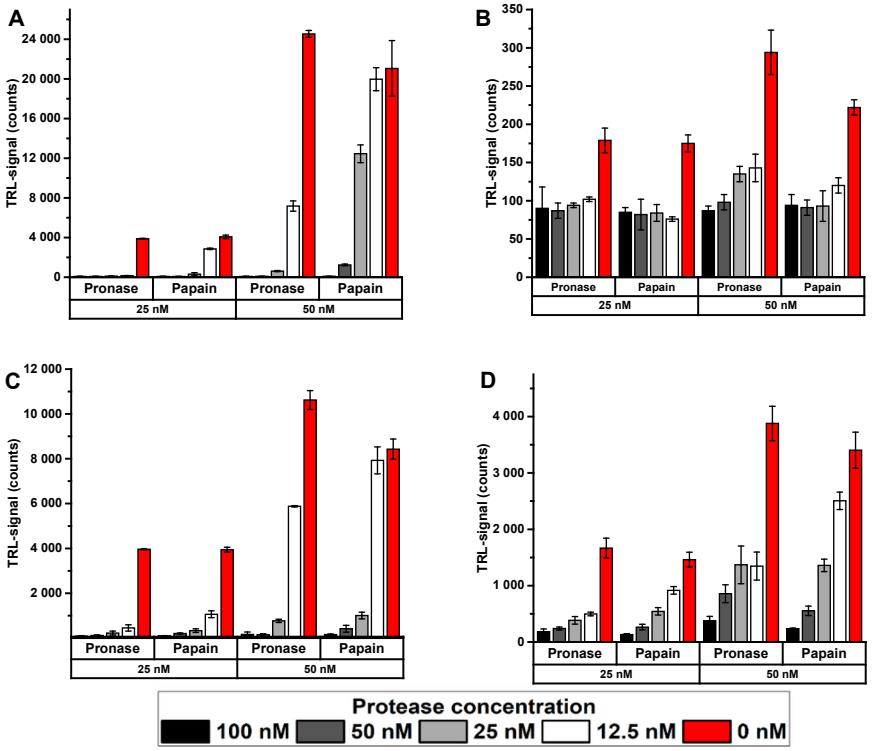

Figure 25. The digestion of MDH and eIF4A by pronase and papain. The digestion activity of pronase and papain (0-100 nM) was monitored by the Protein-Probe with post digestion denatured (**A** & **C**) and native (**B** & **D**) MDH and eIF4A (25 or 50 nM). Native MDH yielded a low TRL-signal, which increased over 90 fold with denaturation. The eIF4A was detectable in the native form with only a slight, 2.9 fold, increase of TRL-signals obtained by denaturation. Data represent mean ± SD (n=3).

The developed Protein-Probe method enables the monitoring of protease activity and inhibition with variety of unmodified substrate proteases in their denatured and native forms. This mimics the digestion of natural protease targets in cellular systems and provides an assay for studying inhibitor and substrate specificity. The Protein-Probe is a highly sensitive and label-free method, requiring only nanomolar levels of proteins and external Eu^{3+}-probe. The versatility of the Protein-Probe was enhanced with post-digestion denaturation of substrates that were at room temperature. This, however, had no effect on the digestion efficiency. These properties, together with the simple one step homogenous protocol, make the Protein-Probe assay highly desirable for protease targeting drug discovery and the first in its class of truly universal methods for proteases and their substrates.

6 Conclusions

Drug development is an incredibly costly and time-consuming process. The initial drug discovery is important for ensuring the safety and effectiveness of the candidate drug before proceeding to the more costly clinical trials. In drug discovery a variety of in vitro and in vivo methods are employed, and new assays are always required to obtain more reliable results and to minimize costs and time consumption. Many of the methods utilized in drug discovery are based on photoluminescence and benefit from quenching, such as the FRET methods and the quenching effect of water discussed in this thesis. FRET and TR-FRET are the basis of many commercial biochemical methods, such as Z'-LYTE, LANCE, HTRF, and TruPoint. Some TR-FRET methods, such as Tag-lite and QRET, utilize living cells to study membrane protein interactions. The fluorescent dye quenching in aqueous solution is utilized in DSF to study, e.g. protein characteristics, aggregation, and interactions in homogenous and label-free format. The methods presented in the literature review and developed during this thesis are compared in **Table 2** at the end of literature review.

The first method in this thesis, QTR-FRET, was developed as a combination of TR-FRET and QRET. The aim of the QTR-FRET approach was to improve the S/B ratio of conventional TR-FRET by reducing the interference of donor emission in the acceptor channel caused by excess donor concentration (**I**). The improvement is achieved by additional soluble quencher, which decreases the emission of the non-bound Eu^{3+}-donor. The donor quenching allows the use of higher donor concentrations, which enables investigation of low affinity interactions (**I**). QTR-FRET also allowed single well monitoring of PLI and the following PPI in a real-time format after energy transfer from donor to acceptor (**II**). This is enabled by monitoring the protein interaction with Eu^{3+}-ligand (donor) at one wavelength (PLI) and the subsequent interaction of this protein-ligand complex with acceptor labelled protein at another wavelength (PPI). QTR-FRET can be used to monitoring the inhibition of both PLI and PPI separately and is suitable for similar targets as conventional TR-FRET. In contrast to multiplexing TR-FRET methods, which requires labeling of at least three compounds, QTR-FRET only requires dual labeling of the ligand with the Eu^{3+}-chelate donor and protein with FRET acceptor

dye. Still, the labeling may complicate the assay conversion to novel target biomolecule interactions and cause steric constraints, which will affect the PLI and PPI. QTR-FRET benefits from the same high sensitivity of time-resolved measurements and simplicity of homogenous assay format as TR-FRET. In the future the QTR-FRET method could be modified for studying multiple PLI and PPI models, e.g. for investigating the inhibition of these interactions. QTR-FRET also has potential for cell-membrane protein studies as QRET is already suitable for GPCR protein studies.

The Protein-Probe method developed during the studies presented in this thesis is based on monitoring the TRL emission of an external probe containing Eu^{3+}-chelate. The emission of the unbound Eu^{3+}-probe is quenched but Eu^{3+}-probe interaction with the target protein prevents this quenching and results in increased TRL emission. In publication **I,** the Eu^{3+}-probe interacted with the unfolding structure of the denaturing target protein and enabled PLI investigation by monitoring the thermal shift of the target protein. The novel Eu^{3+}-probe and the utilized time-resolved measurements of the Protein-Probe resulted in 50-fold improved sensitivity, compared to conventional SYPRO Orange assay (**I**). This improvement lowers assay target protein consumption and thus decreases assay costs. Unfortunately, the component consumption is also increased since the two-step protocol of the Protein-Probe requires individual samples for each temperature. A single-step protocol for the Protein-Probe method is currently under development and promising results have been obtained with an improved external probe. The Protein-Probe method was utilized in publication **II** for monitoring the protease activity though digestion of a variety of unmodified substrate proteins. The activity of proteases is monitored as emission increase and potential inhibitors result in decreased TRL-signal. The assay detectability of substrate protein is enhanced by thermal denaturation of the substrate, thus reducing the amount of substrate, protease and inhibitor required. The method functions at nM range and enables a multitude of protease and substrate combinations for screening a variety of inhibitors.

In articles apart from those presented in this thesis, the Protein-Probe method has also been used to investigate a multitude of PPIs and the aggregation of antibodies. These PPIs have included complex formation of multiple proteins, and the aggregation monitoring capabilities were utilized for formulation studies. The potential of the Protein-Probe method for other enzyme studies apart from proteases is yet unexplored and could result in interesting new assays for enzyme activity investigations.

Acknowledgements

This doctoral thesis was carried out under the drug research doctoral programme in the Detection Technology laboratory from 2018 to 2021. My deepest gratitude goes to the Drug Research Doctoral Programme and Instrumentarium Science Foundation for their financial support towards my work. I am also grateful to the heads of the chemistry department Prof. Pasi Virta, Prof. Juha-Pekka Salminen, and Prof. Carita Kvarnström for the opportunity to perform my studies in their department. I also wish to thank the pre-examiners who took time and effort to evaluate and comment my work, as well as my opponent for immersing himself in my research.

I want to thank my supervisors Docent Harri Härmä and Dr. Kari Kopra. As the head of our group, Harri is a continuous source of ideas and concepts. Whenever there was a moment I found myself lost, Harri found a way for me to continue. Thank you for choosing me for this journey. And thank you for your support, Kari, starting from our first talk about the doctoral thesis, when I was unsure if I even wanted to start walking this road. Your expectations and helpfulness have pushed me forward. I always felt I could approach either of you when I had problems and questions about our research.

Now, I would like to draw attention to the heroes of the chemistry department. I was always armed with the best computers and IT-support from Kari Loikas. I cannot believe you will retire soon. Machines also seemed to break near me, but Mauri Nauma was always there to fix them when needed. Thank you for modding my microscope and saving our incubator from a trip to China. I also needed so many tubes, tips, and reagents for my studies and I could always email Kirsi Laaksonen and she would find them for me. Especially when I struggled setting up our cell lab and made huge orders of pipette tips, you were always willing to help.

I also wish to thank the personnel at City-Lab and Biotop, who always found even the most obscure things I needed. It was always a pleasure to visit you, as I left with my hands full of candy and chocolate to share with my lab mates. I hope your business continues to grow.

I am grateful to thank the other people who were part of our lab when I was walking along my path. Ville was there when I first started as a foolish cell-culture summer worker. It was nice to have someone who I could talk about our doctoral

programmes' inner workings and Star Wars. I was also lucky to meet our new doctoral students, Nazia and Randa, and I hope you'll succeed in your projects. I also want to wish a nice last year of master's studies to the students who came to visit our lab: Titta, Milja, Suvituuli, and Juho. I hope you learned as much from me as I learned from you. I will do my best to improve as a teacher in the future. If you ever need help, just send me a text.

Can you believe this Salla?! I never would have made it through without you and your support. You have helped me from placing the commas to vanquishing melancholy. You are like the twin that I never had. We share a love for games, animals, music, and writing, but also the plight of worrying too much and trying to please everyone. I know that with your attitude you will do great in everything you decide to try! May we stay good friends in the years to come. Let us go to the dog park when you finally get your corgi named Rane. To both of you Salla and Jani, you are incredibly awesome! Thank you for introducing me to Annu and Cy, they are the best! Let our games never end.

And my childhood friend Merja. Without you, I never would have set foot in Turku nor its university. Thank you for the crazy notebook we wrote in the middle of the night and all the supporting talks we have had. Thank you for sharing so many things with me and letting me loisia. To all our wonderful memories, I will raise my finest glass of juice. Let there be more and more plants and laughs to remember. I wish all the happiness in the world to you and Roope. You are so epic! Zilmä!

And Huda. It was a near thing that we never met, but it also feels like it was meant to be. Your compassion shines, and seldom have I met a person more motivated and passionate to improve as you. I hope our paths continue to cross. Let us continue our hair growing competition, mine is 110 cm now! I really hope you and Jon have an incredible life!

And my friends Sini and Suvi. We have our nation of Herne. Now Työväki has become highly educated and our nation will be prosperous. Puolustusvoimat has an army of tiny monsters, cool partner Toni, and one amazing girl, Erin, to govern them. Hallitus has decided fitness is the craze and studying the finest aspiration. Our friendship is the sun, never waning and ever shining. Even when the world rotates and we are far apart, the sun shines on. The dawn will come, and we shall meet again, and all is as before. Sini, Toni, and Erin, we really need to buy a duplex house!

I love you, mom. As years fly by, the more I find myself agreeing with you. *Not all that glitters is gold.* As life is not always kind, let us be kind instead. You are the one most proud of me in the world, and I am proud to be your daughter. You taught me to be accepting and understanding, and to me this is more important than success. I know that I have inherited my smarts from you. Thank you for everything!

I also wish to thank other members of my family, especially my dad Heke, brother Joona, grandparents Saara and Pekka, Kaisa, Jouni, Lauri, Satu, Sari, Tero,

and cousins, Osku, Jaakko, Anni, Ville, Sofia, and Pihla. I'm always having fun when meeting you all, and your help has saved me multiple times. Thank you for thinking about me and stay awesome! Also Mila, why are you so cool? Your perseverance and determination in the face of difficulties have truly inspired me. You will conquer the world and bring your dreams to reality.

I am grateful to have so many people to thank. I want to acknowledge my friends and teachers from my earlier studies at biochemistry and virology departments, especially Sisko, Nelli, Noora, Laura, Milla, Pinja, and Vilma. I also wish to mention my friends from the chemistry department, especially Ade and Winnie. I am the worst at keeping in touch with my friends, but you keep dragging me into fun and interesting things.

Finally, I wish to thank all the healthcare personnel who have made sure my body and mind can take this journey, especially Susanna Ahola. These three years have been more difficult than all the rest of my years combined, but all the compassion and help I have received has humbled me. And even if you do not have your name mentioned here, be assured that I have thought about you when writing this. Also thank you, dear reader, I hope you have enjoyed at least the pictures I have drawn for this thesis. Sadly, paper is limited, and we have reached the conclusion.

Oh! How could I ever forget?! Thank you Reika, Ayako, and Doppio for always allowing me to scratch your ears. Sometimes it is important to remember that the world is found from walks through the forest and soft fur full of unconditional love.

I dedicate this work to you, my soulmate. You are always the first to stand up for me and protect me. You are my support and my home. You have taught me the meaning of love and through your eyes I ever continue to see my worth. ***The blood of the covenant is thicker than the water of the womb.*** We have shared all our battles and I will stand by you, as you have stood by me. There exists a world in us, and to you I gift mine. From the beginning of Time to the end of it and Beyond. May Destiny be kind and let us stay together for all Eternity.

10.11.2021

Emmiliisa Vuorinen

References

(1) Wouters, O. J.; McKee, M.; Luyten, J. Estimated Research and Development Investment Needed to Bring a New Medicine to Market, 2009-2018. *JAMA - Journal of the American Medical Association*. American Medical Association March 3, 2020, pp 844–853. https://doi.org/10.1001/jama.2020.1166.

(2) Matthews, H.; Hanison, J.; Nirmalan, N. "Omics"-Informed Drug and Biomarker Discovery: Opportunities, Challenges and Future Perspectives. *Proteomes* **2016**, *4* (3), 28. https://doi.org/10.3390/proteomes4030028.

(3) Hughes, J. P.; Rees, S. S.; Kalindjian, S. B.; Philpott, K. L. Principles of Early Drug Discovery. *British Journal of Pharmacology*. March 1, 2011, pp 1239–1249. https://doi.org/10.1111/j.1476-5381.2010.01127.x.

(4) Keseru, G. M.; Makara, G. M. Hit Discovery and Hit-to-Lead Approaches. *Drug Discovery Today*. Elsevier Current Trends August 1, 2006, pp 741–748. https://doi.org/10.1016/j.drudis.2006.06.016.

(5) Gong, Z.; Hu, G.; Li, Q.; Liu, Z.; Wang, F.; Zhang, X.; Xiong, J.; Li, P.; Xu, Y.; Ma, R.; Chen, S.; Li, J. Compound Libraries: Recent Advances and Their Applications in Drug Discovery. *Curr. Drug Discov. Technol.* **2017**, *14* (4). https://doi.org/10.2174/1570163814666170425155154.

(6) Dandapani, S.; Rosse, G.; Southall, N.; Salvino, J. M.; Thomas, C. J. Selecting, Acquiring, and Using Small Molecule Libraries for High-Throughput Screening. *Curr. Protoc. Chem. Biol.* **2012**, *4* (3), 177–191. https://doi.org/10.1002/9780470559277.ch110252.

(7) Hevener, K. E.; Pesavento, R.; Ren, J. H.; Lee, H.; Ratia, K.; Johnson, M. E. Hit-to-Lead: Hit Validation and Assessment. In *Methods in Enzymology*; Academic Press Inc., 2018; Vol. 610, pp 265–309. https://doi.org/10.1016/bs.mie.2018.09.022.

(8) Wunberg, T.; Hendrix, M.; Hillisch, A.; Lobell, M.; Meier, H.; Schmeck, C.; Wild, H.; Hinzen, B. Improving the Hit-to-Lead Process: Data-Driven Assessment of Drug-like and Lead-like Screening Hits. *Drug Discovery Today*. Elsevier Current Trends February 1, 2006, pp 175–180. https://doi.org/10.1016/S1359-6446(05)03700-1.

(9) Faqi, A. S. *A Comprehensive Guide to Toxicology in Preclinical Drug Development*; Faqi, A. S., Ed.; Academic Press: London ;, 2013.

(10) Jorgensen, W. L. Efficient Drug Lead Discovery and Optimization. *Acc. Chem. Res.* **2009**, *42* (6), 724–733. https://doi.org/10.1021/ar800236t.

(11) Akhondzadeh, S. The Importance of Clinical Trials in Drug Development. *Avicenna Journal of Medical Biotechnology*. Avicenna Research Institute October 1, 2016, p 151.

(12) Turner, J. R.; Hoofwijk, T. J. Clinical Trials in New Drug Development. *Journal of Clinical Hypertension*. J Clin Hypertens (Greenwich) May 2013, pp 306–309. https://doi.org/10.1111/jch.12085.

(13) Robuck, P. R.; Wurzelmann, J. I.; Merrick, M. Understanding the Drug Development Process. *Inflamm. Bowel Dis.* **2005**, *11* (SUPPL. 1). https://doi.org/10.1097/01.MIB.0000184851.46440.a3.

(14) Carnero, A. High Throughput Screening in Drug Discovery. *Clin. Transl. Oncol.* **2006**, *8* (7), 482–490. https://doi.org/10.1007/s12094-006-0048-2.
(15) Cowan, K. J. On Assay Robustness: The Importance of Early Determination and Science-Driven Decision-Making. *Bioanalysis*. Bioanalysis June 2013, pp 1317–1319. https://doi.org/10.4155/bio.13.101.
(16) Horrocks, W. D. W. [21] Luminescence Spectroscopy. *Methods Enzymol.* **1993**, *226* (C), 495–538. https://doi.org/10.1016/0076-6879(93)26023-3.
(17) Lakowicz, J. R. *Principles of Fluorescence Spectroscopy*; Springer, 2006. https://doi.org/10.1007/978-0-387-46312-4.
(18) Birks, J. B. Fluorescence Quantum Yield Measurements. *J. Res. Natl. Bur. Stand. Sect. A Phys. Chem.* **1976**, *80A* (3), 389. https://doi.org/10.6028/jres.080a.038.
(19) Hagan, A. K.; Zuchner, T. Lanthanide-Based Time-Resolved Luminescence Immunoassays. *Analytical and Bioanalytical Chemistry*. Springer July 2011, pp 2847–2864. https://doi.org/10.1007/s00216-011-5047-7.
(20) Brand, L.; Johnson, M. L. *Fluorescence Spectroscopy*; Brand, L., Johnson, M. L., Eds.; Methods in enzymology, v. 450; Academic Press/Elsevier: San Diego, Calif. ;, 2008.
(21) Hemmilä, I.; Laitala, V. Progress in Lanthanides as Luminescent Probes. *J. Fluoresc.* **2005**, *15* (4), 529–542. https://doi.org/10.1007/s10895-005-2826-6.
(22) Doose, S.; Neuweiler, H.; Sauer, M. Fluorescence Quenching by Photoinduced Electron Transfer: A Reporter for Conformational Dynamics of Macromolecules. *ChemPhysChem* **2009**, *10* (9–10), 1389–1398. https://doi.org/10.1002/cphc.200900238.
(23) Hollett, G.; Roberts, D. S.; Sewell, M.; Wensley, E.; Wagner, J.; Murray, W.; Krotz, A.; Toth, B.; Vijayakumar, V.; Sailor, M. J. Quantum Ensembles of Silicon Nanoparticles: Discrimination of Static and Dynamic Photoluminescence Quenching Processes. *J. Phys. Chem. C* **2019**, *123* (29), 17976–17986. https://doi.org/10.1021/acs.jpcc.9b04334.
(24) Clegg, R. M. The History of Fret. In *Reviews in Fluorescence 2006*; Springer US, 2007; pp 1–45. https://doi.org/10.1007/0-387-33016-x_1.
(25) Shrestha, D.; Jenei, A.; Nagy, P.; Vereb, G.; Szöllősi, J. Understanding FRET as a Research Tool for Cellular Studies. *International Journal of Molecular Sciences*. MDPI AG March 25, 2015, pp 6718–6756. https://doi.org/10.3390/ijms16046718.
(26) Förster, T. Energy Migration and Fluorescence. *J. Biomed. Opt.* **2012**, *17* (1), 011002. https://doi.org/10.1117/1.jbo.17.1.011002.
(27) Karvinen, J.; Hurskainen, P.; Gopalakrishnan, S.; Burns, D.; Warrior, U.; Hemmila, I.; Hemmilä, I. Homogeneous Time-Resolved Fluorescence Quenching Assay (LANCE) for Caspase-3. *J. Biomol. Screen.* **2002**, *7* (3), 223–231. https://doi.org/10.1177/108705710200700306.
(28) Härmä, H.; Rozwandowicz-Jansen, A.; Martikkala, E.; Frang, H.; Hemmilä, I.; Sahlberg, N.; Fey, V.; Perälä, M.; Hänninen, P. A New Simple Cell-Based Homogeneous Time-Resolved Fluorescence Qret Technique for Receptor-Ligand Interaction Screening. *J. Biomol. Screen.* **2009**, *14* (8), 936–943. https://doi.org/10.1177/1087057109341657.
(29) Nørskov-Lauritsen, L.; Thomsen, A. R. B.; Bräuner-Osborne, H. G Protein-Coupled Receptor Signaling Analysis Using Homogenous Time-Resolved Förster Resonance Energy Transfer (HTRF®) Technology. *International Journal of Molecular Sciences*. Int J Mol Sci February 13, 2014, pp 2554–2572. https://doi.org/10.3390/ijms15022554.
(30) Zwier, J. M.; Roux, T.; Cottet, M.; Durroux, T.; Douzon, S.; Bdioui, S.; Gregor, N.; Bourrier, E.; Oueslati, N.; Nicolas, L.; Tinel, N.; Boisseau, C.; Yverneau, P.; Charrier-Savournin, F.; Fink, M.; Trinquet, E. A Fluorescent Ligand-Binding Alternative Using Tag-Lite Technology. *J. Biomol. Screen.* **2010**, *15* (10), 1248–1259. https://doi.org/10.1177/1087057110384611.
(31) Dobretsov, G. E.; Syrejschikova, T. I.; Smolina, N. V. On Mechanisms of Fluorescence Quenching by Water. *Biophys. (Russian Fed.* **2014**, *59* (2), 183–188. https://doi.org/10.1134/S0006350914020079.

(32) Maillard, J.; Klehs, K.; Rumble, C.; Vauthey, E.; Heilemann, M.; Fürstenberg, A. Universal Quenching of Common Fluorescent Probes by Water and Alcohols. *Chem. Sci.* **2021**, *12* (4), 1352–1362. https://doi.org/10.1039/d0sc05431c.

(33) Gao, K.; Oerlemans, R.; Groves, M. R. Theory and Applications of Differential Scanning Fluorimetry in Early-Stage Drug Discovery. *Biophysical Reviews*. Springer February 1, 2020, pp 85–104. https://doi.org/10.1007/s12551-020-00619-2.

(34) Simeonov, A. Recent Developments in the Use of Differential Scanning Fluorometry in Protein and Small Molecule Discovery and Characterization. *Expert Opinion on Drug Discovery*. NIH Public Access September 2013, pp 1071–1082. https://doi.org/10.1517/17460441.2013.806479.

(35) Reed, C. E.; Fenton, S. E. Exposure to Diethylstilbestrol during Sensitive Life Stages: A Legacy of Heritable Health Effects. *Birth Defects Research Part C - Embryo Today: Reviews*. NIH Public Access June 2013, pp 134–146. https://doi.org/10.1002/bdrc.21035.

(36) Vargesson, N. The Teratogenic Effects of Thalidomide on Limbs. *Journal of Hand Surgery: European Volume*. SAGE Publications Ltd January 1, 2019, pp 88–95. https://doi.org/10.1177/1753193418805249.

(37) Scavone, C.; Di Mauro, G.; Mascolo, A.; Berrino, L.; Rossi, F.; Capuano, A. The New Paradigms in Clinical Research: From Early Access Programs to the Novel Therapeutic Approaches for Unmet Medical Needs. *Frontiers in Pharmacology*. Frontiers Media S.A. February 13, 2019, p 111. https://doi.org/10.3389/fphar.2019.00111.

(38) Seyhan, A. A. Lost in Translation: The Valley of Death across Preclinical and Clinical Divide – Identification of Problems and Overcoming Obstacles. *Transl. Med. Commun.* **2019**, *4* (1), 1–19. https://doi.org/10.1186/s41231-019-0050-7.

(39) Owens, J. Determining Druggability. *Nat. Rev. Drug Discov.* **2007**, *6* (3), 187–187. https://doi.org/10.1038/nrd2275.

(40) Blake, R. A. Target Validation in Drug Discovery. *Methods Mol. Biol.* **2007**, *356*, 367–377. https://doi.org/10.1385/1-59745-217-3:367.

(41) Smith, C. Drug Target Validation: Hitting the Target. *Nature* **2003**, *422* (6929), 341–347. https://doi.org/10.1038/422341a.

(42) Strimbu, K.; Tavel, J. A. What Are Biomarkers? *Current Opinion in HIV and AIDS*. NIH Public Access November 2010, pp 463–466. https://doi.org/10.1097/COH.0b013e32833ed177.

(43) Knowles, J.; Gromo, G. Target Selection in Drug Discovery. *Nature Reviews Drug Discovery*. Nature Publishing Group January 2003, pp 63–69. https://doi.org/10.1038/nrd986.

(44) Gashaw, I.; Ellinghaus, P.; Sommer, A.; Asadullah, K. What Makes a Good Drug Target? *Drug Discovery Today*. Elsevier Current Trends December 1, 2011, pp 1037–1043. https://doi.org/10.1016/j.drudis.2011.09.007.

(45) Emmerich, C. H.; Gamboa, L. M.; Hofmann, M. C. J.; Bonin-Andresen, M.; Arbach, O.; Schendel, P.; Gerlach, B.; Hempel, K.; Bespalov, A.; Dirnagl, U.; Parnham, M. J. Improving Target Assessment in Biomedical Research: The GOT-IT Recommendations. *Nature Reviews Drug Discovery*. Nature Research January 1, 2021, pp 64–81. https://doi.org/10.1038/s41573-020-0087-3.

(46) Galloway, W. R. J. D.; Isidro-Llobet, A.; Spring, D. R. Diversity-Oriented Synthesis as a Tool for the Discovery of Novel Biologically Active Small Molecules. *Nature Communications*. Nature Publishing Group September 21, 2010, pp 1–13. https://doi.org/10.1038/ncomms1081.

(47) Reymond, J. L.; Van Deursen, R.; Blum, L. C.; Ruddigkeit, L. Chemical Space as a Source for New Drugs. *MedChemComm*. The Royal Society of Chemistry July 1, 2010, pp 30–38. https://doi.org/10.1039/c0md00020e.

(48) Dobson, C. M. Chemical Space and Biology. *Nature*. December 16, 2004, pp 824–828. https://doi.org/10.1038/nature03192.

(49) Wigglesworth, M.; Hodder, P. Hit Discovery Methodology. *SLAS Discovery*. SAGE Publications Inc. February 1, 2021, pp 165–167. https://doi.org/10.1177/2472555220982257.

(50) Thomford, N. E.; Senthebane, D. A.; Rowe, A.; Munro, D.; Seele, P.; Maroyi, A.; Dzobo, K. Natural Products for Drug Discovery in the 21st Century: Innovations for Novel Drug Discovery. *International Journal of Molecular Sciences*. MDPI AG January 1, 2018, p 1578. https://doi.org/10.3390/ijms19061578.

(51) Lancini, G.; Demain, A. L. Bacterial Pharmaceutical Products. In *The Prokaryotes: Applied Bacteriology and Biotechnology*; Springer-Verlag Berlin Heidelberg, 2013; Vol. 9783642313318, pp 257–280. https://doi.org/10.1007/978-3-642-31331-8_28.

(52) Gullo, V. P.; McAlpine, J.; Lam, K. S.; Baker, D.; Petersen, F. Drug Discovery from Natural Products. In *Journal of Industrial Microbiology and Biotechnology*; 2006; Vol. 33, pp 523–531. https://doi.org/10.1007/s10295-006-0107-2.

(53) Shin, W.-H.; Christoffer, C. W.; Kihara, D. In Silico Structure-Based Approaches to Discover Protein-Protein Interaction-Targeting Drugs. **2017**. https://doi.org/10.1016/j.ymeth.2017.08.006.

(54) Ekins, S.; Mestres, J.; Testa, B. In Silico Pharmacology for Drug Discovery: Methods for Virtual Ligand Screening and Profiling. *British Journal of Pharmacology*. Wiley-Blackwell September 2007, pp 9–20. https://doi.org/10.1038/sj.bjp.0707305.

(55) Brogi, S.; Ramalho, T. C.; Kuca, K.; Medina-Franco, J. L.; Valko, M. Editorial: In Silico Methods for Drug Design and Discovery. *Frontiers in Chemistry*. Frontiers Media S.A. August 7, 2020, p 612. https://doi.org/10.3389/fchem.2020.00612.

(56) Kim, H.; Kim, E.; Lee, I.; Bae, B.; Park, M.; Nam, H. Artificial Intelligence in Drug Discovery: A Comprehensive Review of Data-Driven and Machine Learning Approaches. *Biotechnology and Bioprocess Engineering*. Korean Society for Biotechnology and Bioengineering December 1, 2020, pp 895–930. https://doi.org/10.1007/s12257-020-0049-y.

(57) Mak, K. K.; Pichika, M. R. Artificial Intelligence in Drug Development: Present Status and Future Prospects. *Drug Discovery Today*. Elsevier Ltd March 1, 2019, pp 773–780. https://doi.org/10.1016/j.drudis.2018.11.014.

(58) Morley, A. D.; Pugliese, A.; Birchall, K.; Bower, J.; Brennan, P.; Brown, N.; Chapman, T.; Drysdale, M.; Gilbert, I. H.; Hoelder, S.; Jordan, A.; Ley, S. V.; Merritt, A.; Miller, D.; Swarbrick, M. E.; Wyatt, P. G. Fragment-Based Hit Identification: Thinking in 3D. *Drug Discovery Today*. Elsevier Current Trends December 1, 2013, pp 1221–1227. https://doi.org/10.1016/j.drudis.2013.07.011.

(59) de Souza Neto, L. R.; Moreira-Filho, J. T.; Neves, B. J.; Maidana, R. L. B. R.; Guimarães, A. C. R.; Furnham, N.; Andrade, C. H.; Silva, F. P. In Silico Strategies to Support Fragment-to-Lead Optimization in Drug Discovery. *Frontiers in Chemistry*. Frontiers Media S.A. February 18, 2020, p 93. https://doi.org/10.3389/fchem.2020.00093.

(60) Bérubé, G. An Overview of Molecular Hybrids in Drug Discovery. *Expert Opinion on Drug Discovery*. Taylor and Francis Ltd March 3, 2016, pp 281–305. https://doi.org/10.1517/17460441.2016.1135125.

(61) Decker, M. *Design of Hybrid Molecules for Drug Development*; Decker, M., Ed.; Elsevier: London, [England, 2017.

(62) Kort, E.; Jovinge, S. Drug Repurposing: Claiming the Full Benefit from Drug Development. *Curr. Cardiol. Rep.* **2021**, *23* (6), 62. https://doi.org/10.1007/s11886-021-01484-5.

(63) Roessler, H. I.; Knoers, N. V. A. M.; van Haelst, M. M.; van Haaften, G. Drug Repurposing for Rare Diseases. *Trends in Pharmacological Sciences*. Elsevier Ltd April 1, 2021, pp 255–267. https://doi.org/10.1016/j.tips.2021.01.003.

(64) Sharlow, E. R. Revisiting Repurposing. *Assay Drug Dev. Technol.* **2016**, *14* (10), 554–556. https://doi.org/10.1089/adt.2016.766.

(65) Lipinski, C. A.; Lombardo, F.; Dominy, B. W.; Feeney, P. J. Experimental and Computational Approaches to Estimate Solubility and Permeability in Drug Discovery and Development Settings. *Adv. Drug Deliv. Rev.* **2001**, *46* (1–3), 3–26. https://doi.org/10.1016/S0169-409X(00)00129-0.

(66) Benet, L. Z.; Hosey, C. M.; Ursu, O.; Oprea, T. I. BDDCS, the Rule of 5 and Drugability. *Advanced Drug Delivery Reviews*. Elsevier B.V. June 1, 2016, pp 89–98. https://doi.org/10.1016/j.addr.2016.05.007.

(67) Doak, B. C.; Kihlberg, J. Drug Discovery beyond the Rule of 5 - Opportunities and Challenges. *Expert Opinion on Drug Discovery*. Taylor and Francis Ltd February 1, 2017, pp 115–119. https://doi.org/10.1080/17460441.2017.1264385.

(68) Martín, A.; Nicolaou, C. A.; Toledo, M. A. Navigating the DNA Encoded Libraries Chemical Space. *Commun. Chem.* **2020**, *3* (1), 1–9. https://doi.org/10.1038/s42004-020-00374-1.

(69) Lyu, J.; Wang, S.; Balius, T. E.; Singh, I.; Levit, A.; Moroz, Y. S.; O'Meara, M. J.; Che, T.; Algaa, E.; Tolmachova, K.; Tolmachev, A. A.; Shoichet, B. K.; Roth, B. L.; Irwin, J. J. Ultra-Large Library Docking for Discovering New Chemotypes. *Nature* **2019**, *566* (7743), 224–229. https://doi.org/10.1038/s41586-019-0917-9.

(70) Michael, S.; Auld, D.; Klumpp, C.; Jadhav, A.; Zheng, W.; Thorne, N.; Austin, C. P.; Inglese, J.; Simeonov, A. A Robotic Platform for Quantitative High-Throughput Screening. *Assay and Drug Development Technologies*. Mary Ann Liebert, Inc. October 1, 2008, pp 637–657. https://doi.org/10.1089/adt.2008.150.

(71) Ekins, S.; Clark, A. M.; Dole, K.; Gregory, K.; Mcnutt, A. M.; Spektor, A. C.; Weatherall, C.; Litterman, N. K.; Bunin, B. A. Data Mining and Computational Modeling of High-Throughput Screening Datasets. In *Methods in Molecular Biology*; Humana Press Inc., 2018; Vol. 1755, pp 197–221. https://doi.org/10.1007/978-1-4939-7724-6_14.

(72) Rudnicki, S.; Johnston, S. Overview of Liquid Handling Instrumentation for High-Throughput Screening Applications. *Curr. Protoc. Chem. Biol.* **2009**, *1* (1), 43–54. https://doi.org/10.1002/9780470559277.ch090151.

(73) Jones, E.; Michael, S.; Sittampalam, G. S. *Basics of Assay Equipment and Instrumentation for High Throughput Screening*; Eli Lilly & Company and the National Center for Advancing Translational Sciences, 2004.

(74) Armstrong, J. A Review of High-Throughput Screening Approaches for Drug Discovery. *Am. Biotechnol. Lab.* **1999**, *17*, 26–28.

(75) Martis, E. A. *High-Throughput Screening: The Hits and Leads of Drug Discovery-An Overview*; Vol. 01, pp 02–10.

(76) Yasgar, A.; Shinn, P.; Jadhav, A.; Auld, D.; Michael, S.; Zheng, W.; Austin, C. P.; Inglese, J.; Simeonov, A. Compound Management for Quantitative High-Throughput Screening. *J. Lab. Autom.* **2008**, *13* (2), 79–89. https://doi.org/10.1016/j.jala.2007.12.004.

(77) Aldewachi, H.; Al-Zidan, R. N.; Conner, M. T.; Salman, M. M. High-Throughput Screening Platforms in the Discovery of Novel Drugs for Neurodegenerative Diseases. *Bioengineering*. MDPI AG February 1, 2021, pp 1–20. https://doi.org/10.3390/bioengineering8020030.

(78) Delvecchio, C.; Tiefenbach, J.; Krause, H. M. The Zebrafish: A Powerful Platform for in Vivo, HTS Drug Discovery. *Assay and Drug Development Technologies*. Assay Drug Dev Technol August 1, 2011, pp 354–361. https://doi.org/10.1089/adt.2010.0346.

(79) Lee, D. W.; Doh, I.; Nam, D. H. Unified 2D and 3D Cell-Based High-Throughput Screening Platform Using a Micropillar/Microwell Chip. *Sensors Actuators, B Chem.* **2016**, *228*, 523–528. https://doi.org/10.1016/j.snb.2016.01.011.

(80) Cader, Z.; Graf, M.; Burcin, M.; Mandenius, C. F.; Ross, J. A. Cell-Based Assays Using Differentiated Human Induced Pluripotent Cells. In *Methods in Molecular Biology*; Humana Press Inc., 2019; Vol. 1994, pp 1–14. https://doi.org/10.1007/978-1-4939-9477-9_1.

(81) Fröhlich, F.; Kessler, T.; Weindl, D.; Shadrin, A.; Schmiester, L.; Hache, H.; Muradyan, A.; Schütte, M.; Lim, J. H.; Heinig, M.; Theis, F. J.; Lehrach, H.; Wierling, C.; Lange, B.; Hasenauer, J. Efficient Parameter Estimation Enables the Prediction of Drug Response Using a Mechanistic Pan-Cancer Pathway Model. *Cell Syst.* **2018**, *7* (6), 567-579.e6. https://doi.org/10.1016/j.cels.2018.10.013.

(82) Stoddart, L. A.; White, C. W.; Nguyen, K.; Hill, S. J.; Pfleger, K. D. G. Fluorescence- and Bioluminescence-Based Approaches to Study GPCR Ligand Binding. *Br. J. Pharmacol.* **2016**, *173* (20), 3028–3037. https://doi.org/10.1111/bph.13316.
(83) Fang, Y. Ligand-Receptor Interaction Platforms and Their Applications for Drug Discovery. *Expert Opinion on Drug Discovery*. Expert Opin Drug Discov October 2012, pp 969–988. https://doi.org/10.1517/17460441.2012.715631.
(84) Landry, J. P.; Fei, Y.; Zhu, X.; Ke, Y.; Yu, G.; Lee, P. Discovering Small Molecule Ligands of Vascular Endothelial Growth Factor That Block VEGF-KDR Binding Using Label-Free Microarray-Based Assays. *Assay Drug Dev. Technol.* **2013**, *11* (5), 326–332. https://doi.org/10.1089/adt.2012.485.
(85) Murray, D.; Wigglesworth, M. Chapter 1. HTS Methods: Assay Design and Optimisation; Royal Society of Chemistry, 2016; pp 1–15. https://doi.org/10.1039/9781782626770-00001.
(86) Wesolowski, S. S.; Brown, D. G. The Strategies and Politics of Successful Design, Make, Test, and Analyze (DMTA) Cycles in Lead Generation; John Wiley & Sons, Ltd, 2016; pp 487–512. https://doi.org/10.1002/9783527677047.ch17.
(87) Davis, A. M.; Plowright, A. T.; Valeur, E. Directing Evolution: The next Revolution in Drug Discovery? *Nature Reviews Drug Discovery*. Nature Publishing Group October 1, 2017, pp 681–698. https://doi.org/10.1038/nrd.2017.146.
(88) Plowright, A. T.; Johnstone, C.; Kihlberg, J.; Pettersson, J.; Robb, G.; Thompson, R. A. Hypothesis Driven Drug Design: Improving Quality and Effectiveness of the Design-Make-Test-Analyse Cycle. *Drug Discovery Today*. January 2012, pp 56–62. https://doi.org/10.1016/j.drudis.2011.09.012.
(89) T, B.; G, G. Preclinical Drug Development. *Acta Pol. Pharm.* **2010**, *67* (6).
(90) Shegokar, R. Preclinical Testing—Understanding the Basics First. In *Drug Delivery Aspects*; Elsevier, 2020; pp 19–32. https://doi.org/10.1016/b978-0-12-821222-6.00002-6.
(91) OECD Series on Principles of Good Laboratory Practice (GLP) and Compliance Monitoring - OECD https://www.oecd.org/chemicalsafety/testing/oecdseriesonprinciplesofgoodlaboratorypracticeglpandcompliancemonitoring.htm (accessed May 30, 2021).
(92) Turnheim, D. The OECD Policy for the Implementation of the Principles of Good Laboratory Practice. *Ann. Ist. Super. Sanita* **1994**, *30* (4), 395–400.
(93) New Drug Application (NDA) | FDA https://www.fda.gov/drugs/types-applications/new-drug-application-nda (accessed May 15, 2021).
(94) Olivencia, S. B.; Sasangohar, F. Investigating the Food and Drug Administration Biotherapeutics Review and Approval Process: Narrative Review. *JMIR Formative Research*. JMIR Publications Inc. March 1, 2021. https://doi.org/10.2196/14563.
(95) Cinquanta, L.; Fontana, D. E.; Bizzaro, N. Chemiluminescent Immunoassay Technology: What Does It Change in Autoantibody Detection? *Autoimmun. Highlights* **2017**, *8* (1). https://doi.org/10.1007/s13317-017-0097-2.
(96) Fan, F.; Wood, K. V. Bioluminescent Assays for High-Throughput Screening. *Assay and Drug Development Technologies*. Assay Drug Dev Technol February 2007, pp 127–136. https://doi.org/10.1089/adt.2006.053.
(97) Li, J.; Chen, L.; Du, L.; Li, M. Cage the Firefly Luciferin! – A Strategy for Developing Bioluminescent Probes. *Chem. Soc. Rev.* **2013**, *42* (2), 662–676. https://doi.org/10.1039/c2cs35249d.
(98) Berezin, M. Y.; Achilefu, S. Fluorescence Lifetime Measurements and Biological Imaging. *Chem. Rev.* **2010**, *110* (5), 2641–2684. https://doi.org/10.1021/cr900343z.
(99) Sittampalam, G. S.; Coussens, N. P.; Editor, A. S.; Arkin, M.; Auld, D.; Austin, C.; Bejcek, B.; Glicksman, M.; Inglese, J.; Iversen, P. W.; Mcgee, J.; Mcmanus, O.; Minor, L.; Napper, A.; Peltier, J. M.; Riss, T.; Trask, O. J.; Weidner, J. *Assay Guidance Manual*; Eli Lilly & Company and the National Center for Advancing Translational Sciences, 2004.

(100) Fletcher, K. A.; Fakayode, S. O.; Lowry, M.; Tucker, S. A.; Neal, S. L.; Kimaru, I. W.; McCarroll, M. E.; Patonay, G.; Oldham, P. B.; Rusin, O.; Strongin, R. M.; Warner, I. M. Molecular Fluorescence, Phosphorescence, and Chemiluminescence Spectrometry. *Analytical Chemistry*. NIH Public Access June 15, 2006, pp 4047–4068. https://doi.org/10.1021/ac060683m.

(101) Phillips, D. A Lifetime in Photochemistry; Some Ultrafast Measurements on Singlet States. *Proceedings of the Royal Society A: Mathematical, Physical and Engineering Sciences*. Royal Society of London June 1, 2016. https://doi.org/10.1098/rspa.2016.0102.

(102) Sir ohn F rederick W illiam H erschel, B. J. IV. 'Αμόρφωγa, No. I.— on a Case of Superficial Colour Presented by a Homogeneous Liquid Internally Colourless. *Philos. Trans. R. Soc. London* **1845**, *135*, 143–145. https://doi.org/10.1098/rstl.1845.0004.

(103) Gao, Z.; Hao, Y.; Zheng, M.; Chen, Y. A Fluorescent Dye with Large Stokes Shift and High Stability: Synthesis and Application to Live Cell Imaging. *RSC Adv.* **2017**, *7* (13), 7604–7609. https://doi.org/10.1039/c6ra27547h.

(104) Ren, T. B.; Xu, W.; Zhang, W.; Zhang, X. X.; Wang, Z. Y.; Xiang, Z.; Yuan, L.; Zhang, X. B. A General Method to Increase Stokes Shift by Introducing Alternating Vibronic Structures. *J. Am. Chem. Soc.* **2018**, *140* (24), 7716–7722. https://doi.org/10.1021/jacs.8b04404.

(105) Binnemans, K. Interpretation of Europium(III) Spectra. *Coordination Chemistry Reviews*. Elsevier B.V. January 1, 2015, pp 1–45. https://doi.org/10.1016/j.ccr.2015.02.015.

(106) Huang, H.; Nishi, K.; Tsai, H. J.; Hammock, B. D. Development of Highly Sensitive Fluorescent Assays for Fatty Acid Amide Hydrolase. *Anal. Biochem.* **2007**, *363* (1), 12–21. https://doi.org/10.1016/j.ab.2006.10.041.

(107) Czaplinska, B.; Malarz, K.; Mrozek-Wilczkiewicz, A.; Slodek, A.; Korzec, M.; Musiol, R. Theoretical and Experimental Investigations of Large Stokes Shift Fluorophores Based on a Quinoline Scaffold. *Molecules* **2020**, *25* (11). https://doi.org/10.3390/molecules25112488.

(108) Barrio, J. R.; Tolman, G. L.; Leonard, N. J.; Spencer, R. D.; Weber, G. *Flavin 1, N6-Ethenoadenine Dinucleotide: Dynamic and Static Quenching of Fluorescence (FAD/i,N6-Ethenoadenine Derivative/Fluorescence Emission/Coenzyme Analogue/Energy Transfer)*; 1973; Vol. 70.

(109) Blatr, E.; Chatelier, R. C.; Sawyer, W. H. *EFFECTS OF QUENCHING MECHANISM AND TYPE OF QUENCHER ASSOCIATION ON STERN-VOLMER PLOTS IN COMPARTMENTALIZED SYSTEMS*; Vol. 50. https://doi.org/10.1016/S0006-3495(86)83468-3.

(110) Evale, B. G.; Hanagodimath, S. M. Static and Dynamic Quenching of Biologically Active Coumarin Derivative by Aniline in Benzeneacetonitrile Mixtures. *Journal of Luminescence*. North-Holland August 1, 2010, pp 1330–1337. https://doi.org/10.1016/j.jlumin.2010.03.011.

(111) Chen, C. T.; Wagner, H.; Still, W. C. Fluorescent, Sequence-Selective Peptide Detection by Synthetic Small Molecules. *Science (80-.).* **1998**, *279* (5352), 851–853. https://doi.org/10.1126/science.279.5352.851.

(112) Marras, S. A. E.; Kramer, F. R.; Tyagi, S. Efficiencies of Fluorescence Resonance Energy Transfer and Contact-Mediated Quenching in Oligonucleotide Probes. *Nucleic Acids Res.* **2002**, *30* (21), e122–e122. https://doi.org/10.1093/nar/gnf121.

(113) Pérez-Ibave, D. C.; Burciaga-Flores, C. H.; Elizondo-Riojas, M. Á. Prostate-Specific Antigen (PSA) as a Possible Biomarker in Non-Prostatic Cancer: A Review. *Cancer Epidemiology*. Elsevier Ltd June 1, 2018, pp 48–55. https://doi.org/10.1016/j.canep.2018.03.009.

(114) Le Reste, L.; Hohlbein, J.; Gryte, K.; Kapanidis, A. N. Characterization of Dark Quencher Chromophores as Nonfluorescent Acceptors for Single-Molecule FRET. *Biophys. J.* **2012**, *102* (11), 2658–2668. https://doi.org/10.1016/j.bpj.2012.04.028.

(115) Jernigan, F. E.; Lawrence, D. S. A Broad Spectrum Dark Quencher: Construction of Multiple Colour Protease and Photolytic Sensors. *Chem. Commun.* **2013**, *49* (60), 6728–6730. https://doi.org/10.1039/c3cc42628a.

(116) Ortiz, E.; Avila, M.; Mancera, D.; Morales, E. Quenching of Fluorescence Caused by Graphene Oxide as an Immunosensing Platform in a Microwell Plate Format. In *Proceedings of The 1st International Electronic Conference on Biosensors*; MDPI: Basel, Switzerland, 2020; p 7017. https://doi.org/10.3390/IECB2020-07017.
(117) Suzuki, M.; Husimi, Y.; Komatsu, H.; Suzuki, K.; Douglas, K. T. Quantum Dot FRET Biosensors That Respond to PH, to Proteolytic or Nucleolytic Cleavage, to DNA Synthesis, or to a Multiplexing Combination. *J. Am. Chem. Soc.* **2008**, *130* (17), 5720–5725. https://doi.org/10.1021/ja710870e.
(118) Geißler, D.; Charbonnière, L. J.; Ziessel, R. F.; Butlin, N. G.; Löhmannsröben, H. G.; Hildebrandt, N. Quantum Dot Biosensors for Ultrasensitive Multiplexed Diagnostic. *Angew. Chemie - Int. Ed.* **2010**, *49* (8), 1396–1401. https://doi.org/10.1002/anie.200906399.
(119) Shamirian, A.; Ghai, A.; Snee, P. T. QD-Based FRET Probes at a Glance. *Sensors (Switzerland)* **2015**, *15* (6), 13028–13051. https://doi.org/10.3390/s150613028.
(120) Kokko, T. *Lanthanide Chelates as Donors in Fluorescence Resonance Energy Transfer: Exciting Prospects for Bioaffinity Assay Detection*; 2009.
(121) Glen Report 17.14 - Expanding Our Repertoire of Dark Quenchers: Black Hole Quenchers https://www.glenresearch.com/reports/gr17-14 (accessed Jul 6, 2021).
(122) LAURENCE, D. J. A Study of the Adsorption of Dyes on Bovine Serum Albumin by the Method of Polarization of Fluorescence. *Biochem. J.* **1952**, *51* (2), 168–180. https://doi.org/10.1042/bj0510168.
(123) Gessner, T.; Mayer, U. Triarylmethane and Diarylmethane Dyes. In *Ullmann's Encyclopedia of Industrial Chemistry*; Wiley-VCH Verlag GmbH & Co. KGaA, 2000. https://doi.org/10.1002/14356007.a27_179.
(124) Noga, E. J.; Udomkusonsri, P. Fluorescein: A Rapid, Sensitive, Nonlethal Method for Detecting Skin Ulceration in Fish. *Vet. Pathol.* **2002**, *39* (6), 726–731. https://doi.org/10.1354/vp.39-6-726.
(125) Korlach, J.; Baird, D. W.; Heikal, A. A.; Gee, K. R.; Hoffman, G. R.; Webb, W. W. Spontaneous Nucleotide Exchange in Low Molecular Weight GTPases by Fluorescently Labeled γ-Phosphate-Linked GTP Analogs. *Proc. Natl. Acad. Sci. U. S. A.* **2004**, *101* (9), 2800–2805. https://doi.org/10.1073/pnas.0308579100.
(126) Das, R.; Mitra, S.; Mukherjee, S. Ground and Excited State Proton Transfer of 4-Methyl-2,6-Diformylphenol in Different Solvent Mixtures. *Chem. Phys. Lett.* **1994**, *221* (5–6), 368–372. https://doi.org/10.1016/0009-2614(94)00284-3.
(127) Dubois, M. R.; Dubois, D. L. Development of Molecular Electrocatalysts for CO2 Reduction and H2 Production/Oxidation. *Acc. Chem. Res.* **2009**, *42* (12), 1974–1982. https://doi.org/10.1021/AR900110C.
(128) *SelectScreen ® Biochemical Kinase Profiling Service Z'-LYTE ® Screening Protocol and Assay Conditions Z'-LYTE ® ASSAY CONDITIONS*.
(129) Shin, S. B.; Woo, S. U.; Lee, Y. J.; Yim, H. Comparative Analysis of a Fret-Based Plk1 Kinase Assay to Identify Plk1 Inhibitors for Chemotherapy. *Anticancer Res.* **2017**, *37* (3), 1177–1183. https://doi.org/10.21873/anticanres.11431.
(130) Kang, N. S.; Lee, G. N.; Kim, C. H.; Bae, M. A.; Kim, I.; Cho, Y. S. Identification of Small Molecules That Inhibit GSK-3β through Virtual Screening. *Bioorganic Med. Chem. Lett.* **2009**, *19* (2), 533–537. https://doi.org/10.1016/j.bmcl.2008.10.120.
(131) Gustiananda, M.; Liggins, J. R.; Cummins, P. L.; Gready, J. E. Conformation of Prion Protein Repeat Peptides Probed by FRET Measurements and Molecular Dynamics Simulations. *Biophys. J.* **2004**, *86* (4), 2467–2483. https://doi.org/10.1016/S0006-3495(04)74303-9.
(132) Karvinen, J.; Hurskainen, P.; Gopalakrishnan, S.; Burns, D.; Warrior, U.; Hemmila, I. Homogeneous Time-Resolved Fluorescence Quenching Assay (LANCE) for Caspase-3. *J. Biomol. Screen.* **2002**, *7* (3), 223–231. https://doi.org/10.1177/108705710200700306.
(133) PerkinElmer. *DELFIA, LANCE and TruPoint Technologies: Sensitivity and Dynamic Range Using PerkinElmer Instrumentation and Microplates*.

(134) Hemmilä. LANCEtrade Mark: Homogeneous Assay Platform for HTS. *J. Biomol. Screen.* **1999**, *4* (6), 303–308. https://doi.org/10.1177/108705719900400604.
(135) Devices, M. *IMAP Technology for Kinases, Phosphatases and Phosphodiesterases A Complete Platform for Assay Development and High-Throughput Screening DATA SHEET*; 2020.
(136) Sharlow, E. R.; Leimgruber, S.; Yellow-Duke, A.; Barrett, R.; Wang, Q. J.; Lazo, J. S. Development, Validation and Implementation of Immobilized Metal Affinity for Phosphochemicals (IMAP)-Based High-Throughput Screening Assays for Low-Molecular-Weight Compound Libraries. *Nat. Protoc.* **2008**, *3* (8), 1350–1363. https://doi.org/10.1038/nprot.2008.111.
(137) Zeng, H.; Wu, J.; Bedford, M. T.; Sbardella, G.; Hoffmann, F. M.; Bi, K.; Xu, W. A TR-FRET-Based Functional Assay for Screening Activators of CARM1. *ChemBioChem* **2013**, *14* (7), 827–835. https://doi.org/10.1002/cbic.201300029.
(138) Carazo, A.; Pávek, P. The Use of the LanthaScreen TR-FRET CAR Coactivator Assay in the Characterization of Constitutive Androstane Receptor (CAR) Inverse Agonists. *Sensors (Switzerland)* **2015**, *15* (4), 9265–9276. https://doi.org/10.3390/s150409265.
(139) Degorce, F.; Card, A.; Soh, S.; Trinquet, E.; Knapik, G. P.; Xie, B. HTRF: A Technology Tailored for Drug Discovery - A Review of Theoretical Aspects and Recent Applications. *Current Chemical Genomics*. Curr Chem Genomics 2009, pp 22–32. https://doi.org/10.2174/1875397300903010022.
(140) Acker, M. G.; Auld, D. S. Considerations for the Design and Reporting of Enzyme Assays in High-Throughput Screening Applications. *Perspect. Sci.* **2014**, *1* (1–6), 56–73. https://doi.org/10.1016/j.pisc.2013.12.001.
(141) Einhorn, L.; Krapfenbauer, K. HTRF: A Technology Tailored for Biomarker Determination-Novel Analytical Detection System Suitable for Detection of Specific Autoimmune Antibodies as Biomarkers in Nanogram Level in Different Body Fluids. *EPMA J.* **2015**, *6* (1). https://doi.org/10.1186/s13167-015-0046-y.
(142) Ylikoski, A.; Elomaa, A.; Ollikka, P.; Hakala, H.; Mukkala, V. M.; Hovinen, J.; Hemmilä, I. Homogeneous Time-Resolved Fluorescence Quenching Assay (TruPoint) for Nucleic Acid Detection. *Clin. Chem.* **2004**, *50* (10), 1943–1947. https://doi.org/10.1373/clinchem.2004.036616.
(143) Oueslati, N.; Hounsou, C.; Belhocine, A.; Rodriguez, T.; Dupuis, E.; Zwier, J. M.; Trinquet, E.; Pin, J. P.; Durroux, T. Time-Resolved FRET Strategy to Screen GPCR Ligand Library. *Methods Mol. Biol.* **2015**, *1272*, 23–36. https://doi.org/10.1007/978-1-4939-2336-6_2.
(144) *Tag-Lite ® Binding Assays THE EASY WAY TO APPROACH COMPLEX BIOLOGY TAG-LITE ® Cisbio Offers a Wide Selection of Ligand Binding Solutions, Covering over 18 GPCRs*.
(145) Blanc, E.; Wagner, P.; Plaisier, F.; Schmitt, M.; Durroux, T.; Bourguignon, J. J.; Partiseti, M.; Dupuis, E.; Bihel, F. Design and Validation of a Homogeneous Time-Resolved Fluorescence Cell-Based Assay Targeting the Ligand-Gated Ion Channel 5-HT3A. *Anal. Biochem.* **2015**, *484*, 105–112. https://doi.org/10.1016/j.ab.2015.03.035.
(146) Rozwandowicz-Jansen, A.; Laurila, J.; Martikkala, E.; Frang, H.; Hemmilä, I.; Scheinin, M.; Hänninen, P.; Härmä, H. Homogeneous GTP Binding Assay Employing QRET Technology. *J. Biomol. Screen.* **2010**, *15* (3), 261–267. https://doi.org/10.1177/1087057109358921.
(147) K, K.; N, T.-O.; M, L.; V, E.; PJ, K.; H, H. Homogeneous Peptide-Break Assay for Luminescent Detection of Enzymatic Protein Post-Translational Modification Activity Utilizing Charged Peptides. *Anal. Chim. Acta* **2019**, *1055*, 126–132. https://doi.org/10.1016/J.ACA.2018.12.041.
(148) Moreau, M. J. J.; Morin, I.; Schaeffer, P. M. Quantitative Determination of Protein Stability and Ligand Binding Using a Green Fluorescent Protein Reporter System. *Mol. Biosyst.* **2010**, *6* (7), 1285–1292. https://doi.org/10.1039/c002001j.
(149) Bond, T. E. H.; Sorenson, A. E.; Schaeffer, P. M. A Green Fluorescent Protein-Based Assay for High-Throughput Ligand-Binding Studies of a Mycobacterial Biotin Protein Ligase. *Microbiol. Res.* **2017**, *205*, 35–39. https://doi.org/10.1016/j.micres.2017.08.014.

(150) Sorenson, A. E.; Schaeffer, P. M. High-Throughput Differential Scanning Fluorimetry of GFP-Tagged Proteins. In *Methods in Molecular Biology*; Humana Press Inc., 2020; Vol. 2089, pp 69–85. https://doi.org/10.1007/978-1-0716-0163-1_5.
(151) Rogers, M. V. Light on High-Throughput Screening: Fluorescence-Based Assay Technologies. *Drug Discov. Today* **1997**, *2* (4), 156–160. https://doi.org/10.1016/S1359-6446(97)01016-7.
(152) Huynh, K.; Partch, C. L. Analysis of Protein Stability and Ligand Interactions by Thermal Shift Assay. *Curr. Protoc. protein Sci.* **2015**, *79*, 28.9.1-28.9.14. https://doi.org/10.1002/0471140864.ps2809s79.
(153) Niesen, F. H.; Berglund, H.; Vedadi, M. The Use of Differential Scanning Fluorimetry to Detect Ligand Interactions That Promote Protein Stability. *Nat. Protoc.* **2007**, *2* (9), 2212–2221. https://doi.org/10.1038/nprot.2007.321.
(154) Ericsson, U. B.; Hallberg, B. M.; DeTitta, G. T.; Dekker, N.; Nordlund, P. Thermofluor-Based High-Throughput Stability Optimization of Proteins for Structural Studies. *Anal. Biochem.* **2006**, *357* (2), 289–298. https://doi.org/10.1016/j.ab.2006.07.027.
(155) Newman, J. Novel Buffer Systems for Macromolecular Crystallization. *Acta Crystallogr. Sect. D Biol. Crystallogr.* **2004**, *60* (3), 610–612. https://doi.org/10.1107/S0907444903029640.
(156) Li, Y.; Mach, H.; Blue, J. T. High Throughput Formulation Screening for Global Aggregation Behaviors of Three Monoclonal Antibodies. *J. Pharm. Sci.* **2011**, *100* (6), 2120–2135. https://doi.org/10.1002/jps.22450.
(157) Jones, L. J.; Haugland, R. P.; Singer, V. L. Development and Characterization of the NanoOrange® Protein Quantitation Assay: A Fluorescence-Based Assay of Proteins in Solution. *Biotechniques* **2003**, *34* (4), 850–861. https://doi.org/10.2144/03344pt03.
(158) Nielsen, L.; Khurana, R.; Coats, A.; Frokjaer, S.; Brange, J.; Vyas, S.; Uversky, V. N.; Fink, A. L. Effect of Environmental Factors on the Kinetics of Insulin Fibril Formation: Elucidation of the Molecular Mechanism. *Biochemistry* **2001**, *40* (20), 6036–6046. https://doi.org/10.1021/bi002555c.
(159) Xue, C.; Lin, T. Y.; Chang, D.; Guo, Z. Thioflavin T as an Amyloid Dye: Fibril Quantification, Optimal Concentration and Effect on Aggregation. *R. Soc. Open Sci.* **2017**, *4* (1). https://doi.org/10.1098/rsos.160696.
(160) LeVine, H. Quantification of β-Sheet Amyloid Fibril Structures with Thioflavin T. *Methods Enzymol.* **1999**, *309*, 274–284. https://doi.org/10.1016/S0076-6879(99)09020-5.
(161) McClure, S. M.; Ahl, P. L.; Blue, J. T. High Throughput Differential Scanning Fluorimetry (DSF) Formulation Screening with Complementary Dyes to Assess Protein Unfolding and Aggregation in Presence of Surfactants. *Pharm. Res.* **2018**, *35* (4). https://doi.org/10.1007/s11095-018-2361-1.
(162) Kroeger, T.; Frieg, B.; Zhang, T.; Hansen, F. K.; Marmann, A.; Proksch, P.; Nagel-Steger, L.; Groth, G.; Smits, S. H. J.; Gohlke, H. EDTA Aggregates Induce SYPRO Orange-Based Fluorescence in Thermal Shift Assay. *PLoS One* **2017**, *12* (5), e0177024. https://doi.org/10.1371/journal.pone.0177024.
(163) Bruce, D.; Cardew, E.; Freitag-Pohl, S.; Pohl, E. How to Stabilize Protein: Stability Screens for Thermal Shift Assays and Nano Differential Scanning Fluorimetry in the Virus-X Project. *J. Vis. Exp.* **2019**, No. 144, 58666. https://doi.org/10.3791/58666.
(164) Mackintosh, J. A.; Veal, D. A.; Karuso, P. Fluoroprofile, a Fluorescence-Based Assay for Rapid and Sensitive Quantitation of Proteins in Solution. *Proteomics* **2005**, *5* (18), 4673–4677. https://doi.org/10.1002/pmic.200500095.
(165) Coghlan, D. R.; Mackintosh, J. A.; Karuso, P. Mechanism of Reversible Fluorescent Staining of Protein with Epicocconone. *Org. Lett.* **2005**, *7* (12), 2401–2404. https://doi.org/10.1021/ol050665b.
(166) Karuso, P.; Crawford, A. S.; Veal, D. A.; Scott, G. B. I.; Choi, H. Y. Real-Time Fluorescence Monitoring of Tryptic Digestion in Proteomics. *J. Proteome Res.* **2008**, *7* (1), 361–366. https://doi.org/10.1021/pr0704480.

(167) NM, G. Avidin and Streptavidin. *Methods Enzymol.* **1990**, *184* (C), 51–67. https://doi.org/10.1016/0076-6879(90)84259-J.

(168) M, H.; DJ, C.; K, G.; PC, D.; MR, G.; NL, K.; A, E.-H.; AY, T. A Monovalent Streptavidin with a Single Femtomolar Biotin Binding Site. *Nat. Methods* **2006**, *3* (4), 267–273. https://doi.org/10.1038/NMETH861.

(169) Wang, Q.; Nono, K. N.; Syrjänpää, M.; Charbonnière, L. J.; Hovinen, J.; Härmä, H. Stable and Highly Fluorescent Europium(III) Chelates for Time-Resolved Immunoassays. *Inorg. Chem.* **2013**, *52* (15), 8461–8466. https://doi.org/10.1021/IC400384F.

(170) Umezawa, H.; Aoyagi, T.; Morishima, H.; Matsuzaki, M.; Hamada, M.; Takeuchi, T. Pepstatin, A New Pepsin Inhibitor Produced by Actinomygetes. *J. Antibiot. (Tokyo).* **1970**, *23* (5), 259–262. https://doi.org/10.7164/antibiotics.23.259.

(171) Roberts, N. B.; Taylor, W. H. Comparative Pepstatin Inhibition Studies on Individual Human Pepsins and Pepsinogens 1,3 and 5(Gastricsin) and Pig Pepsin A. *J. Enzyme Inhib. Med. Chem.* **2003**, *18* (3), 209–217. https://doi.org/10.1080/1475636031000076888.

(172) Matsumoto, K.; Mizoue, K.; Kitamura, K.; Tse, W. C.; Huber, C. P.; Ishida, T. Structural Basis of Inhibition of Cysteine Proteases by E-64 and Its Derivatives. *Biopolym. - Pept. Sci. Sect.* **1999**, *51* (1), 99–107. https://doi.org/10.1002/(SICI)1097-0282(1999)51:1<99::AID-BIP11>3.0.CO;2-R.

TURUN
YLIOPISTO
UNIVERSITY
OF TURKU

Painosalama Oy, Turku, Finland 2021

ISBN 978-951-29-8706-1 (PRINT)
ISBN 978-951-29-8707-8 (PDF)
ISSN 0082-7002 (Print)
ISSN 2343-3175 (Online)